CONCEPTUAL STUDY OF PERMANENT MAGNET MACHINE SHIP PROPULSION SYSTEMS

R.A. Marshall, W. McMurray, E. Richter
H.F. Webster, W. Wyeth

Final Report
Contract No. N00014-77-C-0001

Period Covered
1976 October 1 through 1977 October 31

Prepared for
OFFICE OF NAVAL RESEARCH
MATERIAL SCIENCES DIVISION
ARLINGTON, VIRGINIA

Prepared by
General Electric Company
Corporate Research and Development
Schenectady, New York 12301

1977 December

SRD-77-170

GENERAL ELECTRIC

UNCLASSIFIED

SECURITY CLASSIFICATION OF THIS PAGE (When Data Entered)

REPORT DOCUMENTATION PAGE	READ INSTRUCTIONS BEFORE COMPLETING FORM
1. REPORT NUMBER	2. GOVT ACCESSION NO. 3. RECIPIENT'S CATALOG NUMBER
4. TITLE (and Subtitle) (6) CONCEPTUAL STUDY OF PERMANENT MAGNET MACHINE SHIP PROPULSION SYSTEMS.	5. TYPE OF REPORT & PERIOD COVERED Final Report 1976 October 1-1977 October 31
	6. PERFORMING ORG. REPORT NUMBER (14) SRD-77-170
7. AUTHOR(s) (10) R.A./Marshall, W./McMurray, E./Richter, H.F./Webster, W./Wyeth	8. CONTRACT OR GRANT NUMBER(s) (15) N000014-77-C-0001 NEW
9. PERFORMING ORGANIZATION NAME AND ADDRESS General Electric Company Corporate Research and Development Schenectady, New York 12301	10. PROGRAM ELEMENT, PROJECT, TASK AREA & WORK UNIT NUMBERS (11)
11. CONTROLLING OFFICE NAME AND ADDRESS Office of Naval Research Material Sciences Division Arlington, Virginia	12. REPORT DATE 1977 Dec 77
	13. NUMBER OF PAGES 112
14. MONITORING AGENCY NAME & ADDRESS (if different from Controlling Office)	15. SECURITY CLASS. (of this report) (12) 114p.
	15a. DECLASSIFICATION/DOWNGRADING SCHEDULE

16. DISTRIBUTION STATEMENT (of this Report)

Approved for public release; distribution unlimited

DDC RECEIVED JAN 11 1978 B

17. DISTRIBUTION STATEMENT (of the abstract entered in Block 20, if different from Report)

(9) Final rept. 1 Oct 76-31 Oct 77

18. SUPPLEMENTARY NOTES

19. KEY WORDS (Continue on reverse side if necessary and identify by block number)

Cycloconverters, Electric Propulsion, Generators, Motors, Permanent Magnets, Ship Propulsion, Thyristors

141 740

20. ABSTRACT (Continue on reverse side if necessary and identify by block number)

This study examines the feasibility of incorporating permanent magnet machines into an a-c electric propulsion system for U.S. Navy ships. This systems concept is most attractive using conventional generators and permanent magnet motors. The cycloconverter subsystem is designed using advanced thyristors and can be either water or air cooled. The machine-cycloconverter, many-phase or parallel three-phase connection design offers a drive system with characteristics well matched to a ship propulsion system.

DD FORM 1 JAN 73 1473 EDITION OF 1 NOV 65 IS OBSOLETE

UNCLASSIFIED

SECURITY CLASSIFICATION OF THIS PAGE (When Data Entered)

TABLE OF CONTENTS

TABLE OF CONTENTS [Cont'd]

LIST OF ILLUSTRATIONS

LIST OF ILLUSTRATIONS [Cont'd]

LIST OF ILLUSTRATIONS [Cont'd]

LIST OF TABLES

Section 1

SUMMARY

The objective of this study was to determine the feasibility of using permanent magnet generators and permanent magnet motors as components in electric propulsion systems for U.S. Navy ships. The scope of the study required a look at the complete electric drive systems, i.e., from the gas turbine input shaft to the generator, through the power conditioning system through to the propulsion motor/propeller shaft (shaft-to-shaft). To develop system performance data, nominal hull and horsepower requirements for two types of ships were used: a twin-shaft destroyer using 40 000-hp motors, and a hydrofoil ship using two 20 000-hp motors in pods.

The General Electric Company is participating in the U.S. Navy-sponsored development of superconducting d-c machines for electric drive systems aboard naval ships. This study used many of the same ship and mission parameters that were used in the Phase I superconducting machine system study. As such, some preliminary comparisons may be made between superconducting and permanent magnet machines. The basic circuit for the twin-shaft propulsion system is shown in Figure 1-1. This twin-propeller system has a rating of 40 000 hp per shaft which is generated by four 20 000-hp generators. It is assumed that General Electric LM-2500 gas turbines would be used as the drives.

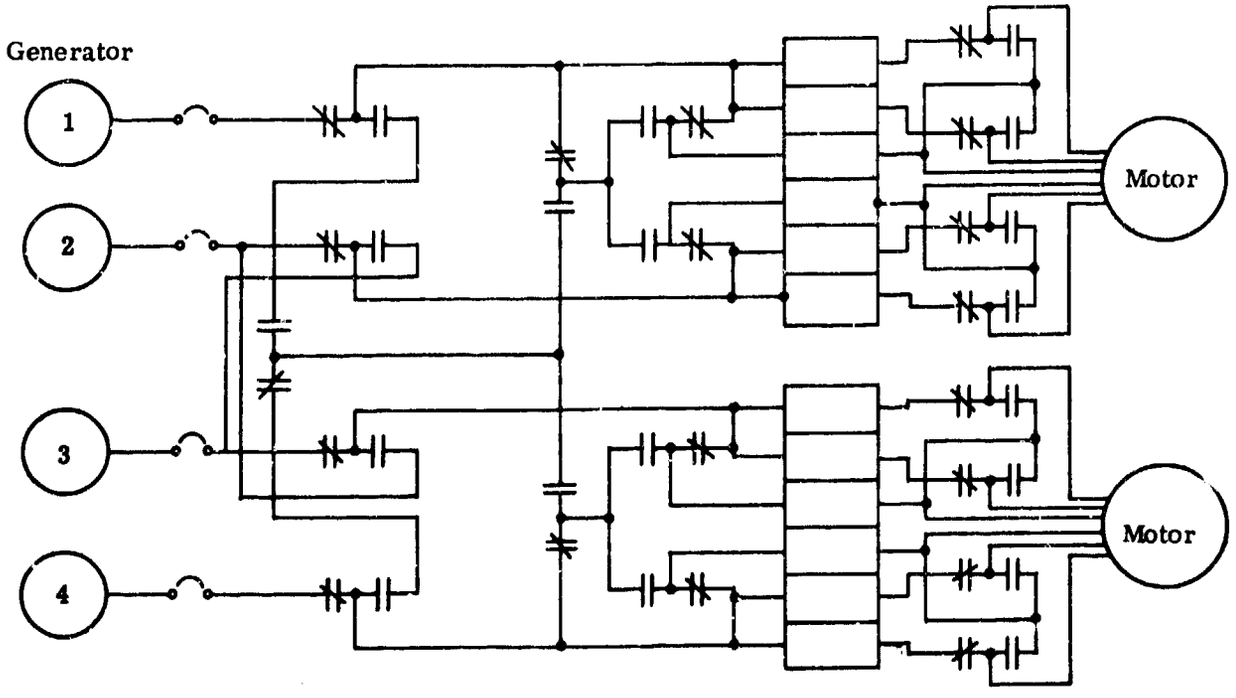

Figure 1-1. Basic Circuit for Twin-shaft Propulsion System

The basic drive system concept proposed for this study utilizes a-c generators to drive a-c motors. This necessitates variable frequency power conditioning equipment to provide the necessary system control for variable speed operation of the ship. Utilization of a cylindrical permanent magnet generator forces the power conditioner to provide for both frequency change and voltage control. The complexity of this dual function made it desirable to also examine the impact on the overall system of using a conventional electrically excited generator.

Originally, it was planned to use a n minal 320-V system having both permanent magnet generators and permanent magnet motors. This system voltage is similar to that used in the superconducting d-c system.

As the study progressed, two areas were noted that needed more emphasis than had originally been planned. It appeared that both of these areas would improve the systems performance:

- Designing a system with motor voltages between 600 V and 700 V, instead of ~ 320 V.
- Designing a system with an electrically excited a-c generator, instead of a permanent magnet generator.

The higher voltage system with permanent magnet generators requires placing SCR's in series in the power conditioning cycloconverter, which slightly complicates the electronics. However, the number of parallel three-phase circuits is reduced. This has a major effect of reducing the size and weight of the high current transmission lines between the cycloconverter and the motor.

The system design using a conventional electrically excited generator should result in lighter weight and simpler electronics over the permanent magnet generator system. These benefits may not make up for the loss in system efficiency due to the power required for excitation of the generator, particularly at cruise or lower propeller speeds.

Another concept that should also be given more detailed consideration is the disc-type permanent magnet generator. This concept involves stacking permanent magnet rotor discs and segment-shaped stator coils backed by laminated stator core iron. The optimum form factor for the disc machine is a large diameter unit which requires more magnet material than for cylindrical machines. This design may win the trade-off analysis for certain applications, most probably as generators.

At the very end of the study, an error was found in the computer program used to design the permanent magnet machinery. The effects of this error were to increase the size and the weight of the permanent magnets in the machines on the order of 2 to 1. The implications are (having run the

critical cases for the 20 000-hp motor and the 40 000-hp motor) that the weight of the machines will go up slightly. The size and the weight for the 20 000-hp generator will increase and exceed the stress limits, thereby becoming impractical with the permanent magnet materials available today. At the end of Section 3, "Permanent Magnet Machine Trade-off Designs," corrected design data for both the 20 000-hp motor and generator and for the 40 000-hp motor are described.

Based on the work in this study and at this point in time, a "best" system for a twin-shaft destroyer, using the following major components, is proposed:

• 20 000-hp Electrically Excited Generator	760 V 6580 ampere/phase 360 Hz, three phase 3600 rpm 40.5 in. dia, 54.5 in. long (frame) 15 100 lb each Exciter power: 64 kW each
• 40 000-hp Power Conditioner	Three phase, six groups of circuits Water-cooled modules 108 SCR's (nominal 2400 V) Size: ~ 230 ft^3 Weight: 4500 lb
• Transmission Lines	18 transmission cables (6 three-phase lines)
• Braking Resistors	To be specified (for crash-back maneuver)
• 40 000-hp Permanent Magnet Motor	640 V 15 625 ampere/phase 78 Hz at 168 rpm 105 in. dia, 106 in. long (frame) 104 000 lb each

An 80 000-hp, twin-shaft ship propulsion system with conventional generators and permanent magnet motors would weigh about 320 000 lb and have a system efficiency of about 95 percent at flank speed.

The hydrofoil system is simpler than the destroyer system because each generator is normally dedicated to a motor, thereby eliminating the cross-connect bus and switches. The higher rpm, smaller diameter, longer motor is a very attractive machine for pod-mounted applications. An advantage of permanent magnet motors that could be exploited is the opportunity to run the machine "flooded," eliminating cooling liquid transfer across the rotating couplings to the rotor. The permanent magnet motor

has no brushes or contacts to break down or require servicing; thus, it should be a very reliable machine. This feature applies to all permanent magnet motors regardless of size and rotational speed.

Based on the trade-off analyses described in detail in this report, the following conclusions have been arrived at:

- It is feasible and practical to consider the development of propulsion equipment using permanent magnet motors. These motors could be in the size range from 5000 hp up to 40 000 hp.
- It is not practical to consider the development of cylindrical permanent magnet generators in the range of 5000 hp to 20 000 hp. The stresses developed in the rotating portions of the generator exceed the materials capabilities for fabricating high-performance rotors at the high drive-turbine speeds considered.
- It was found that the optimum system voltage should fall between 600 V and 700 V. This voltage level is established by the level of insulation in the motors and by the voltage rating of the power control electronic devices (SCR's).
- The use of a water-cooled cycloconverter system to minimize the size and the weight of the power conditioning equipment has been assumed. This is based mainly on the 50 percent overcurrent requirement caused by the crash-back maneuver. It was assumed that the power conditioning equipment would be located immediately adjacent to the generator so that the high-frequency transmission lines will be as short as possible to minimize EMI.

Permanent magnet motors combined with conventional a-c generators and advanced power conditioning equipment are prime candidates for development in marine propulsion systems. Disc-type permanent magnet machines have been studied briefly. It was found that they would not be advantageous for the motor applications. However, their stronger rotor structure and the possibility of being able to regulate the voltage make them prime candidates for generators.

The size, the efficiency, and the weight of these components are equally competitive with other electric drive systems, except for the superconducting d-c machines system. It is accepted that the power density of the components in the superconducting d-c generator and superconducting d-c motor electric drive system is higher than any other machine concept forcasted for the forseeable future. However, reliability evaluations for these superconducting machines and support equipments are, as of this writing, not well documented. It is reasonable to believe that both types of equipment will find their place in future electric propulsion systems.

Section 2

SYSTEM ANALYSIS

The use of permanent magnet synchronous motors and generators with power conditioning equipment offers a comparatively lightweight and compact propulsion system, with a minimum of auxiliary equipment loading on the ship's service system.

The system studied here has been designed in the light of the practicality of the approach, and its special features have been analyzed. The areas where trade-offs are to be considered for a final design have been identified.

The power conditioning equipment provides many positive features:

- Separation from the synchronous tie between the motor and the generator inherent in a-c/a-c systems, where the propeller speed is controlled by the prime mover speed. The prime mover's speed can be considered separately, not as a rigid relationship. It can be operated at constant speed or controlled at speeds for fuel consumption economies.
- The resultant control provides d-c motor characteristics for the propulsion motor. Overload conditions drop the motor speed to the equilibrium value (severe overloads can cause the motor to stall) without pulling out of step, overloading the prime mover, or stalling the prime mover.

  A wide range of speed control, with the torques required for starting, accelerating, and crashback, is possible.
- Use of the power plant is flexible. By means of cross connections at the power conditioning inputs, one generator can supply both propulsion motors and provide completely independent control of the speed and the direction of rotation of each propeller, with an accompanying improvement in fuel economy.

SYSTEM ARRANGEMENT

Figure 2-1 shows the schematic diagrams of the main loop circuit for a destroyer ship propulsion system (twin-shaft, 40 000-hp each). The basic building block is to normally associate one cycloconverter module with each generator. Figure 2-2 shows each motor circuit as a nine-phase machine with two circuits per phase. The generators are correspondingly nine-phase machines with one circuit per phase. This was selected as a more practical arrangement than the use of a 39-phase motor with one circuit per phase. Thus, each generator cycloconverter supplies half of the circuits of each motor. To achieve this arrangement, a minimum voltage of 650 V

(a) Destroyer System

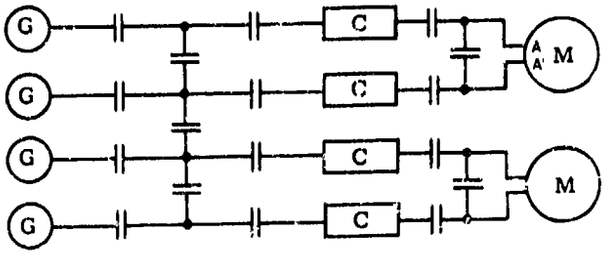

(b) Full Power

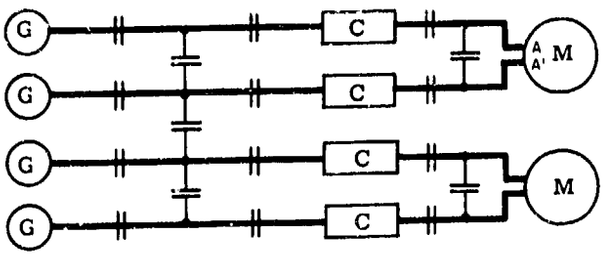

(c) Half Power

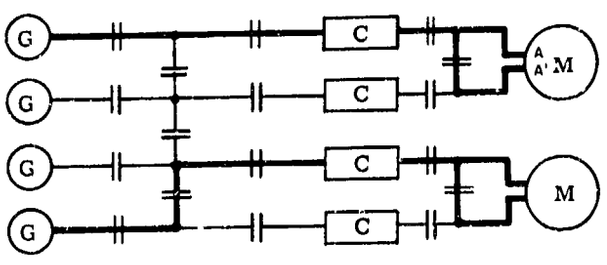

(d) Quarter Power

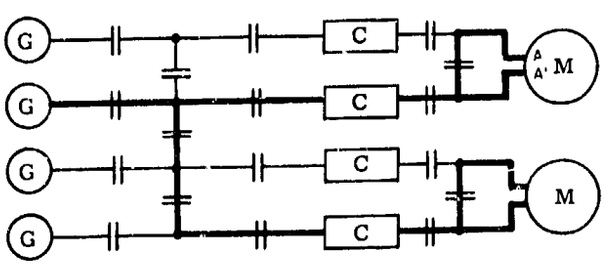

(e) Three-quarter Power
(Unbalanced loading of motors)

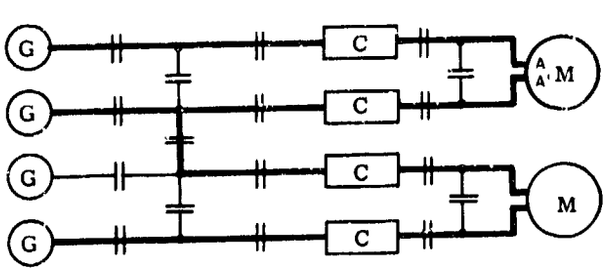

Figure 2-1. Schematic Diagrams of Main Loop Circuit for a Destroyer Ship Propulsion System

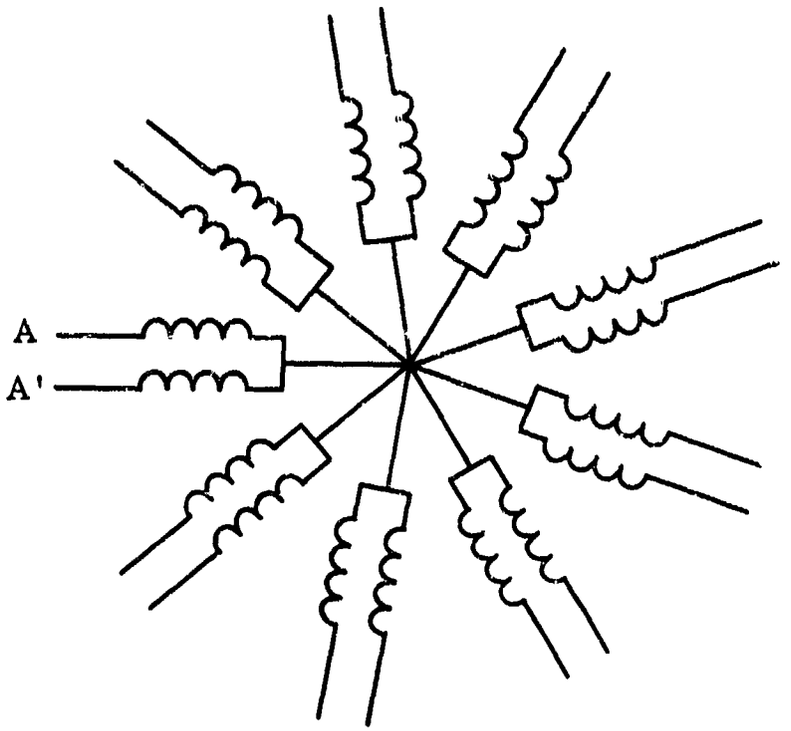

Figure 2-2. Complete Set of Motor Windings

line-to-neutral is required. Each cycloconverter would have nine phases with two cells in series in each leg. This would eliminate the necessity of paralleling thyristors and the consequent need for load sharing.

Higher voltages up to 5 kV can be obtained by use of higher voltage cells or by connecting several cells in series in each bridge leg. Series connection of the cells will require a further analysis to determine trade-offs between machine and cycloconverter sizes.

The use of switches in the main loop circuit, as shown in Figure 2-1a, provides a high degree of flexibility to the propulsion system. The switches on each side of each cycloconverter allows maintenance work to be performed while the rest of the system is still operating. Cross connections between the generators allows for the selection of any number of generators to be connected to the power supply to the two motors for four possible power modes. The cross connections at each motor are so that all of the motor circuits are energized in all of the power modes. Figures 2-1b through 2-1e show the current paths for the four power modes. This circuit arrangement allows a current unbalance in the motor circuits in the three-generator/two-motor power mode, and does not present any problem in cycloconverter control or in motor behavior.

Many other configurations of phases and circuits are possible, e.g., three-phase motors and generators each with six circuits per phase. In

this case, the currents would be balanced in the motor windings for all of the power modes.

The final selection of a system arrangement will require further detailed analysis of such factors as: 1) whether or not the generator is a permanent magnet machine or an electrically excited machine, 2) the number of thyristors in individual or paralleled circuits, 3) the voltage levels and the effects on machine size together with individual or series-connected thyristors, 4) the space and maintenance aspects of a small number of large heavy-current switches or a large number of small lower-current switches.

The hydrofoil system, shown in Figures 2-3a through 2-3c, does not have the three quarter power mode. Therefore, it does not present the same requirements for phase and circuit coordination. The other options of paralleled or individual thyristors, voltage levels, and decisions on the size and the number of main loop switches are still important trade-off determinations.

POWER CONDITIONING

The power conditioning units are three-pulse, midpoint cycloconverters. They are used to convert the generator frequency into a controlled output, such that the drive is operating in the self-controlled mode, where the motor speed directly controls the output frequency of the cycloconverter. Therefore, the motor does not operate out of synchronism, and the permanent magnet propulsion motor has the same characteristics as a d-c motor.

The motor is regulated to operate at unity power factor due to the fact that a motor lagging or leading power factor always results in a lagging power factor at the input to the cycloconverter. This mode of control is accomplished by means of a rotor position sensor which provides signals to the cycloconverter such that the rotor position relative to the stator is known at all times.

The outer control loop is a speed regulator with the speed-regulating amplifier error voltage calibrated in proportion to the required machine torque needed to maintain the set speed (Figure 2-4). A rotor-stator magnetomotive force (MMF) angle control circuit function allows the three-phase reference set to be varied over the necessary range by the speed-regulating amplifier error voltage (Figure 2-5). Thus, the magnitude of the stator current is proportional to the required torque with its frequency controlled by the rotor speed. The stator flux has a definite spatial relationship to the rotor flux; the stator flux is capable of being varied by the MMF control circuit for operation at unity power factor.

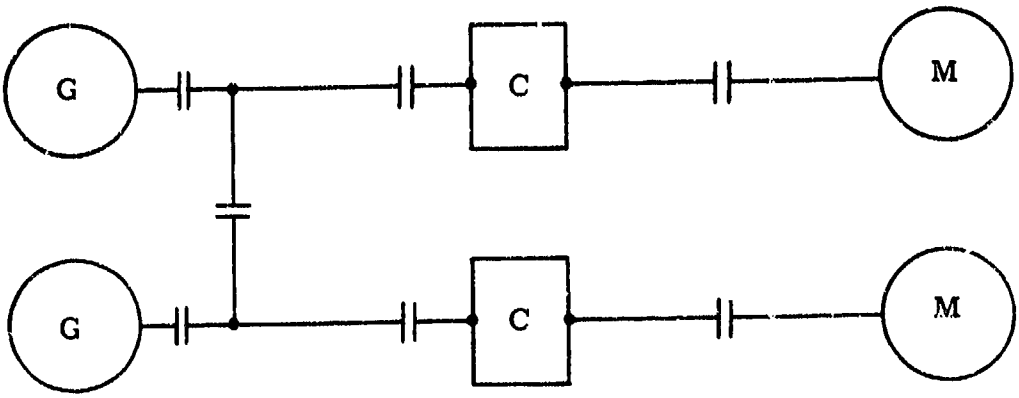

(a) Hydrofoil System

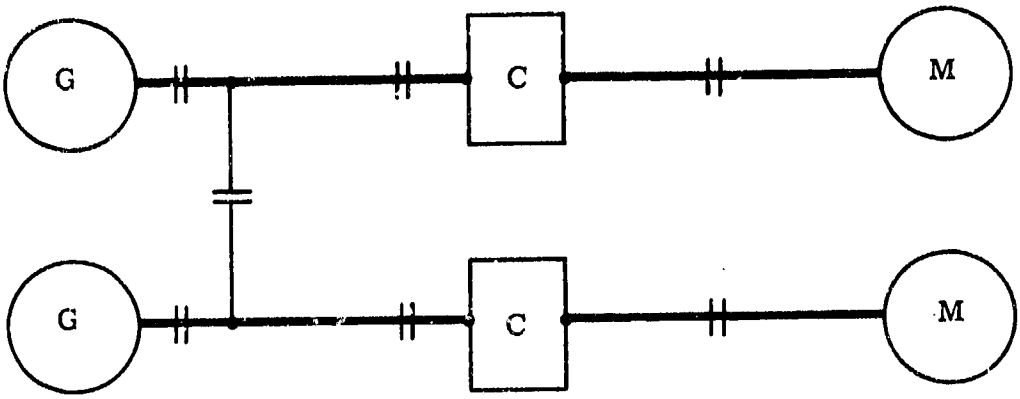

(b) Full Power

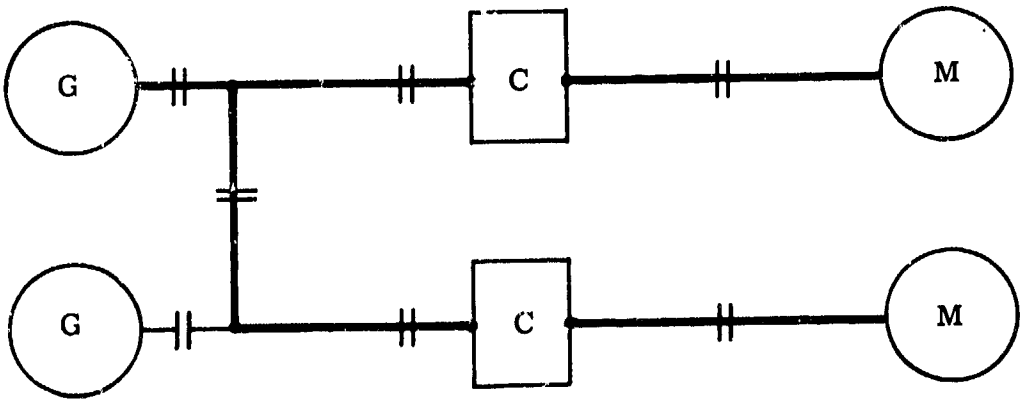

(c) Half Power, Using Both Converters

Figure 2-3. Schematic Diagrams of Main Loop Circuit for Hydrofoil Ship Propulsion System

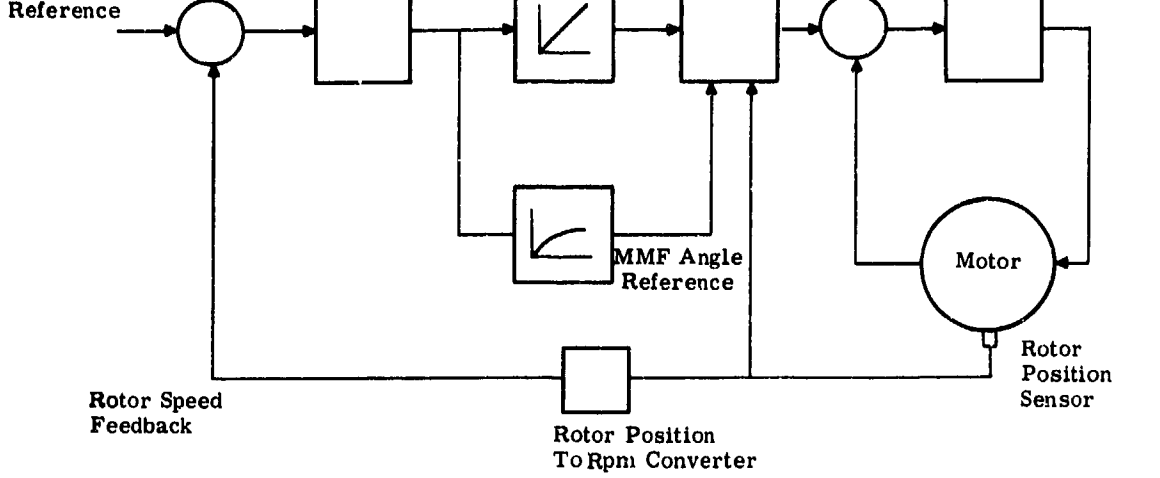

Figure 2-4. Block Diagram of System

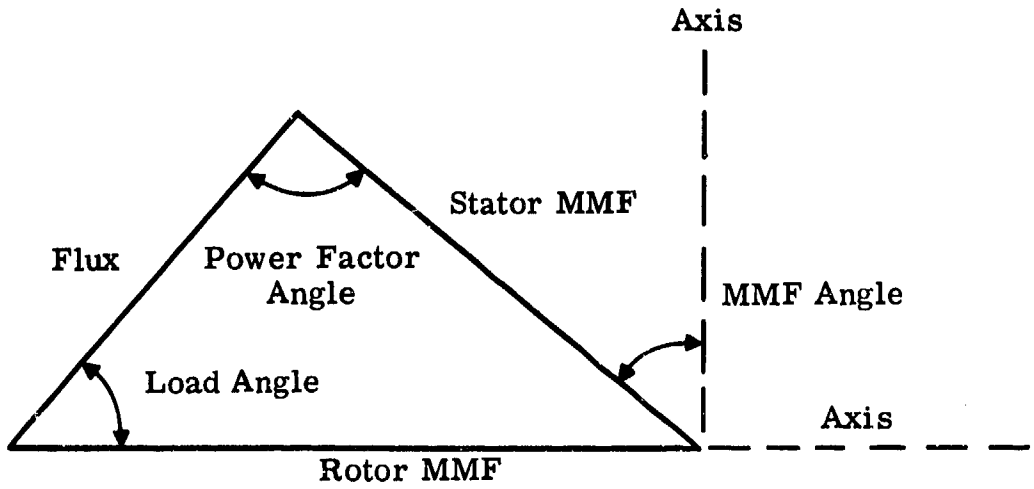

Figure 2-5. Vector Diagram Triangle

CRASH-BACK

Braking resistors are used in the crash reverse operation only and are rated for full regenerative power.

The resistor concept utilizes high-temperature resistor material and the thermal capacity of the material to absorb the regenerative energy. An alternate concept is to liquid cool the resistors. However, this does not seem to be economically justified, because the crash-back operation is seldom performed.

The gas turbine generator set has a capacity for transient and steady-state power absorption. The cycloconverter has the ability for two-way power flow. Therefore, it can be controlled to return some or all of the regenerative power from the propulsion shafts into the gas turbine generator sets. In each phase, the braking resistors would be connected to the motor with shorting switches. The resistor can be sized to dissipate any excess regenerative power over what the gas turbines can absorb. Further analysis using hull and propeller characteristics and required crash-back cycle times will be necessary before correct sizing or even the necessity of braking resistors can be determined.

PROTECTION

System protection requires investigation to determine the level, the requirements, and the methods of implementation. Many of the usual methods of fault detection can be employed; but, due to the permanent magnet machines, the implementation will be different. The cycloconverter can be supplied with fault detection for most of the system fault conditions and used to initiate a suppression circuit whereby an electronic gate suppression circuit will interrupt all firing pulses to the thyristors.

FUEL CONSUMPTION

Values of fuel consumption for the various modes of power utilization are shown for the destroyer ship in Figure 2-6 and Tables 2-1 through 2-3 and for the hydrofoil ship in Figure 2-7 and Tables 2-4 through 2-6. The data are presented in various ways and are all on a per-shaft base.

Figures 2-6 and 2-7 show actual fuel consumed per hour plotted against propeller speed for various power configurations. To avoid confusion by presenting too many curves, in Figure 2-6 the three generators applied to the two-motor mode is not plotted for the destroyer ship, only the maximum point of operation is identified for completeness. Two curves for each power mode are shown for comparison, one for constant speed and one for variable speed. The gas turbines can be operated at a constant speed of 3600 rpm. When the load decreases, the permanent magnet generator voltage rises, and the cycloconverter can operate more phased back to produce the voltage required at the motor terminals. The conventional generator can have its voltage regulated to the values required at the input to the cycloconverter.

Lower fuel consumption is possible, if the gas turbine is operated at reduced speeds for reduced loads. This permits a variable generator speed profile proportioned to the propeller speed. When matched to the turbine economical fuel operation, the propeller load curve produces relatively high generator speeds so that the full-field condition produces excess volts over the requirements. The lower excess volts over the requirements can be accommodated by cycloconverter phase-back or conventional generator voltage regulation

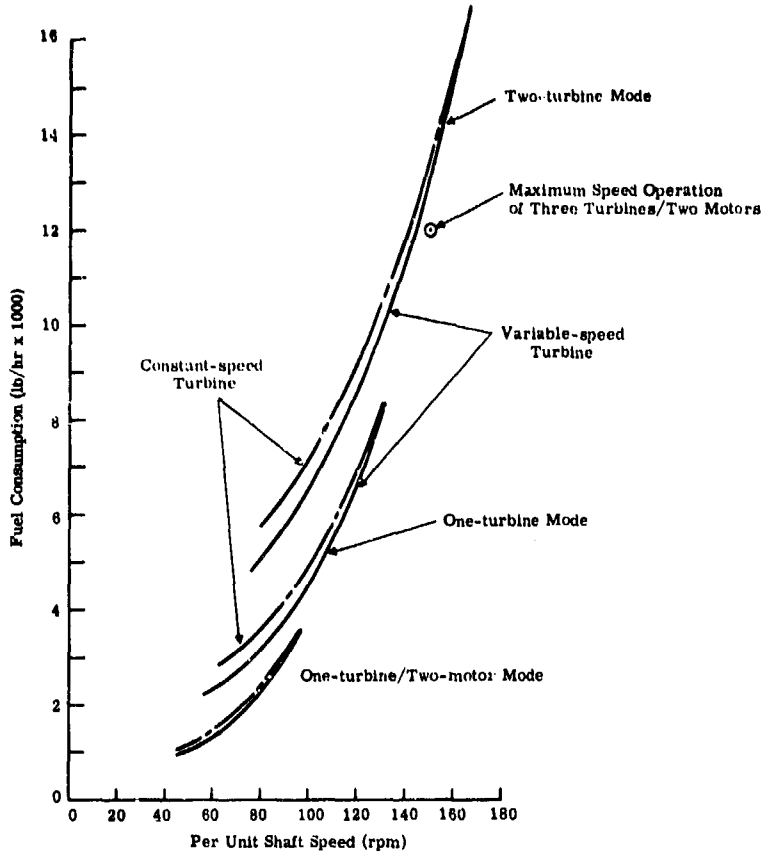

Figure 2-6. Fuel Consumption Versus Propeller Speed per Shaft for Destroyer Ship

Table 2-1

MISSION PROFILE POWER RANGES FOR DESTROYER SHIP

Power Mode	Average Fuel Consumption Per Shaft		
	Propeller Speed (rpm)	Constant Speed Fuel Rate (lb/shp/hr)	Variable Speed Fuel Rate (lb/shp/hr)
Two Generators per Motor	146 - 168	14 002	12 700
Three Generators per Two Motors	120 - 146	9091	8789
One Generator per Motor	95 - 120	5646	5363
One Generator per Two Motors	72 - 95 48 - 72	3291 1661	3003 1399

Table 2-2

PROPULSION PLANT OVERALL FUEL RATE FOR DESTROYER SHIP

Power Mode	Propeller Speed (rpm)	Constant Speed Fuel Rate (lb/shp/hr)	Variable Speed Fuel Rate (lb/shp/hr)
Two Generators per Motor	168	0.417	0.417
Two Generators per Motor	146	0.483	0.483
One Generator per Motor	120	0.472	0.451
One Generator per Motor	95	0.610	0.574
One Generator per Two Motors	72	0.683	0.584
One Generator per Two Motors	48	1.306	1.068

Table 2-3

PROPULSION PLANT FUEL RATE AND EFFICIENCY FOR DESTROYER SHIP

Power Mode	Propeller Speed (rpm)	Overall Fuel Rate (lb/shp/hr)	Overall Efficiency (%)
Four Generators per Two Motors	168	0.417	0.95
Three Generators per Two Motors	152	0.420	0.96
Two Generators per Two Motors	125	0.432	0.96
One Generator per Two Motors	88	0.49	0.94

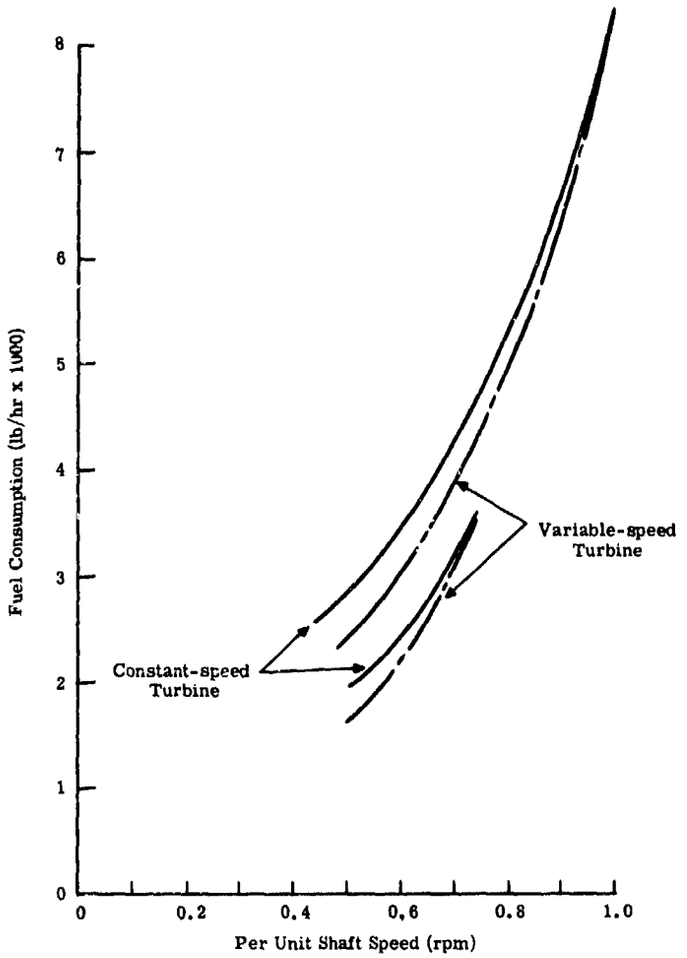

Figure 2-7. Fuel Consumption Versus Propeller Speed per Shaft for Hydrofoil Ship

Table 2-4

MISSION PROFILE POWER RANGES FOR HYDROFOIL SHIP

Propeller Speed (rpm)	Constant Speed Fuel Rate (lb/hr)	Variable Speed Fuel Rate (lb/hr)
1050 - 1200	7366	7269
900 - 1050	5440	5275
750 - 900	3615	3350
600 - 750	2260	1985

Table 2-5

PROPULSION PLANT OVERALL FUEL RATE
FOR HYDROFOIL SHIP

Power Mode	Propeller Speed (rpm)	Constant Speed Fuel Rate (lb/shp/hr)	Variable Speed Fuel Rate (lb/shp/hr)
One Generator per Motor	1200	0.417	0.417
One Generator per Motor	1050	0.465	0.452
One Generator per Motor	900	0.57	0.520
One Generator per Two Motors	750	0.545	0.485
One Generator per Two Motors	600	0.77	0.640

Table 2-6

PROPULSION PLANT FUEL RATE AND EFFICIENCY
FOR HYDROFOIL SHIP

Power Mode	Propeller Speed (rpm)	Overall Fuel Rate (lb/shp/hr)	Overall Efficiency (%)
Two Generators per Two Motors	1200	0.417	0.95
One Generator per Two Motors	890	0.426	0.96

Tables 2-1 and 2-4 show the average pounds per hour of fuel consumed when the system is operating within the various ranges of the mission profile. This could be more representative of what can actually be expected during a mission. Both the constant and variable gas turbine speed types of operation are shown for comparison.

Tables 2-2 and 2-5 compare the overall fuel rates of the propulsion system to the mission profile and include all of the motor generator and cycloconverter losses to obtain the load conditions on the propulsion gas turbines. Thus, the figures show the pounds of fuel per shaft horsepower per hour; not included are the various propulsion system auxiliaries that would be supplied from the ship's service system. These would include such items as pumps and blowers for cooling systems, lubrication oil pumps, and excitation.

Also shown in the tabulation are the overall propulsion plant efficiencies achieved at the various power modes. Again, these figures include the losses of the motors, the generators, and the cycloconverters, but do not include the system auxiliaries. Thus, the efficiencies are from propeller shaft to turbine shaft.

Tables 2-3 and 2-6 show the maximum operating speeds, the shaft horsepowers, and the overall propulsion plant fuel rates for the various power modes. It will be noted that the shaft horsepowers obtained are not the full values expected. For example, in Table 2-2 the one-generator-per-motor mode does not provide half horsepower. The reason for this is based on the use of the motor saturated characteristic curves, where the current contribution, from each generator, in any particular power mode will determine the motor speed. To reach the full available power in all of the modes, the generators will have to be designed for a slightly higher current than the value obtained based on the full-power design point.

CONCLUSIONS

Propulsion equipment utilizing permanent magnet motors and either permanent magnet or conventional generators with cycloconverter control offers an eminently practical power plant that provides a remarkably efficient, flexible, and reliable system.

Further detailed investigations are required in the many trade-off areas to determine the optimum designs and the equipment selections for a final hull/plant coordinated design.

The major areas of trade-off, in addition to those identified in the specific equipment description sections, are:

- Voltage levels
- Individual or parallel thyristors
- Machine phases and circuits
- Crash-back resistors
- Turbine speed control
- System protection
- Maximum values of intermediate power levels

Section 3

PERMANENT MAGNET MACHINE TRADE-OFF DESIGNS

INTRODUCTION

The objective of this propulsion systems study is to study the feasibility of using permanent magnet (PM) machines. Trade-off studies have been performed to establish practical permanent magnet motor and generator designs for several specific machine ratings. The objective is to establish machine designs that are of optimum size, weight, and efficiency and are compatible with the system's requirements. The drive system will consist of a gas turbine directly coupled to an alternator that, through a cycloconverter, drives the propulsion motor.

This part of the study concerns itself with permanent magnet machines for the motor and generator functions as well as the alternative case of a permanent magnet motor with an electrically excited, wound-rotor machine as the generator. Initial system considerations indicated that it may be beneficial to perform the voltage regulation function in the alternator rather than in the cycloconverter. Voltage regulation is impractical in a high-speed permanent magnet alternator, thus a high-speed, wound-rotor machine will be considered.

Furthermore, a section that considers a different type of permanent magnet machine (the disc-type, permanent magnet machine) has been included. Since complete designs of this type of machine would go beyond the scope of this study, only electromagnetic sizing and trade-offs were considered. This should be sufficient to assess this new type of machine in comparison to the conventional cylindrical-type permanent magnet machine.

BASIC SYSTEM CONSIDERATIONS

The scope of this study is to answer the question whether permanent magnet machines are feasible and practical with respect to ship propulsion applications. Several system parameters (e.g., voltage level and current level (for constant power) in the system) have relatively little effect on the size of the electrical machines even though they are very important for the system. The voltage, once it exceeds about 700 V line-to-neutral, will increase the machine size by a few percent because of the added insulation, depending upon the voltage level.

For that reason, when sizing the machines, the voltage levels chosen are set for convenience and do not represent final values for an actual system. The 320-V motor voltage is convenient because at this level one

SCR, of presently available types, can handle all of the voltage (current and frequency) in the cycloconverter. Double voltage would require two present-day production SCR's in series in the inverter. When establishing the generator voltage requirements, the cycloconverter is treated on an ideal basis which can be represented in a circuit diagram as shown in Figure 3-1.

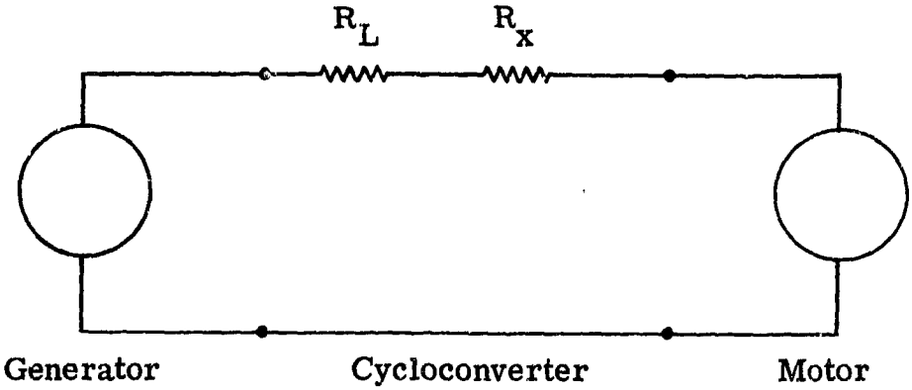

Figure 3-1. Single-phase Equivalent Circuit of System

R_L in the converter represents the losses in the semiconductors and in the main current path. R_x is a wattless resistor that represents the voltage losses in the converter due to wave shaping and commutation. Thus, the generator voltage in the study will reflect the voltage losses in both resistors but not the voltage changes between input and output due to the cycloconverter connection being utilized. These considerations will only be performed for the system portion of this study. Thus, actual voltages for a real system will be different from those used for the motor and generator study. However, selecting the number of turns per phase in both machines will allow adjusting the machine voltage levels.

BASIC DESIGN AND TRADE-OFF CONSIDERATIONS

Designing any rotating electrical machine requires balancing a multitude of independent and interdependent parameters to achieve a reasonable design. To perform trade-off studies on this basis is considered a very uneconomical procedure. Since trade-off study results indicate trends, most of the factors whose contributions are considered insignificant, as far as their range of variation is concerned, can be eliminated.

The resultant calculation method will consider the active motor area, where the windings are located, as a space filled partially by copper, partially by insulation material, and partially by laminated iron. The end-turn extension is calculated based upon the pole geometry, while the stack length and the yoke iron are calculated based upon the amount of flux in the machine.

The permanent magnet geometry in the rotor is carried to such a detail that realistic leakage flux calculations are possible. The structural parts in the rotor and the stator are included in a generalized fashion in order to obtain machine weight information.

The computer program used to carry out the trade-off calculations calculates machine parameters based upon a given voltage and current level. However, this is done for convenience in order to see the effects of the number of turns per phase, and not to indicate that the machine design is fixed and only that voltage level can be accepted. The per unit values of the machine reactances and resistances should not be dependent upon the potential (voltage) level unless more insulation is required! This generally happens for voltages above 700 V to 800 V. The saturation effects are taken into consideration through an increase in air-gap length.

The computer program used for this study was developed on General Electric funds. It is set up to perform machine synthesis in contrast to design analysis. This is accomplished by automatically varying two of the independent parameters until the specified performance goals are achieved. The independent parameters are the stack length (length of laminated core in the axial direction) and the magnet width in the radial direction, the magnet width in the circumferential direction (to some degree), the rotor outside diameter, the number of turns per phase, the per unit pole arc, the ratio of air-gap length to pole pitch, and the current density. The flux density levels in the machine are set at maximum practical levels.

The stack length (symbol Hi) is used to adjust the voltage and thus the power capability of a machine which is fixed in the radial dimension. The magnet width in the radial direction (symbol Hm) is utilized to keep the flux level in the air gap and the stator teeth within a prescribed range. The other independent parameters are varied externally. In some cases, the per unit pole arc is varied automatically to result in the lowest weight machine for a set of given parameters.

The program is equipped with various decision-making features that will allow it to change Hi and Hm in such a fashion as to possibly result in a proper design. The iteration process used employs the Newton-Rapson method for both variables separately. This results at times in convergence problems which, for their solution, would require more advanced multivariable iteration methods. These convergence problems plagued mostly the generator design.

A brief performance analysis program for the unsaturated machine allows the establishment of the maximum power point of the machine as well as to gain some basic performance information. Even though the saturation level is only considered for the full-load point design (through a constant air-gap increase), the program gives useful partial load information if one

considers the possible effects of saturation. This will be discussed in more detail for the individual machines.

MAGNET PACK FOR CYLINDRICAL-TYPE PERMANENT MAGNET MACHINES

All machines discussed previously and below require magnet sizes that exceed, in at least one dimension, the manufacturing capabilities for the rare earth magnets. Therefore, all of the rotor magnets have to be assembled from smaller magnet blocks in one or more directions.

All four machines feature a rotor construction in which the rotor is built up from rings that are either fastened to each other and to the shaft extension or assembled to a shaft. Thus, in the axial direction, a baseline division of the magnets exists. However, since the maximum producible magnet size is about one to two square inches in cross section and one inch in length, the magnets in one pole section in a motor ring have to be assembled from smaller magnets.

At present, it is anticipated that the magnets will be assembled into the rotor ring in the demagnetized condition and held together either by a combination of epoxy glue and mechanical compression for low-stress machines or by mechanical compression alone for high-speed and thus high-stress machines. Magnetization of the magnets will take place after each ring has been completed, since at that stage magnetization of high quality magnets can be handled with relative ease. Magnetization of a complete rotor is only possible if a superconducting magnetization coil can be placed around each magnet at that stage of assembly.

The individually magnetized rings will require special fixturing for assembly into one rotor. Similarly, special fixturing and precaution will have to be used when assembling the rotor into the stator. This can be done in two ways:

- For large diameter machines -- the stator windings can be arranged in such a fashion that the stator can be split into two half-sections. In that case, the rotor will be lowered into the lower stator half and supported. The upper stator half-section will be added subsequently with proper fixturing and support.
- For smaller diameter rotors -- sectioning of the stator may be impractical. In that case, the rotor will be slid into the stator and Teflon® -coated distance pieces will be used to maintain an even clearance around the rotor before the bearings are assembled.

® Registered trademark of the E.I. deNemours duPont & Company, Inc.

The difference between permanent-magnet excited machines and electrically excited machines is only to be found for the unexcited machine. In operation, both types of machines show the same magnetic forces.

40 000-HP MOTOR

TRADE-OFF DESIGNS

The design program provides data for a complete machine. But, the design of the frame, shaft, bearings, and mechanical support structure is done on a simplified generalized basis that prevents designing the mechanical parts for minimum weight. For a given torque rating, the different machine configurations would be treated equally when judged for minimum weight, based upon the generalized mechanical design. It should be pointed out again that the final weight, which should be somewhat lower than given by the program, will only be obtained after a more specific design of the support structure. This will be done after the optimum machine configuration has been selected.

The speed for maximum power output for this motor is fixed at 168 rpm, which automatically specifies the torque at this speed. The 150 percent over-torque requirement will be dealt with later. Since the electromagnetically developed torque is a direct function of the ampere-turns-flux product of the electrical machine, this product is also fixed. By varying the amount of flux in the machine or the number of ampere-turns, different machine configurations can be obtained for the same output power. Emphasis on high flux results in a heavy but low reactance machine, while a high number of turns results in a lower weight but a higher reactance machine.

A high reactance machine also means a larger portion of the magnetization (on the rotor) will be necessary to overcome the demagnetizing action of the armature or load current. This demagnetizing action is further influenced by the operating power factor of the machine: a lagging power factor would reduce the total excitation requirement, while a leading power factor would increase it. It can be shown that the optimum power factor for minimum motor weight lies in the range of 0.98 to 0.96 lagging. However, in this application one would not operate the motor at the optimum power. factor because:

- Any power factor other than unity will generally penalize the generator, since a significant increase in kVA capability of the generating machine will be required.
- The weight difference for unity power factor operation and optimum power factor operation is insignificant.

The rotor diameter is a second important parameter that influences the size and the weight of the machine. In general, an optimum diameter exists, but a detailed analysis has to prove that a practical machine can be built at

that diameter. Other important parameters are: the number of pole pairs and thus the frequency, the ratio of air gap length to pole pitch, the winding current density, and the ratio of pole arc to pole pitch. The latter will always be selected to result in the lowest weight machine. The magnetic flux density in the various sections of the machine will not be considered a parameter, since both thermal limitations (because of iron losses) and saturation limitations influence the selection of practical flux densities. As mentioned before, maximum practical values have been selected.

The current density influences weight and losses in the opposite way, in general; e.g., high current density results in a lower weight but higher loss machine and vice versa. Practical values depend upon the efficiency requirements and the cooling capabilities.

The ratio of air gap length to pole pitch is a magnetic parameter that influences the synchronous reactance level as well as the amount of excitation--and thus the amount of magnets--necessary to achieve a specified air gap flux density.

The number of pole pairs determines the frequency of the machine at a given speed and thus influences the iron losses as well as the synchronous and leakage reactance level. Indirectly, it also determines the size of the individual magnets, since it enters into the leakage flux calculations and determines how many equivalent ampere-turns have to be provided by each magnet at full load.

The arrangement of the magnets in the rotor utilizes the flux-squeezing technique described in the proposals and previous reports and publications (Refs. 1 and 2). That is, two magnets aligned circumferentially feed their magnetic flux into a magnetic pole piece that leads the flux to the air gap, and comprise one pole pair in connection with the flux-collecting pole piece at the other end of these magnets (Figure 2). The result of this arrangement is a flux density in the air gap that is higher than the flux density in the magnets, provided the total magnet cross-section area is bigger than the pole-face area. This magnet arrangement is best suited for rare earth permanent magnets in multipole permanent magnet machines.

The trade-off studies have covered the following ranges for the individual parameters:

Turns per phase, turns	3 to 6
Rotor outside radius, RR	38 in. to 60 in.
Number of pole pairs, PP	12 to 28
Number of poles	24 to 56
Current density, CD	3000 A/in.^{2} to 9000 A/in.^{2}
Air gap length to pole pitch ratio, GPTP	0.010 to 0.05
Pole arc to pole pitch ratio, PUPA	0.44 to 0.72

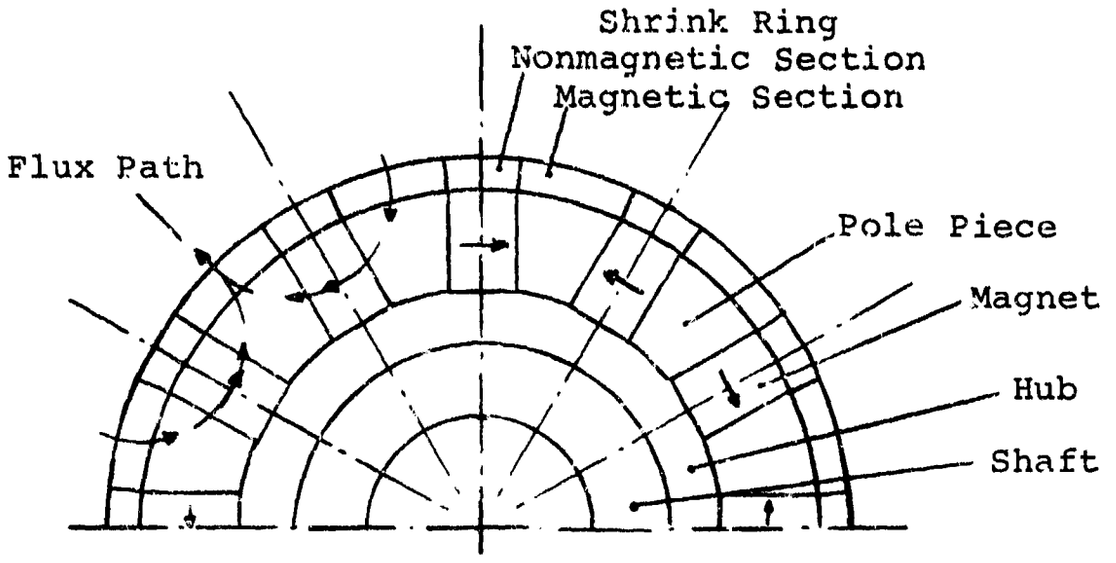

Figure 3-2. General Rotor Construction

The trade-off design computations cover the complete range of the parameters. From these computation results the following machine characteristics are plotted as shown in Figures 3-3 through 3-6 as well as listed in Table 3-1:

	Symbol	Units
Total machine weight	WTOT	klbs
Electromagnetic weight	EMW	klbs
Total electromagnetic losses	PTOT	kW
Overall frame diameter	ODFR	inch
Leakage reactance	Xsig	10^{-3} Ω
Synchronous reactance in quadrature axis	Xaq	10^{-3} Ω

Table 3-1

MACHINE PARAMETERS VERSUS (GAP/POLE PITCH)--RATIO

Parameters	CD = 6000 A/in.^{2} / RR = 44 in. Turns = 5 / Pole Pairs = 24				
Gap/Pole Pitch	0.01	0.02	0.03	0.04	0.05
Total Weight, klb	128	129	129	129	130
Total Losses, UW	645	655	643	653	646
Synchronous Reactance q-Axis, mR	24.7	13.5	9.50	8.18	7.05

ODFR and Xsig show very little or no change for this machine size.

The data in Table 3-1 illustrate that the gap-to-pole-pitch ratio has very little influence upon any machine characteristic, except Xaq. This indicates that sufficient magnet material can be put into the rotor geometry to meet both magnetization and armature reaction magnetomotive force (MMF) requirements. If that is not case, any one of the other parameters will also suffer since the machine will become larger. However, within the range of the parameters considered, only Xaq will be affected, which makes the ratio of air gap length to pole pitch a convenient tool to control the value for Xaq.

The curves plotted in Figures 3-3 through 3-6 show, in general, the expected behavior of the design characteristics, but one needs to assess the impact of a change in parameters in view of the overall design and systems concept. This has to be done with respect to the power rating of the machine and its per unit reactance level.

The rating of 40 000-hp output power corresponds to an electrical output rating of P_r = 29 830 kW. The voltage and current level chosen (these should not be confused with the actual levels pointed out before) of 320 V_{rms} line-to-neutral and 31 750 A per phase (three-phase basis) result in a unit impedance of X_{pu} = 0.01008 Ω or 10.08 mΩ. That means a leakage reactance of 0.7 mΩ is equivalent to a per unit reactance of X_L = 0.069 p.u. or 6.9 percent. An electrical loss figure of 1000 kW is equivalent to a loss of 3.24 percent which is equivalent to an electromagnetic efficiency of 96.81 percent.

Figure 3-3 shows the motor characteristics versus current density of the windings in the stator; current density in this study is the actual rms current density (e.g., rms phase current divided by total copper cross-section area per phase). Current densities in large commercial machines

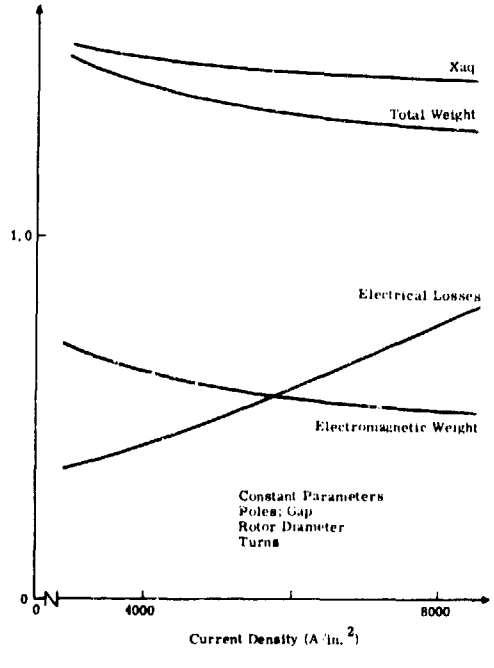

Figure 3-3.

Permanent Magnet Machine Characteristics Versus Current Density (large machine, 40 000 hp)

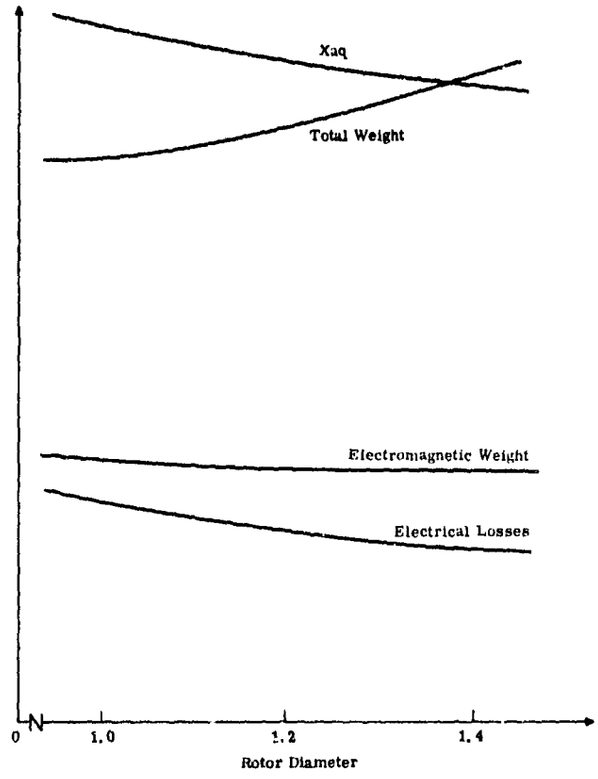

Figure 3-4.

Permanent Magnet Motor Characteristics Versus Rotor Radius (large machine, 40 000 hp). Construction Parameters: Turns/Phase, Poles, Air Gap

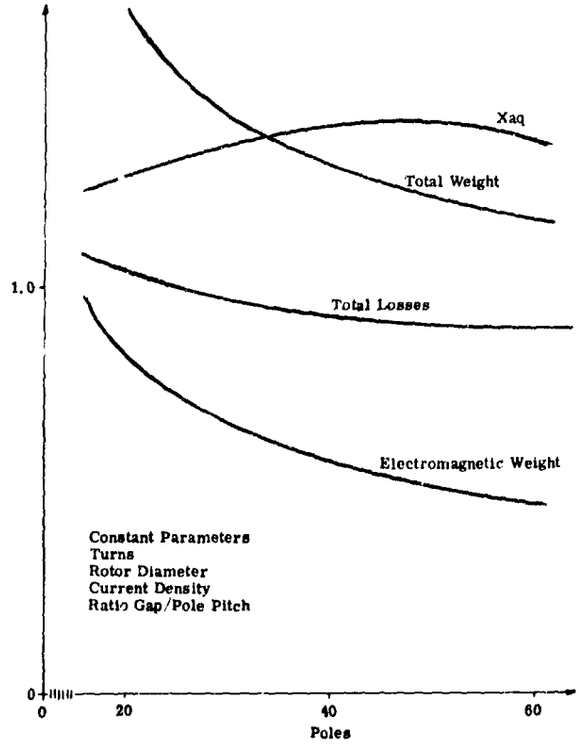

Figure 3-5.

Machine Characteristics Versus Number of Poles (large machine, 40 000 hp). Poles = 2 x Pole Pairs

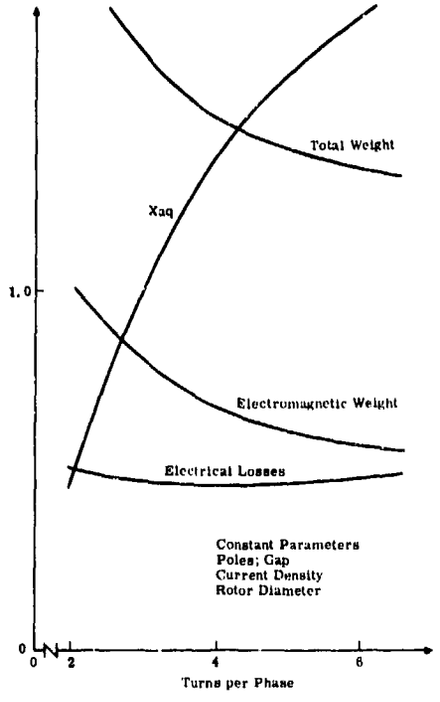

Figure 3-6.

Permanent Magnet Machine Characteristics Versus Turns per Phase (large machine, 40 000 hp)

run below 3000 A/in.^{2} while smaller commercial machines run above that number. Aerospace machinery runs generally between 9 and 12 kA/in.^{2} for air cooling and higher for oil-cooled machines. A deciding point on where to operate depends upon the required machine life and the temperature life capability of the insulation system. Low voltage aerospace insulating systems (up to 800 $V_{L\text{-ground}}$) have a 200 C life of more than ten years. Thus, the allowable current density depends upon the effectiveness of the cooling scheme in the machine.

Preliminary investigations indicate that 6000 A/in.^{2} will be within a reasonable range for this machine. This would (for a machine with RR = 50 inch, 5 turns, 48 poles, and a gap-length-to-pole-pitch ratio of GPTP = 0.0153) result in the following characteristics:

WTOT	=	134 klb	
Xaq	=	14.5 mΩ	≙ 1.44 p.u.
Xsig	=	0.52 mΩ	≙ 0.052 p.u.
ODFR	=	110 in.	
PTOT	=	584 kW	⇒ η = 0.981
EMW	=	56 klb	

Besides the fact that the weight and the synchronous reactance in the q-axis are too high, it might be interesting to compare weight and efficiency changes for a given change in current density as shown in Table 3-2.

Table 3-2

WEIGHT AND EFFICIENCY VERSUS CURRENT DENSITY

CD, A/in.^{2}	3000	6000	9000
WTOT, %	111.6	100	95.9
PTOT, %	63.4	100	145.5
η, %	98.8	98.1	97.2

The total losses change less than the current density for two reasons:

- The machine size, diameter, and length will decrease slightly with increasing current density. Thus, the resistance will increase less than linear.
- The iron losses which are part of the total losses will also decrease slightly with increasing current density.

Figure 3-4 shows the machine characteristics as a function of the rotor radius. In the range considered, the total weight decreases with decreasing radius. But since the stack length grows more than linear with decreasing radius, a minimum weight will be reached at some lower radius than 42 inches. (Note: the electromagnetic weight is already increasing in the range considered.) This also explains the increases in Xaq, Xsig, and PTOT. The general interpretation of Figure 3-4 is that, in the range considered, the decrease in weight with decreasing rotor radius is only due to the structural parts of the machine not to the electromagnetics.

Figure 3-5 shows the machine characteristics as a function of the number of pole pairs. Changing the number of pole pairs for constant operating speed will result in two effects showing opposite trends. Sectionalizing of the flux reduces the iron cross section necessary to carry the flux from one pole to the next. It will also reduce the end-turn length because the windings do not have to brace that large a pole pitch. More pole pairs will increase the frequency and related effects such as iron losses and reactance levels.

These trends are clearly shown, except for the synchronous reactance in the quadrature axis. The synchronous reactance combines the effects of changing the effective air gap, the poles, and the stack length and the effects of changing the per unit pole arc. (The pole arc resulting in the smallest machine is selected.) The losses bottom out because the gain due to shorter end turns is outweighed by the increase in iron losses. Within the range of poles considered, total weight and electromagneto weight decrease (but at a continuously diminishing rate) with an increasing number of pole pairs. There is a limit on how many poles can be put into a given rotor diameter and how small the stator slots can be made.

It is expected and will be demonstrated in detail later that 28 pole pairs represent a reasonable upper limit for the number of pole pairs, because of geometrical limitations. This particular set of curves was obtained for a constant gap-length-to-pole-pitch ratio of GPTP = 0.05. The resultant Xaq of Xaq = 6.95 mΩ ≙ 0.689 p.u. is significantly reduced when compared to the previous curves where Xaq was running between 14 mΩ and 16 mΩ or 1.389 p.u. and 1.587 p.u.

Figure 3-6 shows the machine characteristics as a function of turns. Since the input voltage is kept constant in this case, it means an increase in ampere turns and thus a reduction in flux and, generally, machine size. The weight will come down as shown while the reactance level will go up. The allowable reactance level is determined by the required dynamic behavior of the machine and by the amount of excitation that can be packed into the rotor. Furthermore, a high Xaq will result in a high voltage regulation factor which will be detrimental to the semiconductors.

Voltage regulation is also influenced by saturation. Saturation will have some negative influences on the iron losses to the point that saturation-induced harmonic air gap fields can significantly increase the iron losses. This can only be determined by a detailed analysis of the individual case. Based upon this, it is judged that five to six turns per phase is a reasonable upper limit for this particular machine size, especially since the rate of weight decrease is significantly reduced beyond this point.

The trade-off studies conducted thus far are summarized below. The lowest weight machine will be obtained for the following design:

- Low rotor radius. Limit determined by rotor dynamics and manufacturing considerations.
- High current density. Limit determined by cooling capability and thermal insulation life.
- High number of poles. Limit given by manufacturing considerations.
- High number of turns per phase. Limit given by saturation effects at light load and by voltage regulation considerations as well as by dynamic response requirements.

The next step involves the performance analysis and detail considerations for a selected machine size. Based upon the previous discussions, a machine with the parameters and characteristics shown in Table 3-3 has been selected as a reasonable candidate.

Table 3-3

SELECTED MACHINE CHARACTERISTICS

Pout, kW	29 830	
U rms L-N, V	320	
I rms per phase, A	30 730	
Phases	3	
Power factor, PF	1.0	
Frequency, Hz	78	
Pole pairs	28	
Rpm	168	
Turns per phase	5	
Xaq, mΩ	6.12 (0.606 p.u.)	
Xsig, mΩ	0.71 (0.070 p.u.)	
Rotor radius, in.	44	
Outside frame diameter, in.	98	
Stack length, in.	91	
Length over end-turns, in.	95	
Weight, lb		
Total weight, lb	122 500	
EM weight, lb	52 100	
Magnet weight, lb	8900	
Current density, A/in.^{2}	6000	at full load
Copper losses, kW	554	at full load
Iron losses, kW	90	at full load
Total losses, kW	644	at full load
Full load efficiency	0.979	at full load

PERFORMANCE ANALYSIS

Performance of the selected machine has been analyzed from three different viewpoints:

- Constant speed operation (up to full load).
- Variable-speed operation for given shaft power versus speed characteristic.
- Overload capability at reduced speed.

The original analyses were done for the unsaturated machine. One of the important design criteria found that way is the maximum output power point. For this particular machine size, it has been found that, because of the high A/in. (circumference) loading of the machine, the magnet length has to be increased over what would be the natural length (Figure 3-7). If

that is not done, the maximum power point appears at less than full-load current, resulting in a machine design that is not optimum.

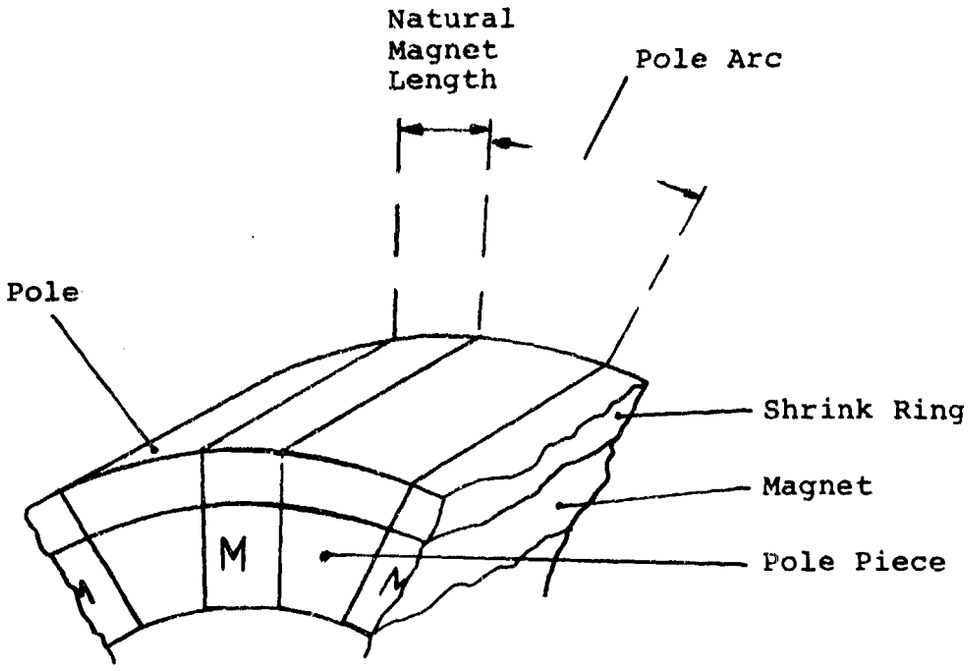

Figure 3-7. Natural Magnet Length

Adjustment of the magnet length resulted in a maximum output power (and torque) point at full-load current of 31 750 A and unity power factor. This is illustrated in Figure 3-8, which shows the machine performance curves at a constant speed of 168 rpm. The solid lines represent the unsaturated values, while the broken lines give the saturated performance curves. The voltage is reduced because of saturation which also decreases the output power. Because of the lower output power the efficiency is somewhat reduced, notably so at less than full-load current. At full-load current, the effect is minimal.

$$\eta_{unsat} = 0.9786 \qquad \eta_{sat} = 0.9782$$

As is apparent, saturation at the full-load point will keep the motor from reaching full power (2.8 percent short). This can be easily rectified by increasing the magnet length somewhat to make up for the increased excitation requirements. A magnet increase of less than 2.8 percent should be sufficient and should cause no difficulties when constructing the machine. It should be noted that, while the iron losses comprise about 11 percent of the total losses in the full-load unsaturated case and 13 percent for the saturated case, at half load the iron losses account for slightly over half of the losses (50.3 percent) in the unsaturated case and for 44 percent of the total losses for the saturated machine.

Figure 3-9 shows the performance and the required input quantities for the machine when operated at variable speed and an output power which is related to the speed as follows:

$$P_{out} = 6.29 \times rpm^3 \ [W]$$

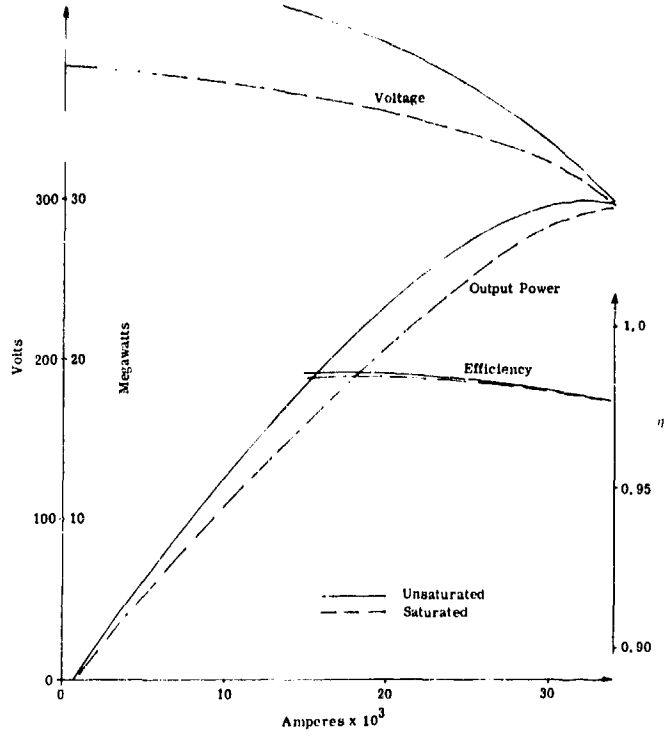

Figure 3-8.

Permanent Magnet Motor Performance at Constant Power Factor (PF = 1.0) and Speed (168 rpm) (40 000-hp machine)

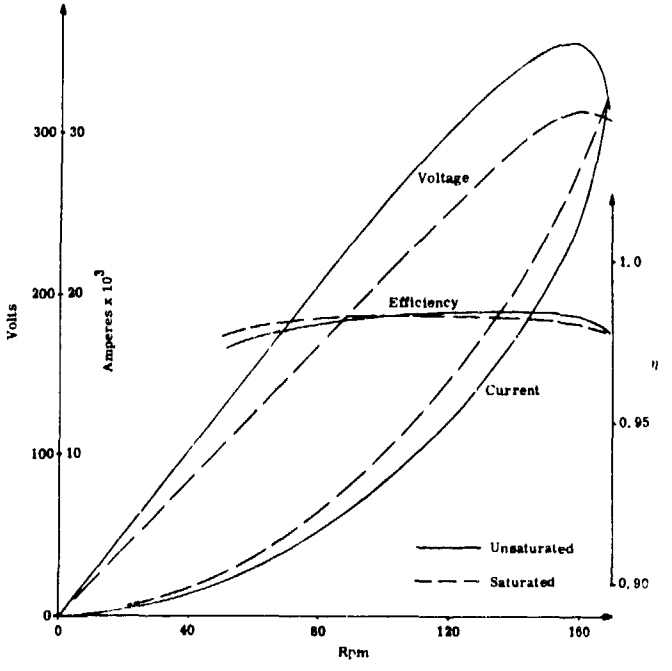

Figure 3-9.

Permanent Magnet Machine Performance for Pout = $6.29 \times Rpm^3$ (40 000-hp motor)

Generally, one would expect constant flux in the machine (as is usually the case in a d-c machine). However, as illustrated before, the decrease in armature reaction with decreasing current causes a significant increase in flux up to the level allowed by the saturation MMF requirements.

For constant flux the following relations are valid:

$$P \sim rpm^3$$

$$T = C_1 \times P/rpm \sim rpm^2$$

$$T = k_1 \times \phi \times Ia \times \cos \measuredangle (\phi, Ia)$$

$$Ia \times \cos \measuredangle (\phi, Ia) \sim rpm^2$$

$$P_{Cu} \sim I^2 \sim \left(\frac{rpm^2}{\cos \measuredangle (\phi, Ia)} \right)^2$$

$$P_{Fe} \sim \phi^2 (k_2 F^2 + k_3 F)$$

where: ϕ = machine flux

C_1, k_n = constants

P_{Cu} = copper losses

P_{Fe} = iron losses

T = torque

P = power

I = current

Since at low frequencies the hysteresis losses are a significant portion of the total iron losses, the iron losses will not show the typical quadratic characteristics with changing frequency as is experienced at high frequencies.

The presence of the iron losses will be felt especially at the lower speed and current levels. In general terms, the efficiency can be expressed as

$$\eta = 1 - \underbrace{k_a \, rpm}_{\text{(copper losses)}} - \underbrace{k_b/rpm}_{\text{(eddy current)}} - \underbrace{k_c/rpm^2}_{\text{(hysteresis)}}$$

which illustrates this trend quite well. ($k_{a, b, c}$ are constants.) If the flux

level increases because of decreased armature reaction, the iron losses will be even more significant at lower speed, torque, and current levels.

Figure 3-9 shows the actual efficiency curves for both saturated and unsaturated conditions. The percentage values for the iron losses in terms of the total losses are given in Table 3-4.

Table 3-4

IRON LOSSES IN PERCENT OF TOTAL LOSSES

Rpm	Saturated	Unsaturated
168	13.6	13.0
140	43.0	27.0
90	70.9	53.1
60	86.5	73.2

Because the iron losses are percentage wise lower for the saturated case, the actual machine will show a better efficiency at low speeds than calculated for the unsaturated machine, as illustrated in Figure 3-9.

So far, the performance characteristics have covered variable speed and constant speed performance up to rated torque at 168 rpm. It should be pointed that at unity power factor the rated load also represents the maximum load capability of the machine. The reason for this lies in the armature reaction which, with increasing current, will demagnetize the magnets and reduce the air gap flux in such a way that beyond the full-load point the voltage will decrease faster than the current will increase.

If the load capability has to be increased, either the magnet length has to be made bigger or the armature reaction has to be reduced. The change in magnet length requires a larger machine in general. The reduction of armature reaction can be affected electrically by changing the operating power factor. A lagging power factor means that magnetizing energy is fed into the machine to partially offset the demagnetizing action of the armature reaction. Since the output power is to stay constant, this requires an increase in input voltage and current. A reduction in efficiency will also result since the I^2R losses will increase.

This technique is mostly suited to cover overload conditions such as the 150 percent torque requirements for this machine. To carry this 150 percent torque requirement to full speed would require an increased VA capability of the generator. If the VA capability of the generating machine is not to exceed the requirements at full load and unity power factor operation (on the motor side), the 150 percent torque capability is limited to somewhat

less than $\frac{1}{1.5}$ of fully rated speed. The exact speed limitation will have to be analyzed later for the complete generator-cycloconverter-motor-system.

Figure 3-10 illustrates (unsaturated only) the motor input and output characteristics for 100 percent to 150 percent torque at 2/3 rated speed. The 100 percent torque point at unity power factor is equivalent to a 20 MW output at 112 rpm. To achieve 150 percent torque, the current will increase to 150 percent rated current while the voltage will increase from 216 V to 234 V (1.083). The power factor will have to be adjusted (phase-angle control through shaft-position control) to 0.94 lagging. Thus, the input power requirement at that point is 30 MW at 234 V and 0.94 lagging power factor.

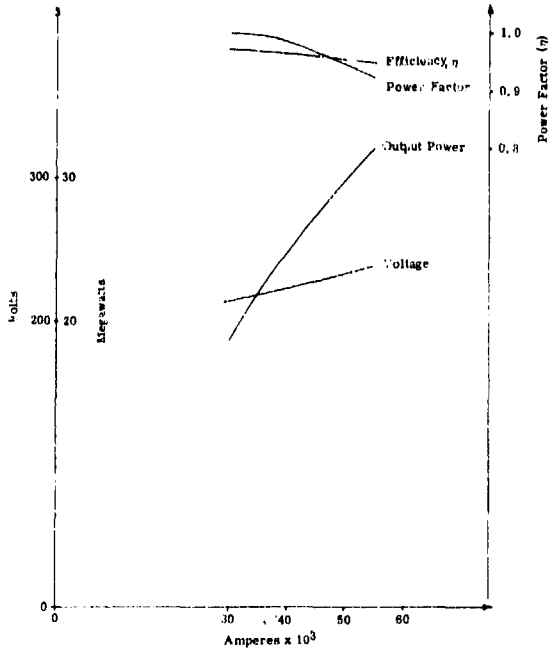

Figure 3-10.

Permanent Magnet Motor Overload Performance at 112 Rpm (40 000-hp machine)

MECHANICAL DESIGN CONSIDERATIONS

The computer program utilized to perform the trade-off studies performs only a generalized mechanical design. A detailed printout of the program for the selected machine is shown in Figure 3-11. The calculated weights are of specific interest. It is worth noting that the electromagnetic weight of the machine (ELM) is 52.1 klb, which is about 43 percent of the total weight; the bearings, weighing almost 37 klb, contribute rather heavily to the total weight of 122.5 klb.

The rotor construction is shown in Figure 3-12. Figure 3-12a shows a portion of the axial cross section with the proposed wedging and dove tail construction which is aided by through-bolts in the center of the pole-piece laminations. A stress analysis of the wedge construction shows a stress level of less than 1500 psi in the pole tip section at 168 rpm. This is considered extremely low. The low centrifugal forces exerted by the

```
INDIVIDUAL PRINTOUT FOR PM-MACHINES(M)

ELECTRICAL DATA
TERM VOLT     320.3    TERM KW   30472.0    P F      1.00
GAP  VOLT     315.2    SHFT KW       0.     F         78.
PHASE CUR   31727.4                         RPM      168.

XSIG 0.7103E-03  FL       0.      BMG 0.5997E-03  PP       28.TURNS      5.
XAQ  0.6115E-02  DELTA    0.531   BMT 0.1199E-02  PUPA    0.36 PHASES    3.
XQ   0.6826E-02  GAMA     0.603   BMP 0.1100E-02  GAP     0.296CIR     48.00
RW   0.1833E-03  COSD     0.862   BMY 0.1000E-02  GAEF    0.311  TPC      1.0
PLE  0.1564E 01  S1     720.00    CD      6000.00  KPKD    0.958  SF     0.660
KM        1.4233  KFI     0.9837  CAQ       0.6271 KF      0.92

DIMENSIONS
STATOR
RIS      44.296  RBS      46.338  ROS      47.450  ODFR    97.900
HI       90.859  OLEM     94.809  OLEC    152.986  OLMF   155.986
HY        1.112  TPP       4.937  CWDG      9.122
TS        0.387  WS        0.176  HSI       1.892  HST      0.150
ROTOR
RR       44.000  RTR      40.109  THR       0.340  THH      1.500
OLER     97.219  OLEB    152.986  OLMS    208.753
BEARINGS&SHAFT
DSHFT    27.883  ODB      55.767  DIS      22.307
MAGNETS
BR    0.000540   MYR       1.050  LM        2.835  HM       2.051

WEIGHTS
CU         7315.  SHR. R.     2535.  BEAR     36777.
CORE      17193.  POL. P.     5755.  SHFT      9604.
FRAME     19668.  MAGNETS     8878.  ROTOR    55588.
ENDB       4317.  HUB        10427.  STAT     66882.
ELAM      52103.  ROT EM     27595.  TOT     122470.

LOSSES
PCU     553.7 PFET   59276.9  PFEY   31017.0  PFE      90.3  PTOT     644.0
```

Figure 3-11. Computer Printout for Selected 40 000-hp Machine

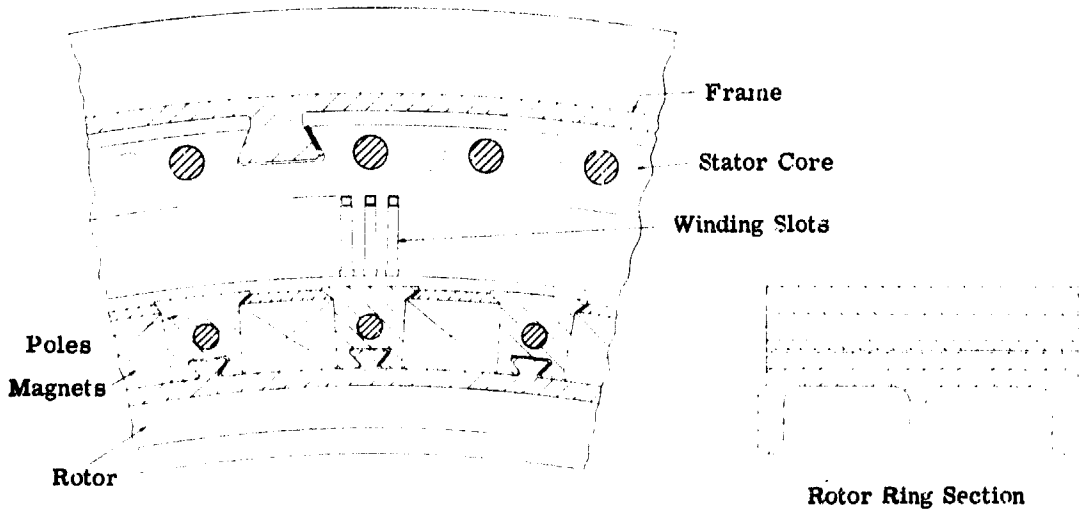

Figure 3-12. Permanent Magnet, 40 000-hp, 168-rpm Motor. Left: Axial Cross Section of Rotor (Detail Segment). Right: Detail of Rotor Hub.

magnet-pole-piece assembly allows a hub construction, as shown in Figure 3-12b, which weighs significantly less than the 1.5-in.-thick ring assumed in the computer program. The magnet assembly, which is similar to all four permanent magnet machines considered, has already been discussed.

The rotor will consist of ten identical rings; a partial cross section is shown in Figure 3-12. The rings will be positioned by a rabbet construction and held together by bolts through the inside flanges and the above-mentioned through-bolts. The two end rings will overhang the rotor end bells (a ring-spoke construction), as shown in Figure 3-13, which will be bolted to the two shaft extensions. The drive-end shaft extension has been dimensioned (25.6-in. o.d.) for a stress of 10 000 psi at rated torque. The drive-end bearing is a force-lubricated, straight sleeve bearing as used in commercial d-c motors.

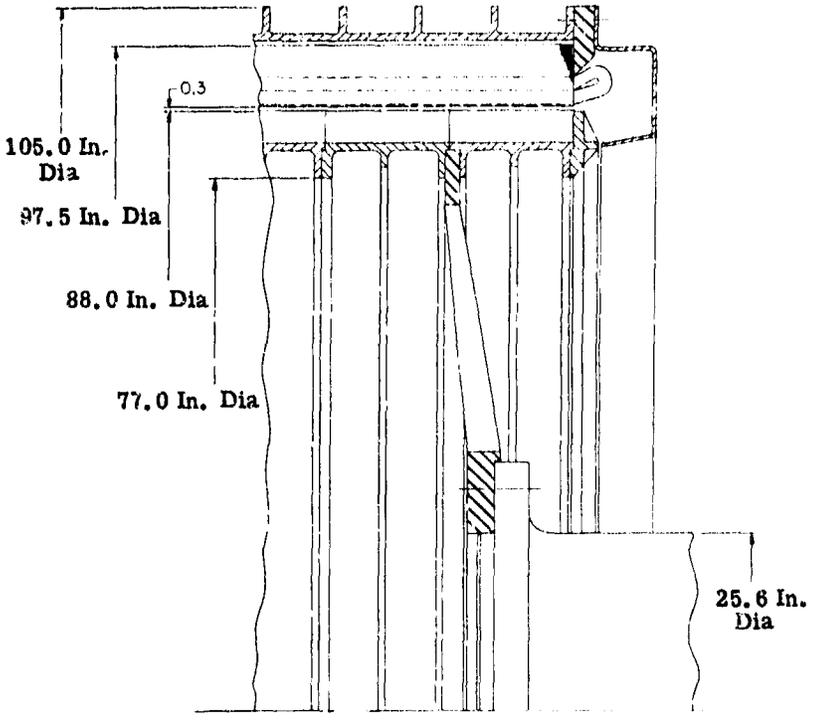

Figure 3-13. Detail of Rotor End of Permanent Magnet, 40 000-hp, 168-rpm Motor

The antidrive-end shaft and bearing also provide for locating the rotor axially. The shaft is dimensioned so that at a shock load of 25 g it can support one-half of the total rotor weight at an approximate stress level of 60 kpsi. The weight analysis of the rotor parts, based upon the changes discussed above, are shown in Table 3-5. The total weight of the rotor is significantly reduced compared to the trade-off results which for the rotor, the shaft extensions, and the bearings amounted to 83 581 lb.

Table 3-5

WEIGHT DETAILS
(In Pounds)

Drive End	Shaft	4650	
	Bearing	4500	
	End bell	1750	
Rotor	Hub	6800	
	Magnets	8878	
	Polepiece and wedges	8290	
	Missal	637	
Antidrive End	Shaft	1025	
	Bearing	4000	(Kingsbury FF23)
	End bell	2700	
Total Rotor		45 000	

The mechanical design of the stator will have to consider the cooling aspects of the windings and the core as well as the support for the stator core. It is anticipated that water or oil cooling will have to be used for this application. The conductors in the slots are not large enough to warrant hollow-conductor cooling. The frequency at 78 Hz will cause high conductor eddy current losses in large conductors. A cooling jacket around the outside of the laminations is impractical because a low temperature differential between the laminated core and the heat sink requires significant pressure levels between these two parts, which is difficult to achieve with segmented punchings. Thus, it is planned to have cooling pipes in the bottom of the slot and in various sections of the core. This will result in an increase in the outside punching diameter and the weight.

Fastening the laminations to the steel frame will be done by dovetail construction. To accommodate this, the yoke height has to be increased in order to avoid local saturation in the yoke. The space between the dovetails allows for additional holes in the laminations. These additional holes will be used for through-bolts to keep the core under axial pressure and for additional cooling pipes to take care of the iron losses. The through-bolts will terminate in press-plates which are added to the end of the core. These plates will also be mounted to the frame. The frame, when made out of a 0.5-in.-thick steel shell with reinforcing ribs welded to the outside, will be more than strong enough to carry the stator weight and the electromagnetic forces. Steel end caps will protect the winding end turns, as shown in Figure 3-14 which pictures the complete machine. The frame is mounted to the machine base separately from the bearings.

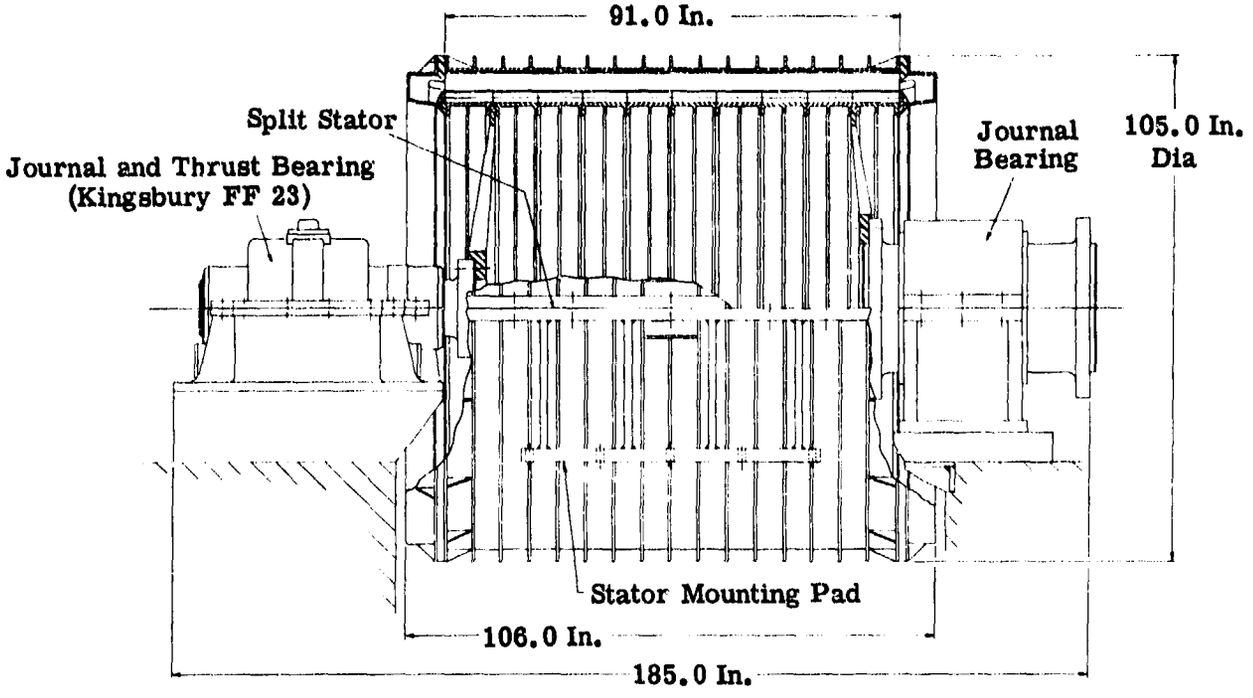

Figure 3-14. Permanent Magnet, 40 000-hp, 168-rpm Propulsion Motor (Total weight: 89 000 lb)

The frame construction and core changes resulted in new weights and dimensions.

	Weight (lb)
Frame	11 099
Core	22 433
Copper	7 315
Caps	1 900
Connections, etc.	1 253
Total Stator	44 000

The maximum dimensions of the machine are:

	Dimensions (in.)
Maximum diameter	105
Maximum length of frame	106
Maximum length of machine	185

The total weight of the machine, which has been designed in more detail than the trade-off program allows, amounts to:

	Weight (lb)
Rotor weight	45 000
Stator weight	44 000
Total machine weight	89 000

20 000-HP GENERATOR

TRADE-OFF CONSIDERATIONS

The input requirements for the 20 000-hp generator are found by combining the input requirements of the motor with the efficiency and power factor of the cycloconverter. Since there are practically no current losses, one generator will have to supply one-half of the full-load motor current. (Note: The voltage and current level are chosen strictly for illustrative purposes; they are not the final values.) The final values will be chosen according to the cycloconverter requirements and the number of turns per machine phase adjusted accordingly. The same procedure is followed to account for the voltage change due to the selected cycloconverter connection. The voltage numbers used in the design do not reflect the final generator voltage.

$$I = 16\,000 \text{ A}$$
$$U = 320/0.98/0.86 = 380 \text{ V}$$

Where 0.98 is the converter efficiency and 0.86 the generator power factor. Parameters being altered for the trade-off studies are, as before, for the 40 000-hp motor.

- Turns per phase — Turns
- Rotor radius — RR
- Number of pole pairs — P
- Current density — CD
- Gap-to-pole-pitch ratio — GPTP
- Per unit pole arc — PUPA

From the 40 000-hp motor study it was learned that in a high flux machine the influence of current density is very small. Thus, an optimum current density for full load has been chosen as CD = 6000 A/in.^{2}. The gap-to-pole-pitch ratio has been selected as large as possible (limits due to pole-form coefficient taken from a limited curve), because the reactance level, basically the commutating reactance, of the generator has to be quite low for successful interfacing with the cycloconverter.

The trends resulting from the computer trade-off studies (Table 3-6) are as expected: an increase from two to three turns per phase and an increase in the number of pole pairs from six to eight reduce the size and the weight but also increase the commutating reactance of the machine.

However, these trade-off calculations do not take into consideration the rotor stress limitations. A quick assessment utilizing previously prepared stress factor calculations shows that those machines with three turns, for example, and a rotor shrink ring thickness of 0.25 in. experience rotor stresses at top speed of more than 200,000 psi, which according to previous experiences (Ref. 1) are too high.

Table 3-6

RESULTS OF TRADE-OFF STUDIES FOR 20 000-HP GENERATOR

Weight, klb	13.9	12.4	12.3	11.4	11.9	10.7	10.8	10.3	10.6	10.1	10.7	9.72
Rotor Radius, in.	14.5	14.5	10.0	10.0	14.5	14.5	10.0	10.0	13.0	14.5	11.5	11.5
Pole Pairs	6	8	6	8	6	8	6	8	6	8	6	8
Turns	2	2	2	2	3	3	3	3	4	4	4	4
Xaq, p.u.	0.444	0.445	0.679	0.673	0.653	0.647	1.013	1.017	1.005	0.854	1.102	1.14
Hi, in.	40.1	38.9	57.1	57.6	28.1	28.3	35.8	40.9	24.1	22.5	31.1	27.9

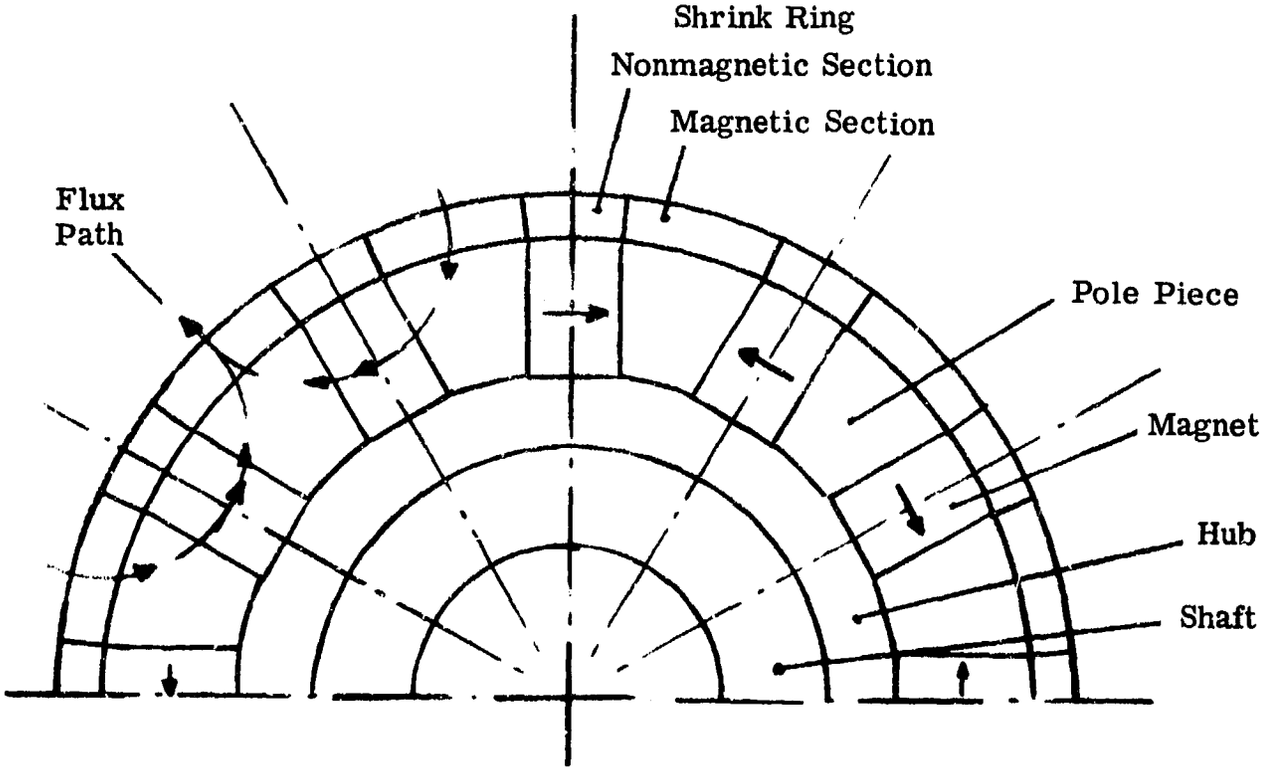

Figure 3-15. Rotor Construction with Shrink Ring

The stress in the rotor shrink ring (Figure 3-15) are calculated in (the following) simplified fashion. It is assumed that the shrink ring carries the full load of magnets and pole pieces which exert a uniform pressure to the inside of the ring. This assumption is only valid if the shrink ring is pre-stressed in such a fashion that the magnet pole piece assembly is under compression up to the maximum allowable speed. The stress then is a function of outside rotor radius (RR), shrink ring thickness (THR), magnet height in the radial direction (HM) rotor speed (rpm), and specific weights of the materials utilized,

$$\sigma = (\text{rpm} \times \text{RR})^2 \cdot 0.71006 \times 10^{-5} \times \text{Ks}$$

where: rpm is in revolutions per minute
RR is in inches

Ks is a stress factor dependent upon the geometry and the material densities. Expressing the ratio of the inside radius (RM) of the shrink ring to the outside radius as x

$$x = \frac{RM}{RR}$$

and the inside radius of the magnet assembly (RIM) to the inside radius of the shrink ring as y

$$y = \frac{RIM}{RM}$$

one can plot Ks for given material densities as a function of x and y as shown in Figure 3-16. Using these curves, one can determine the maximum allowable Ks as a function of rotor radius. With the aid of Ks, the maximum allowable magnet height (HM) can be determined for different shrink ring thicknesses. Table 3-7 shows the allowable HM values for the radii considered and for x = 0.98 and x = 0.97. These restrictions narrow the choice of generator candidates down significantly.

Table 3-7

ALLOWABLE SHRINK RING THICKNESS AND MAGNET HEIGHT FOR SELECTED ROTOR RADII

RR, in.	14.5	13	11.5	10	
THR, in.	0.29	0.26	0.26	0.20	x = 0.98
HM, in.	1.93	2.29	2.85	3.76	
THR, in.	0.435	0.390	0.345	0.300	x = 0.97
HM, in.	3.16	3.88	5.31	76.0	

	Magnet Assembly	Shrink Ring
Material properties		
Poisson Ratio	0.3	0.316
Density	0.3	0.297 lb/in.^{3}
Rpm = 3600		

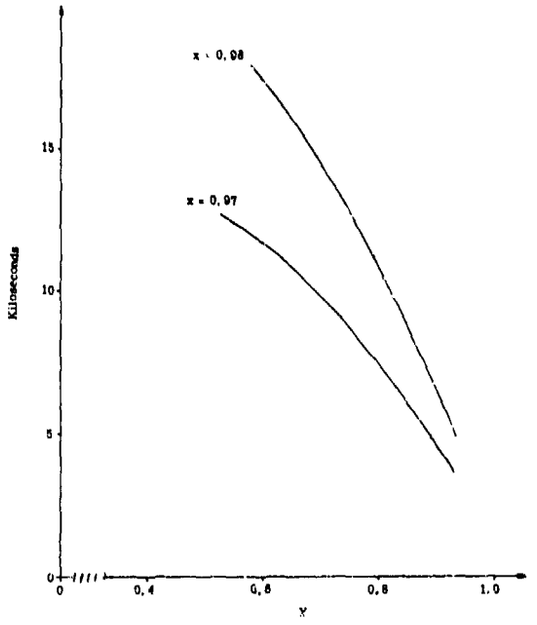

Figure 3-16.

Stress Factor Ks Versus y at Two Values of x

The thinner shrink ring (x = 0.98) reduces the maximum allowable rotor radius at three turns per phase but results in the lowest possible weights. A thicker shrink ring (x = 0.97) makes it possible to use the machines with a larger rotor radius and three turns per phase which tend to have lower reactance levels, as illustrated in Figure 3-17 but higher weights. Lowering the number of turns will allow smaller magnets because of reduced armature reaction. This results in lower reaction levels as well as increased weights. Table 3-8 lists possible machine configurations for three selected numbers of pole pairs. From these results, curves have been plotted which give a relationship between weight and reactance level, as shown in Figure 3-18.

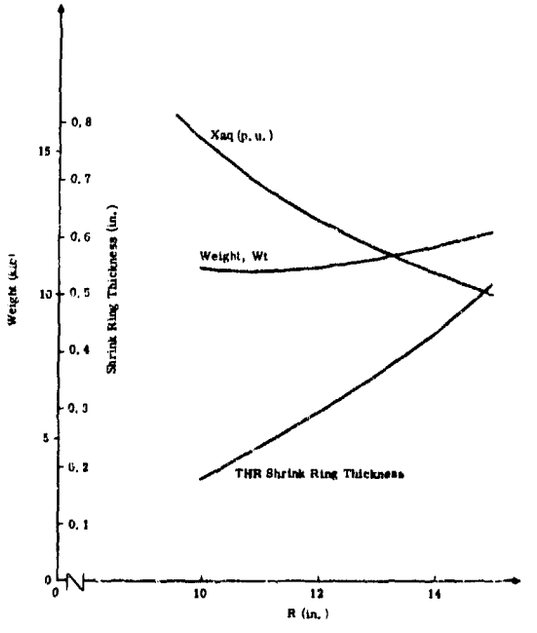

Figure 3-17.

Machine Parameters Versus Rotor Radius, R, for 20 000-hp, 12-pole, 3600-rpm Generator

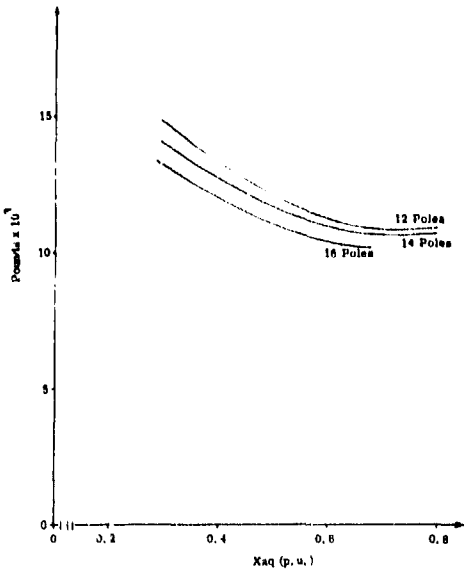

Figure 3-18.

Weight Versus Synchronous Reactance, q Axis, for Permanent Magnet, 20 000-hp, 3600-rpm Generator

Table 3-8

POSSIBLE GENERATOR CONFIGURATIONS

Pole Pairs	Turns	Rotor Radius (in.)	THR (in.)	Pole Arc (in.)	Xaq (p.u.)	Weight (klb)
6	2	10.0	0.20	0.56	0.56	12.3
6	2	11.5	0.23	0.56	0.49	12.5
6	2	13.0	0.26	0.44	0.38	13.3
6	2	14.5	0.435	0.56	0.35	14.3
7	2	10.0	0.20	0.56	0.56	11.8
7	2	11.5	0.23	0.52	0.46	12.2
7	2	13.0	0.26	0.52	0.41	12.4
7	2	14.5	0.435	0.52	0.36	13.4
8	2	10.0	0.20	0.60	0.59	11.4
8	2	11.5	0.23	0.56	0.48	11.6
8	2	13.0	0.26	0.48	0.39	12.2
8	2	14.5	0.29	0.44	0.33	12.7

So far the synchronous reactance in the quadrature axis (Xaq) has been taken as representative for the commutating reactance level, since it is most easily calculated. Actually the leakage reactance, the synchronous reactances in both axes as well as any amortisseur reactances on the rotor, representing the magnetic energy of any currents either in the solid rotor surfaces or in possible amortisseur cages, enter into the commutating reactance calculation.

A high-speed solid rotor is more easily built without an amortisseur cage. In that case, the commutating reactance will be quite close to the average value of the two synchronous reactances, since the effective amortisseur reactance of the solid pole pieces is quite high because of poor coupling and high resistance. Thus, in order to maintain the required low level of commutating reactance the synchronous reactance level has to be kept low. For this case, it is considered necessary to keep Xaq within the range of Xaq $\leq$ 0.4 p.u. The eight-pole-pair machine for this case would have the following characteristics:

P	8/F = 480 Hz
Turns	2
Xaq	0.39 p.u.
Weight	12.2×10^3 lb
THR	0.26 in.
RR	13.0 in.

A seven-pole-pair machine would have the following characteristics:

P	7/F = 420 Hz
Turns	2
Xaq	0.39 p.u.
Weight	12.5×10^3 lb
THR	0.26 in.
RR	13.0 in.

A comparable six-pole-pair machine would weigh about $13.3 > 10^3$ lb.

If an amortisseur cage is added to the rotor, which can be done at the expense of rotor complexity and cost, a higher synchronous reactance level can be allowed. The actual level cannot be predicted yet since a detailed analysis beyond the scope of this program is necessary. However, it appears that a synchronous reactance level corresponding to Xaq = 0.66 p.u. could be tolerated. The seven-pole-pair machine would feature the following characteristics:

P	7/F = 420 Hz
Turns	3
Xaq	0.66 p.u.
Weight	10.5×10^3 lb
THR	0.23 in.
RR	11.5 in.

A comparable eight-pole-pair machine would weigh 10.2×10^3 lb. The comparable six-pole-pair machine (F = 360 Hz) would have the following characteristics:

P	6/F = 360 Hz
Turns	3
Xaq	0.66 p.u.
Weight	10.9×10^3 lb
THR	0.26 in.
RR	11.5 in.

Because of the frequency requirement established for the cycloconverter (F = 360 Hz), emphasis will be put on the six-pole-pair (12-pole) machine. The selection of 360 Hz over 480 Hz (six pole pairs versus eight) carries, at three turns, a weight penalty for the generator of roughly 700 lb.

PERFORMANCE ANALYSIS

As pointed out previously, the motor requires 150 percent torque at reduced speed which at the time was set at 67 percent of rated speed. At that point, the motor power requirement amounts to 33.7 MVA at a power factor of cos ϕ = 0.94 and a voltage of 1.083 of rated voltage at that reduced speed. Taking the cycloconverter losses of 562 kW at 150 percent current and the power factor of the cycloconverter into consideration, one finds that the generator power capability at 150 percent current amounts to 39.8 MVA at a power factor of cos ϕ = 0.81 and a voltage of 276 V.

A quick check of the performance curves at 3600 rpm for the selected 12-pole machine indicates that at 150 percent current (or 24 000 A per phase) the output voltage will be down to 59 V per phase; this machine will have sufficient output at 16 000 A but not at 24 000 A. The reason for the rapid fall-off of the voltage is the limited excitation built into the rotor in connection with the high armature reaction. Magnet length can be increased somewhat but not enough to raise the voltage at 24 000 A current significantly. Armature reaction can be reduced by decreasing the number of turns per phase which also reduces the reactance level.

A design was done for six pole pairs, two turns per phase and a magnet length increased to 30 percent above the natural magnet length as determined by Figure 3-19. The voltage at 24 000 A and 0.81 PF amounts to 269 V per phase, just short of the required 276 V. An additional increase in magnet length would theoretically increase the voltage; but, practically, this would not help because the rotor-pole piece would saturate. One would have to go to one turn per phase to achieve the goal of 276 V. This would result in a significant weight penalty for the generator, which in the two turn per phase version is already heavier than the three turn per phase version, as indicated below:

P	6/F = 360 Hz
Turns	2
Xaq	0.334 p.u.
Weight	14.18×10^3 lb
THR	0.435 in.
RR	14.5 in.

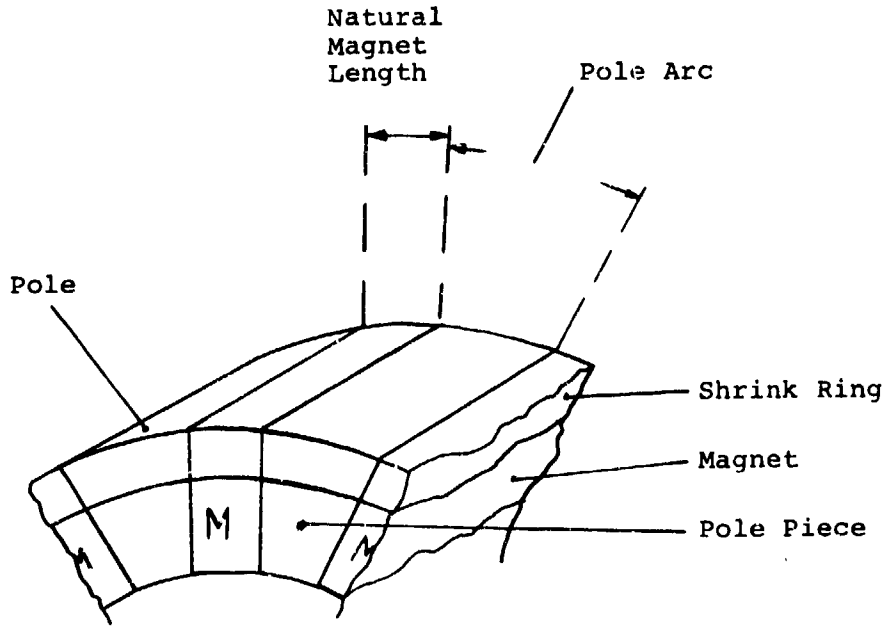

Figure 3-19. Natural Magnet Length

To consider six-pole-pair machines for smaller diameters will result in a machine that will not provide sufficient overload voltage capability, because the current loading per inch of rotor circumference will increase, which is the underlying factor for the reactance dependence, and require more magnet magnetization force than for a larger rotor diameter.

Because of the slight voltage shortcoming of the generator, 150 percent current and therefore motor torque will be possible up to 65 percent speed rather than 66.7 percent (109 rpm). This seems to be acceptable from the overall system point of view.

The next step involves the system performance at a cruise speed of 90 rpm. At this point, one motor requires 8200 A. Thus, one generator can supply the two motors at a generator current of 16 400 A per phase. The motor input voltage has been found to be Um = 190 V per phase (saturated). The comparable voltage level at the generator would be 225 V.

The generator output power at 225 V, 16 400 A cos ϕ = 0.86 (lead) is 9505 kW or 12 750 hp. The input, except friction and windage, amounts to 12 911 hp (η_{el} = 0.987). In addition, one has to add 20 hp for journal

bearing friction losses (μ = 0.015, weight of rotor 7000 lb, 3600 rpm, 6.59 in. shaft diameter) and 11 hp for windage losses at 3600 rpm for a total of ~12 950 hp. According to specific fuel consumption curves for the LM2500 marine turbine, the speed for optimum fuel consumption at 12 950 hp is around 2800 rpm (SFC = 0.45 lb total hp-hr). The change in friction and windage losses is small compared to the total power, thus it will be neglected.

Performance computations for variable leading power factor at 2800 rpm indicate that at a power factor of Cos ϕ = 0.73 leading the generator will provide the proper output power. The output voltage of the cycloconverter will be reflected to the generator at a value of 267 V. The efficiency of the generator will be

$$\eta_{el} = 0.985$$

$$\eta_{tot} = 0.984$$

This is slightly lower by about 0.002 than the efficiency the generator would achieve if voltage matching would be done by speed reduction rather than by power factor adjustment. Since a reduction in turbine speed would result in a significantly poorer specific fuel consumption, voltage regulation by power factor adjustment is preferred over voltage adjustment by speed. It should be noted that the small change in efficiency, when changing power factor, is due to the fact that the iron losses represent the major portion of the losses.

So far, all of the considerations have dealt only with the unsaturated generator. To illustrate the saturated case the same procedure has to be used, with the present design tools, as for the 40 000-hp motor. This has not been done for this case because: 1) the general trends are not changed significantly by saturation, and 2) a slight increase in magnet length can compensate for the saturation, as shown before, without influencing the total machine weight. Furthermore, the saturation is less effective, in the case of the load requirements, at the cruise load point where a reduction in power factor is used to reduce the output voltage and thus the saturation level by means of increased effective armature reaction.

To summarize the performance considerations, it should be pointed out that the machine (the major parameters are listed in Table 3-9) will meet the requirements of the operation as follows: at full speed of 3600 rpm and full load of 16 000 A per phase at 0.86 power factor leading, the input to the generator is 15.89 MW or 21 300 hp for a total efficiency of 98.68 percent including 23 kW of friction and windage losses.

This machine, the magnet length of which has been increased by 30 percent over the natural length as determined by the chosen pole arc of 44 percent, will supply 150 percent current leading power factor of 0.81 and a

Table 3-9

MAJOR GENERATOR PARAMETERS

Speed	3600 rpm	Three phases	
Poles	12	Two turns per phase	
Frequency	600 Hz	Gap	0.456 in.
X sig	4.1 percent	Xaq	33.4 percent
Rotor diameter	29.0 in.	Stator base	29.9 in.
Stack length	44.4 in.		

maximum generator speed of 3600 rpm up to about 65 percent motor speed for the crashback reversal maneuver. The input power requirements are 21 400 hp at a generator efficiency of 98.55 percent.

At a cruise point of 90 rpm motor speed, the drive turbine will operate at 2800 rpm for optimum fuel consumption and supply 12 950 hp to the generator which will convert this mechanical input power to electrical output power at an efficiency of 98.4 percent. The power factor of the generator will be 0.73 leading because of the voltage regulation in the cycloconverter to match the required motor input voltage at that point.

The generator efficiency does not change very much for those three points, because the iron losses are the major portion of the generator losses.

MECHANICAL DESIGN CONSIDERATIONS

As explained for the 40 000-hp motor, the design trade-off computer program utilizes a generalized mechanical design to accomplish the tradeoff calculations. In this section, the design will be detailed to a point that a layout can be drawn and a more exact weight prediction can be made.

The drive-end shaft diameter, as required by ship building rules, at 16 000 hp and 3600 rpm amounts to

$$D = \sqrt[3]{\frac{64 \times 20\,000}{3600}} = \sim 7.2 \text{ in.}$$

The antidrive-end shaft, which basically supports the rotor and carries the thrust bearing, has a diameter of 5.4 in. At present, the design (Figure 3-20) calls for the drive-end bearing to be a straight journal bearing and the antidrive-end bearing to be a combined journal and thrust bearing. Ball and roller bearings could also be considered for this generator, which would result in somewhat lower bearing friction losses and some weight reduction (w. 1000 lb).

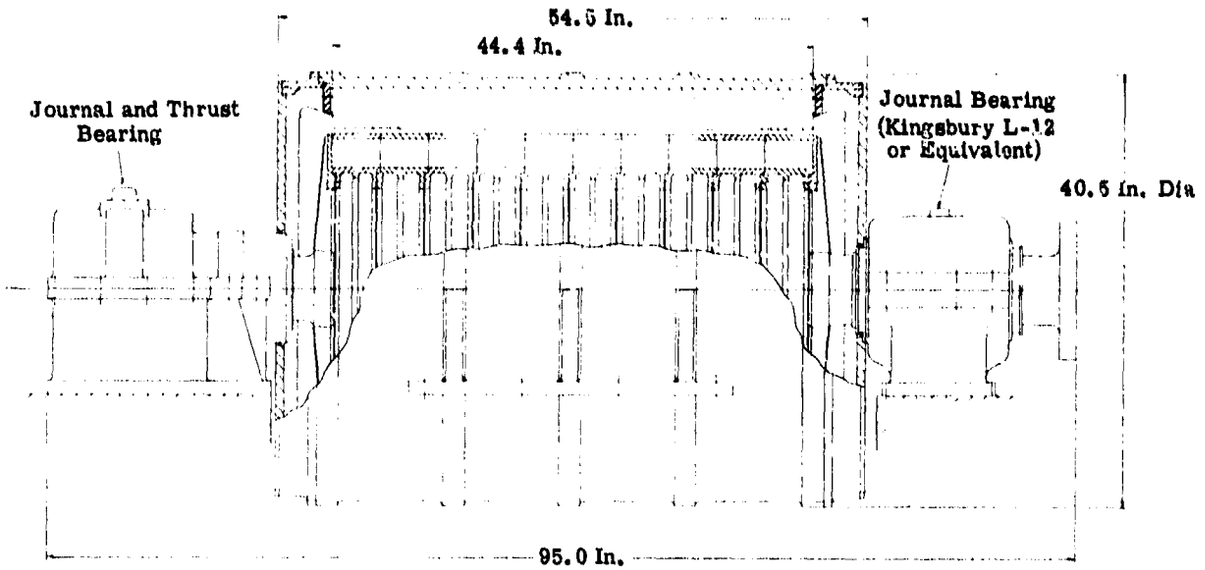

Figure 3-20. Permanent Magnet, 20 000-hp, 3600-rpm Generator (13 000 lb)

The rotor consists, as does the 40 000-hp motor rotor, of a combination of rotor ring assemblies bolted together to form the rotor, and supported by a spider construction which connects to the corresponding shaft extensions. The spider portions carry an aluminum shield in order to minimize rotor-end windage losses which, with open rotor and spider construction, could be significant at 3600 rpm.

Each rotor ring consists of a hub, the magnet-pole piece ring assembly, and the supporting shrink ring (Figures 3-21 and 3-22). The hub has to be made from nonmagnetic material such as any of the 300 series stainless steels. The pole pieces, made from magnetic steel, are wedged between the magnet packs which are basically 5.342 in. in the direction of magnetization (parellel with the circumference) and have an axial ring length of 4.437 in. by 2.470 in. in cross section. A high-strength shrink ring welded together from Inconel 718* (as a nonmagnetic material) and CTX1** (as a magnetic material capable of shrink ring stresses in excess of 150,000 psi) will hold the magnet-pole piece assembly together up to the required overspeed. The shrink ring is assembled to the rotor ring with an interference fit sufficient to maintain a compression level in the rotor ring from standstill to overspeed, thereby avoiding any stress concentration†. During this assembly, the magnets will be demagnetized. Magnetization will take place after each ring has been completed.

* Trademark of the International Nickel Company
** Trademark of the Carpenter Technology Corporation
† Air Force Aero-Propulsion Laboratory, 150 kVA Samarium Cobalt VSCF Starter Generator Electrical System (Phase 1), Report No. AFAPL TR 76-8, Wright Patterson Air Force Base, Ohio

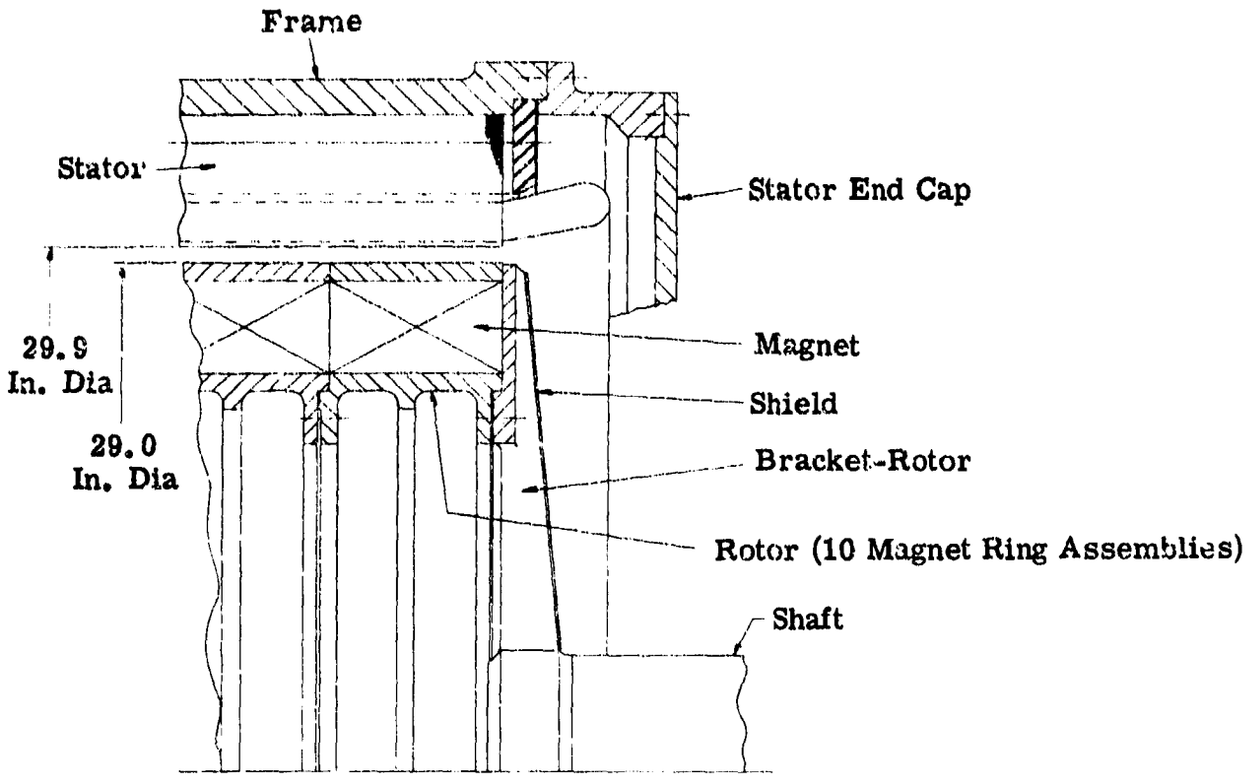

Figure 3-21. Machine End Detail of Permanent Magnet 20 000-hp, 3600-rpm Generator

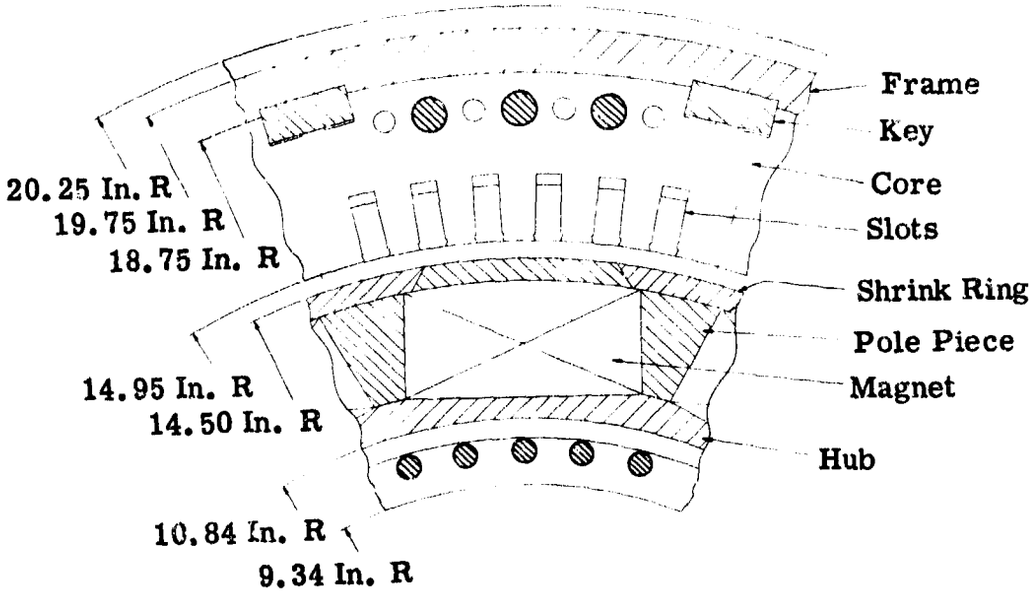

Figure 3-22. Electromagnetic Detail of Permanent Magnet 20 000-hp, 3600-rpm Generator

Assembly of the rotor will have to be done with the magnets magnetized. This will require extensive fixturing to master the repulsive forces of the magnet rings. Wooden or other nonmagnetic spacers in the 0.45-in. wide air gap that will keep the rotor and the stator separated during assembly. The stator core manufactured from single-piece punchings, which are bolted together and fastened to the frame by keys, features cooling pipes in the yoke and in the slot bottom to effectively cool the windings and the core. The frame is made from a 1-in.-thick aluminum ring with reinforcing ribs. The winding end turns are protected by fabricated aluminum end caps. The cover plates of these end caps feature a rubber seal to the bearing housings and are 0.5-in.-thick for ruggedness.

The total weight of this machine is 13 000 lb with the overall dimensions of 40.5-in. diameter, 54.5-in. frame length, and 95-in. overall length, as shown in the layout sketch. A detailed weight analysis is given in Table 3-10.

Table 3-10

WEIGHT DETAILS FOR 20 000-HP GENERATOR
(In Pounds)

Stator	
Core	3827
Copper	785
Frame	748
Hardware	855
	6215
Rotor	
Shrirk Ring	516
Hub	910
Magnets and Pole Pieces	2800
Brackets	292
	4518
Shaft Extensions	488
Drive-end Bearing	550
Antidrive-end Bearing	600
Miscellaneous	629
Total Weight	13 000

20 000-HP MOTOR

TRADE-OFF PERFORMANCE AND ANALYSES

The design specifications for the 20 000-hp motor are:

Maximum rating (continuous)	20 000 hp 450 rpm
Cruise speed	75% of 450 rpm
Torque-speed curve	$T = C \times rpm^2$
Constant C determined from rating data	

The motor is to be driven from a cycloconverter-generator system, whose maximum frequency has been fixed, as before, at 360 Hz. This limits the maximum motor frequency to 120 Hz which at 450 rpm results in a maximum number of pole pairs, p

$$p = \frac{60 \times f}{rpm} = \frac{60 \times 120}{450} = 16$$

The motor voltage level is chosen at 320 V, as was done for the 40 000-hp motor. Again, it should be emphasized that the potential level of the machine can be changed as long as the rating stays the same, without affecting the machine size, except when the insulation level has to be increased which should be done upward of 700 V line-to-ground. Chosing a voltage level is necessary to account for voltage "losses" (voltage drops) in the system. The related current level amounts to 15 700 A per phase on a three-phase basis. Subdividing the windings into more than three phases will reduce the phase current accordingly. But it will not influence the weight and the performance of the machine.

The trade-off design studies are done only for a limited range of parameters, since the trends established for the 40 000-hp motor are generally the same as for the 20 000-hp motor. Correlating the two machines, the following results for the various parameters:

1. Number of Pole Pairs -- p = 8 to 16 or 16 to 32 poles, the maximum of which is determined by the frequency limits.

2. Turns per Phase -- turns = 2 to 4. The upper limit of turns is again determined by the reactance limit put on the machine for cycloconverter operation. At the present level of design detail, this limit is more a recommendation than a limit, since only a detailed system analysis can establish limits.

3. Rotor Radius -- RR = 32 in. to 20 in. based upon peripheral velocities and results of the 40 000-hp machine.

4. Gap-length-to-pole-pitch Ratio -- GPTP = 0.06. This is done for a low reactance level based upon the 40 000-hp machine results.

5. Current Density -- CD = 6000. As discussed before, it does not appear justified to push up the current density to gain some small weight benefit without a detailed thermal analysis, which is not within the scope of this study. Furthermore, the efficiency impact has to be studied closely before recommending an increase.

6. Per Unit Pole Arc -- will be established with respect to size, weight, and reactance level of the machine.

The trade-off studies are summarized in Table 3-11. The results clearly indicate that a 16-pole-pair machine at a 20-in. rotor radius and four turns per phase with a resultant reactance level of Xaq = 0.547 p.u. will be a very attractive machine, which will also accommodate the reactance requirements of the system. The detail results for this machine are shown in Figure 3-23, which indicates a computer calculated weight of 39 000 lb. and a stack length of 91 in.

Table 3-11

RESULT OF TRADE-OFF CALCULATIONS

Pole Pairs	16	12	8
Turns Range	2 ÷ 4	2 ÷ 4	2 ÷ 4
Radius Range, in.	32 ÷ 20	32 ÷ 20	32 ÷ 20
Weight Range, klb	10 ÷ 39	79 ÷ 42	97 ÷ 48
Reactance Range			
X aq, Ω	0.0112 ÷ 0.0033	0.0108 ÷ 0.0032	0.0109 ÷ 0.0032
X leak, Ω	0.0015 ÷ 0.0003	0.0012 ÷ 0.0003	0.0009 ÷ 0.0002
X aq, p.u.	0.547 ÷ 0.162	0.527 ÷ 0.158	0.539 ÷ 0.154
X leak, p.u.	0.073 ÷ 0.015	0.058 ÷ 0.012	0.042 ÷ 0.010

Per unit Reactance

Xpu = 0.204 Ω

```
INDIVIDUAL PRINTOUT FOR PM-MACHINES(M)

ELECTRICAL DATA
TERM VOLT    320.3   TERM KW  15198.1   P F     1.00
GAP  VOLT    316.5   SHFT KW      0.    F      120.
PHASE CUR  15825.6                      RPM    450.

XSIG 0.1484E-02  FL      0.     BMG 0.5991E-03  PP      16.TURNS      4.
XAQ  0.1115E-01  DELTA   0.490  BMT 0.1198E-02  PUPA   0.60 PHASES     3.
XQ   0.1263E-01  GAMA    0.564  BMP 0.1100E-02  GAP   0.236CIR     24.00
RW   0.2904E-03  COSD    0.882  BMY 0.1000E-02  GAEF  0.252  TPC       1.0
PLE  0.2379E 01  S1    288.00   CD     6000.00  KPKD  0.958  SF      0.660
KM       1.3803  KFI     0.9985 CAQ      0.6586  KF     0.92

DIMENSIONS
STATOR
RIS     20.236  RBS     22.038  ROS     22.963  ODFR   48.926
HI      90.935  OLEM    94.077  OLEC   129.188  OLMF  132.188
HY       0.925  TPP      3.927  CWDG     6.436
TS       0.441  WS       0.202  HSI      1.652  HST      0.150
ROTOR
RR      20.000  RIR     16.098  THR      0.350  THH      1.500
OLER    97.301  OLEB   129.188  OLMS   161.075
BEARINGS&SHAFT
DSHFT   15.944  ODB     31.867  DIS     12.755
MAGNETS
BR   0.000540  MYR      1.050  LM       1.543  HM       2.052

WEIGHTS
CU        2896.   SHR. R.     1181.   BEAR      6875.
CORE      7057.   POL. P.     3572.   SHFT      1478.
FRAME     8171.   MAGNETS     2764.   ROTOR    16736.
ENDB       918.   HUB         4303.   EL M     22480.
STAT     21773.   ROT EM     11820.   TOT      39216.

LOSSES
PCU    218.2 PFRT  43726.6  PFEY  22146.9  PFE     65.9  PTOT    284.1
```

Figure 3-23. Computer Printout of 20 000-hp Motor

The unsaturated performance curves are presented in Figures 3-24 through 3-26. Figure 3-24 shows the machine's performance at 450 rpm and unity power factor. Of interest is the flat efficiency curve over a wide current range and the fact that the rated power point is also the maximum power point at unity power factor. Figure 3-25 shows the machine's performance at variable speed for an output power which is defined as $P_{out} = C \times rpm^3$. It should be pointed out that, for all practical purposes, the electrical efficiency between full load at 450 rpm and a cruise speed of 338 rpm does not change. It takes a speed decrease to 170 rpm to lower the efficiency by one percent. The different effects of iron and copper losses are responsible for the efficiency shape. At present, the machine is designed so that at full load the iron losses are about 23 percent of the total losses at the cruise speed point. If that loss number is to be changed at the cruise speed point, a bigger and heavier machine will result, especially since two-thirds of the iron losses are located in the teeth area.

Figure 3-26 shows the constant speed performance curves at cruise speed. (Note: the flat efficiency curve and the built-in torque reserve at that speed.) If any torque above 100 percent rated torque is to be delivered, this motor has to be operated at a lagging power factor in the same fashion discussed for the 40 000 motor.

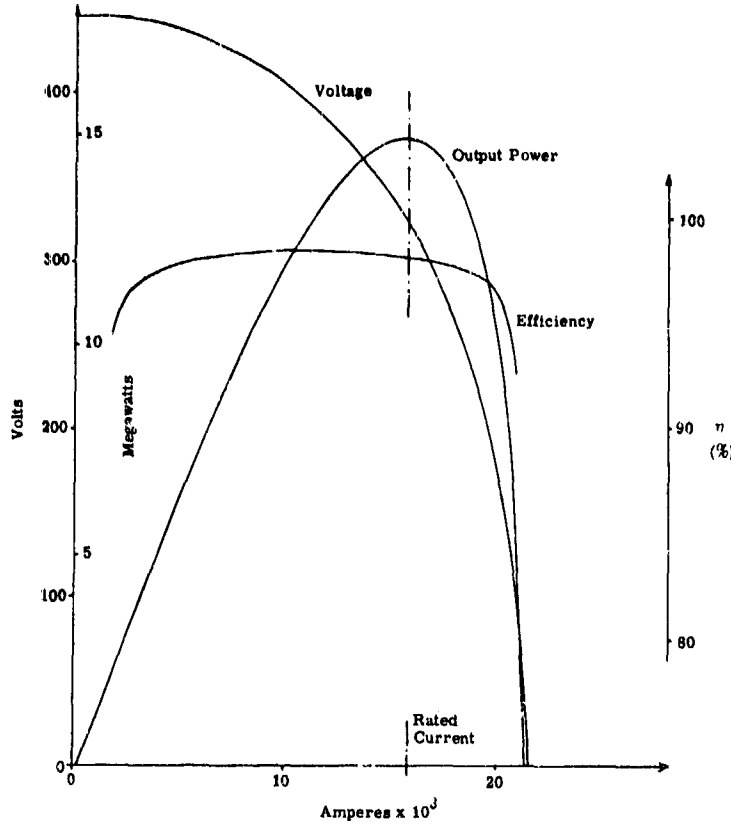

Figure 3-24.

Performance of Permanent Magnet, 20 000-hp, 450-rpm Motor at Constant Speed and Unity Power Factor

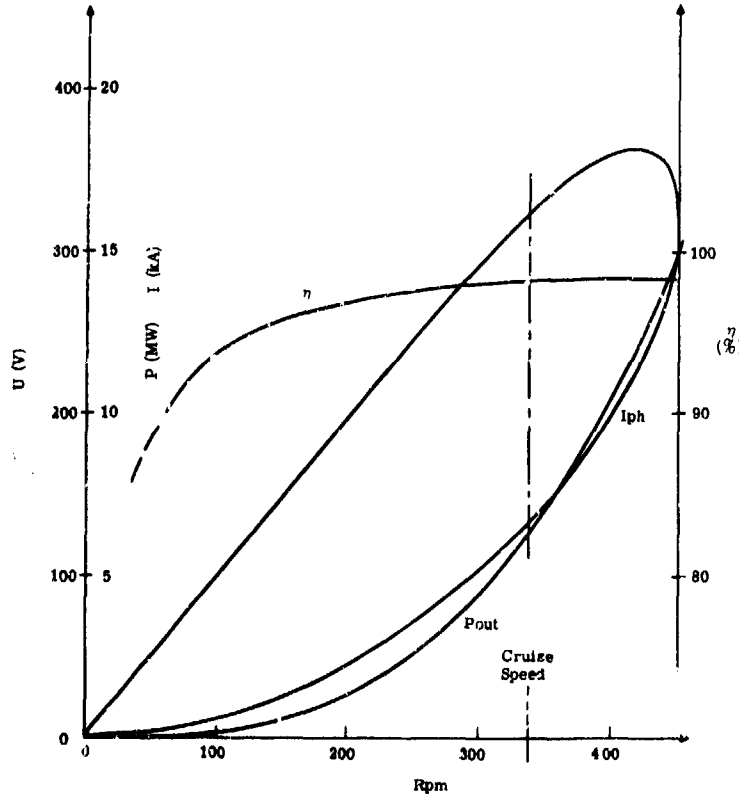

Figure 3-25.

Load Performance of Permanent Magnet, 20 000-hp Motor. Pout = 0.1637 = rpm^3 at 1.0 PF

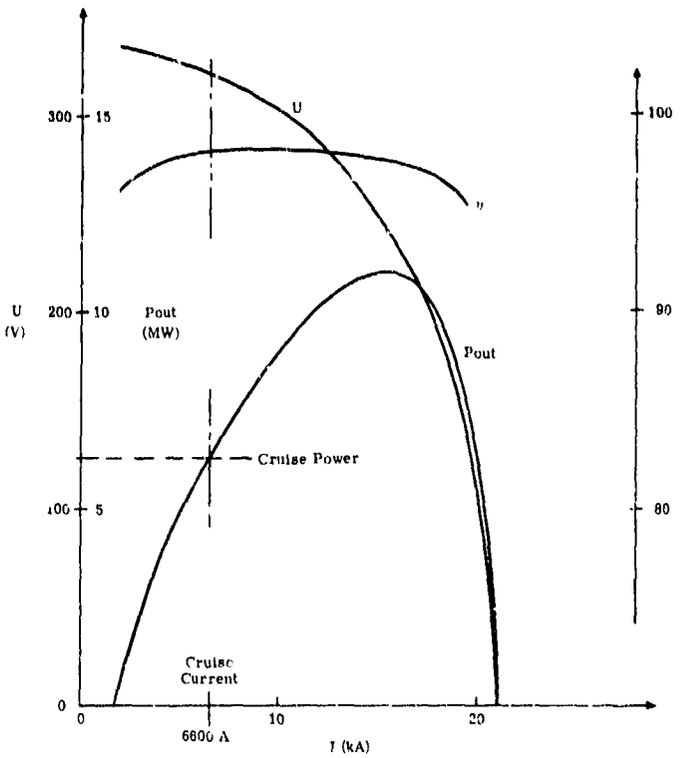

Figure 3-26. Constant Speed Performance of Permanent Magnet, 20 000-hp Motor at Cruise Speed of 337.5 rpm, Cos y = 1.0

MECHANICAL DESIGN CONSIDERATIONS

A layout sketch of the 20 000-hp, 450-rpm motor is shown in Figure 3-27. The basic construction characteristics discussed for the 40 000-hp motor have also been used for this machine. At this speed range, roller bearings may be applicable and could result in a significant weight savings.

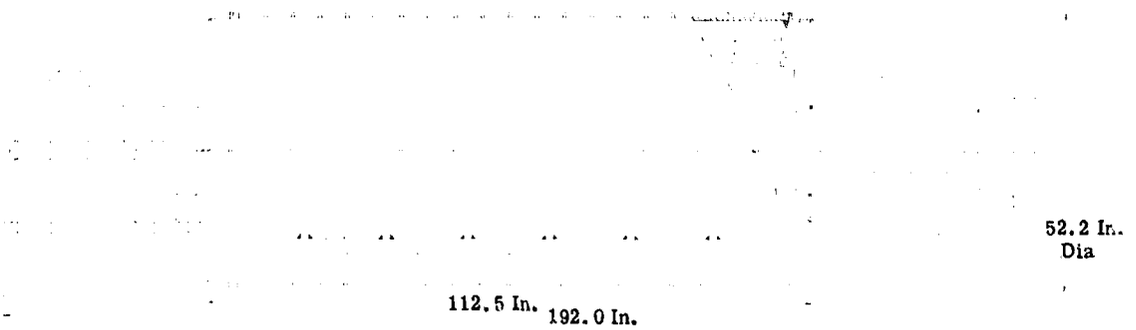

Figure 3-27. Permanent Magnet, 20 000-hp, 450-rpm Motor (Total weight: 38 000 lb)

Two points need checking as far as the layout is concerned. The first one is the mechanical strength of the rotor structure at top speed. The rotor construction chosen is similar to the one used for the 40 000-hp motor (Figure 3-11), using wedges and dovetails to fasten the magnets and poles to

the rotor hub ring. In general, the peripheral velocity of the 450-rpm machine at this speed is 78.5 ft/s, which is slightly higher than the peripheral velocity of the 40 000-hp, 163-rpm machine at rated speed of 64.5 ft/s. The comparison shows that the stresses should be about 50 percent higher than for the 40 000-hp machine or 2500 psi for the wedge construction. That appears to be quite acceptable.

A different approach is taken for the dovetail design: the combined weight of the wedge, the magnets, and the pole piece per pole pitch and 1-in. stack length is 2.7 lb. At 450 rpm, the centrifugal force of this section amounts to 309 lb. The minimum cross section of the dovetail is 0.787 in.^{2}. This would result in a straight stress in that section without consideration of a stress concentration factor of 400 psi. Even a stress concentration factor of ten will not cause unacceptable dovetail stresses.

The second point to be checked is the actual weight of the machine, as shown in Figure 3-27. The shaft diameter of the drive end is determined according to marine standards as:

$$Dsh = \sqrt[3]{\frac{64 \times Hp}{Rpm}} = 14.2 \text{ in.}$$

This shaft requires a Type-L27 (Kingsbury) journal bearing (Figure 3-27). It weighs 3800 lb. The antidrive-end shaft is sized according to shock loading with a diameter of 10.25 in. which also requires a large and heavy combined journal and thrust bearing. The remainder of the weight details are given in Table 3-12 which shows a total machine weight of 38 000 lb. This is not very much lower than the computed weight (Table 3-11), but the weights of the various components have shifted appreciably.

Table 3-12

WEIGHT DETAILS
FOR 20 000-HP MOTOR

Stator	
Core	7057
Copper	2896
Frame	5980
End caps	280
	16 213
Rotor	
Hub	2873
Magnet	2764
Pole pieces	3572
Pole top and wedge	1811
	11 020
Shaft Extensions	3750
Drive-end Bearing	3800
Antidrive-end Bearings	2500
Miscellaneous	717
	10 767
Total Weight	38 000

5000-HP GENERATOR

TRADE-OFF DESIGN

The electrical power, voltage, and current rating for the 5000-hp generator, which is to be operated at 7200 rpm at rated output, have been established in the same way as discussed for the 20 000-hp generator. The voltage losses in the power conditioner and those due to the power factor change have been taken into account, while the voltage change due to the cycloconverter connection has not been accounted for. This and the actual voltage level of the system once established for the complete system can, in general, easily be accommodated in the machine without any significant influence on the machine's size, provided no additional insulation material is required. The voltage and current level for this machine are established as:

Rated voltage	U = 380 V
Rated current	I = 3800 A/phase
Power factor	$\cos\phi$ = 0.86 leading

The design trade-off procedure is similar to the one used before and, in general, the same parameters can be varied. However, besides the current density and the gap-to-pole-pitch ratio, which are based upon previous trade-off experience (CD = 6000 A/m^2, GPTP = 0.06), other parameters can be narrowed down in their range before the actual trade-off calculations are performed, based upon system and other requirements.

The generator frequency is limited at the low end by the requirements of the cycloconverter, which calls for the input frequency to be, as a minimum, three times the output frequency. Since the output frequency could go as high as 120 Hz (e.g., in the 20 000-hp motor), the minimum generator frequency should be 360 Hz. The switching capability of the power semiconductors may limit the upper frequency to about 500 Hz.

At 7200 rpm, there are only two numbers of pole pairs capable of producing frequencies in that range:

Four pole pairs	F = 480 Hz	7200 rpm
Three pole pairs	F = 360 Hz	

Because of the cycloconverter operation, the combination of reactance requirements and the rotor stress capability limit quite severely the range of the remaining three parameters (turns per phase (Turns), rotor radius (RR), and the per unit pole arc (PUPA)). This was determined during the studies for the 20 000-hp generator. As a matter of fact, the per unit pole arc previously selected to provide for the lightest machine will have to play

a vital role to keep the reactance level low. Based upon the experience gained for the 20 000-hp generator, the synchronous reactance level should not be much larger than 0.333 p.u.

In order to limit the rotor radius range to practical values, the previously discussed method of shrink ring stress calculation is again employed.

$$\sigma = (\text{rpm} \times R)^2 \times Ks \times 0.71 \times 10^{-5}$$

For rpm = 7200, one gets

$$\sigma = 368.1 \times R^2 \times Ks$$

For a given stress level, a curve of rotor radius (RR) versus stress factor, Ks, can be plotted, as is done for σ = 130,000 psi and 150,000 psi in Figure 3-28. In the same figure, curves of magnet height (hm) versus Ks are shown for constant X which relates the shrink ring thickness (THR) to the rotor radius,

$$THR = RR \times (1 - X)$$

This second set of curves is shown for σ = 130 000 psi and the following rotor material data:

	Shrink Ring	Magnet Ring
Poisson ratio (average)	0.316	0.3
Density (average) (lb/in^3)	0.297	0.3

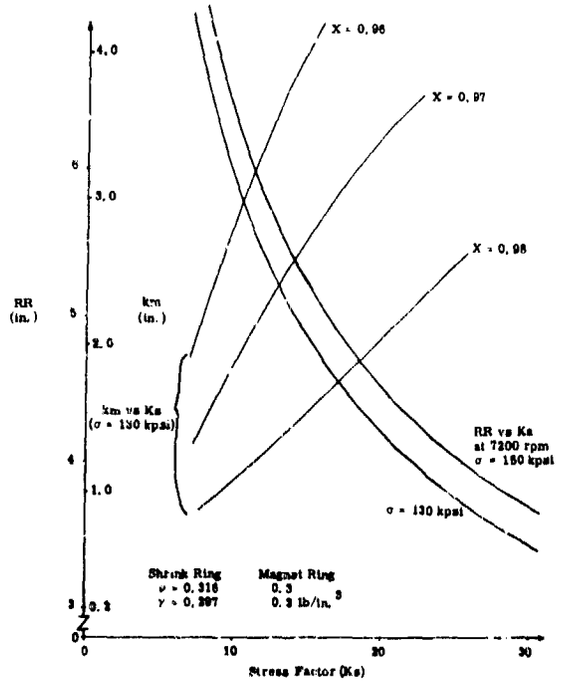

Figure 3-28.

Rotor Radius and Maximum Magnet Height for 5000-hp, 7200-rpm Machine

On those curves (hm versus Ks), points are marked for various rotor radii. It can be seen that X = 0.98 requires rather small rotor radii in order to meet the stress limitations for reasonable magnet heights. A value of X = 0.97, which calls for a shrink ring thickness of 3 percent of the outer rotor radius, allows larger rotor radii for a given magnet height.

This grid of feasible rotor dimensions was then superimposed over the trade-off calculation which had been performed for the following ranges of the previously not fixed parameters:

RR	4 in. to 6.4 in.
Turns	2 to 4
PUPA	0.44 to 0.72

Two generalized mechanical designs were selected that best fit the reactance requirements and the stress limitations. The general data of the three-pole-pair and four-pole-pair designs selected are presented in Table 3-13. It should be pointed out that the four-pole-pair design with a frequency of 480 Hz is about 9 percent lower in weight than the three-pole-pair design. Both designs have magnets that are 20 percent longer than the natural length in order to meet the performance requirements.

Table 3-13

GENERAL DATA FOR SELECTED 5000-HP, 7200-RPM GENERATORS

Rotor Radius, in.	5.6	5.6
Pole Pairs	4	3
Frequency, Hz	480	360
Turns	3	3
Magnet Height, in.	1.61	2.08
Xaq, p.u.	0.337	0.339
Lm, p.u.	1.2	1.2
PUPA, p.u.	0.52	0.52
Stack Length, in.	33.4	35.5
Weight, lb	3292	3610
Losses, kW	69.1	53.1
Efficiency, p.u.	0.947	0.959

The three-pole-pair machine was selected as the candidate to be presented in a layout sketch because of the frequency concern for the power conditioning semiconductors. The layout sketch is shown in Figure 3-29. The machine features ball bearings (90-mm, ABEC7, angular contact type bearings with oil lubrication) and an oil-cooled stator with the cooling jacket

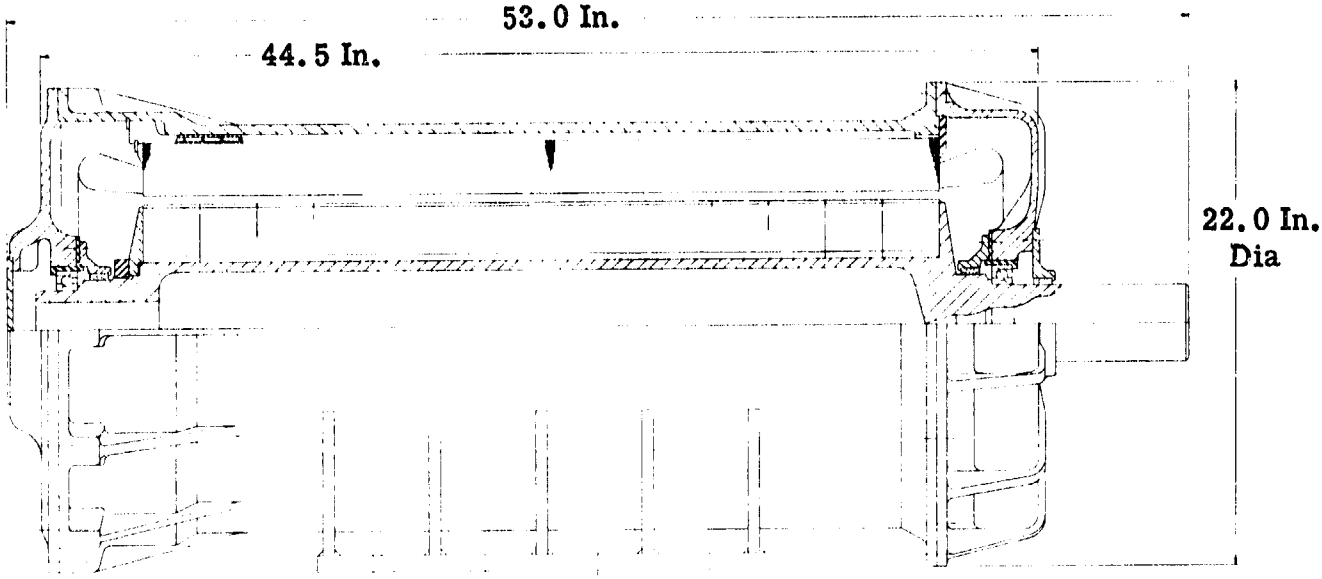

Figure 3-29. Permanent Magnet, 5000-hp, 7200-rpm Generator (Total weight: 2700 lb)

between the laminations and the aluminum housing. The overall dimensions of this machine are:

	Dimension (in.)
Maximum diameter (flanges)	22.0
Total length of frame	44.5
Total length over shaft	53.0

A refined weight analysis based upon the layout results in a total machine weight of 2700 lb, of which 1730 lb are attributable to the stator and 880 lb to the rotor.

Performance calculations have not been performed for the 5000-hp generator. Instead a preliminary design of an electrically excited 20 000-hp generator was done in order to have some comparison between an all permanent magnet motor generator system and a permanent magnet motor -- wound-rotor generator system.

20 000-HP, 3600-RPM, WOUND-ROTOR GENERATOR

The permanent magnet generator has several disadvantages, especially when it is a high-speed machine. One disadvantage is the fact that the permanent magnet generator does not contain any means of field control or voltage regulation, which, in this case, means that the voltage control function (e.g., cruise speed operation) has to be done by the cycloconverter.

Voltage regulation in the cycloconverter is performed by additional phase back of the firing angle. This results in a higher time harmonic content of the voltage and the current and thus higher harmonic losses.

A second disadvantage occurs when a permanent magnet generator has to operate into a cycloconverter. This generally requires a rather low commutating reactance of the generator. For conventional, electrically excited, wound-rotor generators a low commutating reactance is achieved by means of an amortisseur winding on the rotor. This can be accomplished even in high-speed machines. The present design for high-speed permanent magnet machines does not readily allow incorporation of an amortisseur winding on the rotor. Thus, in order to achieve a low commutating reactance level, the synchronous reactance has to be kept very low. As shown in Appendix B, "The Influence of Machine Characteristics upon the Weight and Volume of a Synchronous Generator", this results in a rather heavy machine.

For these two reasons, an attempt has been made to conceptually design a wound-rotor synchronous generator of the same rating as the 20 000-hp permanent magnet generator,

P	20 000 hp	3600 rpm
U	380 V	16 000 A/phase
Phases	3	360 Hz
		12 poles

The basic rotor and machine dimensions are the same as for the originally designed 20 000-hp permanent magnet generator shown in Table 3-9.

The wound rotor would be made out of high-strength vanadium Permendur laminations, which can stand stress levels in excess of 70 000 psi. The rotor design is dominated by the maximum strength required to support the windings on the pole and the amount of copper to be put into the field windings to maintain reasonable excitation losses. The stress analysis of the rotor is done by means of a computer program developed by the Aerospace Controls and Electrical Systems Product Department of the General Electric Company and has been successfully used for rotor stress analysis of high-speed aircraft alternators.

The field windings in the rotor are liquid cooled with the liquid flowing through the hollow conductors. The center wedges and stuffing wedges, which are required to maintain the rotor winding well positioned, are made from a magnesium alloy for rotor stress reasons. The top sticks are made from titanium for strength and weight reasons. The general stress level in the rotor does not exceed 50 000 psi, as indicated for selected points in Figure 3-30, except for point No. 2, which is 74 000 psi, at the tooth overhang root.

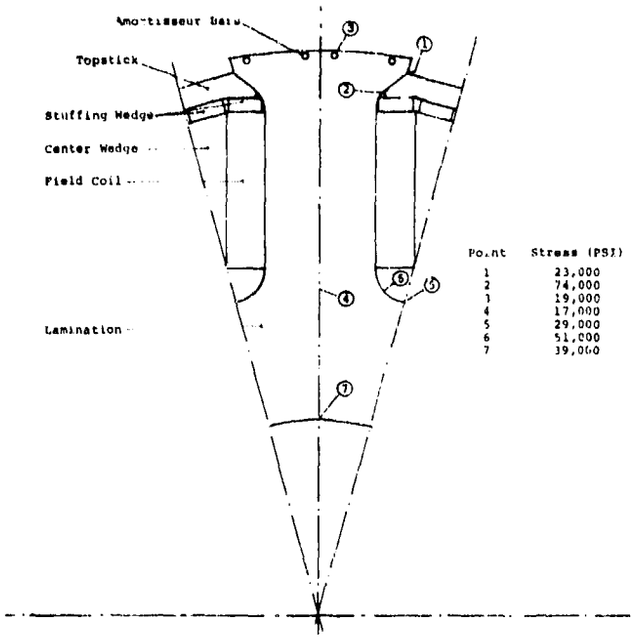

Figure 3-30.

Wound Rotor Construction and Stress Levels

This stress level is calculated for an over speed of 115 percent and is close to the capability limit of the material. Should a detail design of this machine follow, a finite element stress analysis of this rotor section should be performed to determine a more accurate stress level. It is expected, based upon experience, that the computer results obtained so far are rather pessimistic and that accurate stress values at this point will be below 70 000 psi at the over-speed point.

A weight analysis of the wound rotor has resulted in a weight of 6650 lb for the rotor without shaft extensions. This is 46 percent higher than the rotor for the preliminary permanent magnet generator design. The total machine length will increase somewhat over that of the preliminary permanent magnet machine because of the slip rings necessary to provide excitation power to the rotor. Excitation power for the generator when providing power for cruise operation amounts to

$$P_{ex} = 64 \text{ kW}.$$

This will have to be traded off against the increase in system losses due to the increased electrical systems harmonics in case voltage regulation is done by the inverter. This trade-off analysis requires a detail component and interface design that goes beyond the scope of this study.

DISC PERMANENT MAGNET MACHINE

An alternate approach for permanent magnet machines for electrical ship propulsion systems is the use of disc-type permanent magnet machines. The basic unit of this type of machine, shown in Figure 3-31, consists of: segment-shaped permanent magnets arranged with alternating polarity on the

rotor discs and backed by magnetic iron as a return path, and segment-shaped stator coils arranged in a three-phase array and backed by laminated stator core iron. This type of machine constitutes an air-gap winding machine, since the windings are not embedded in the stator slots.

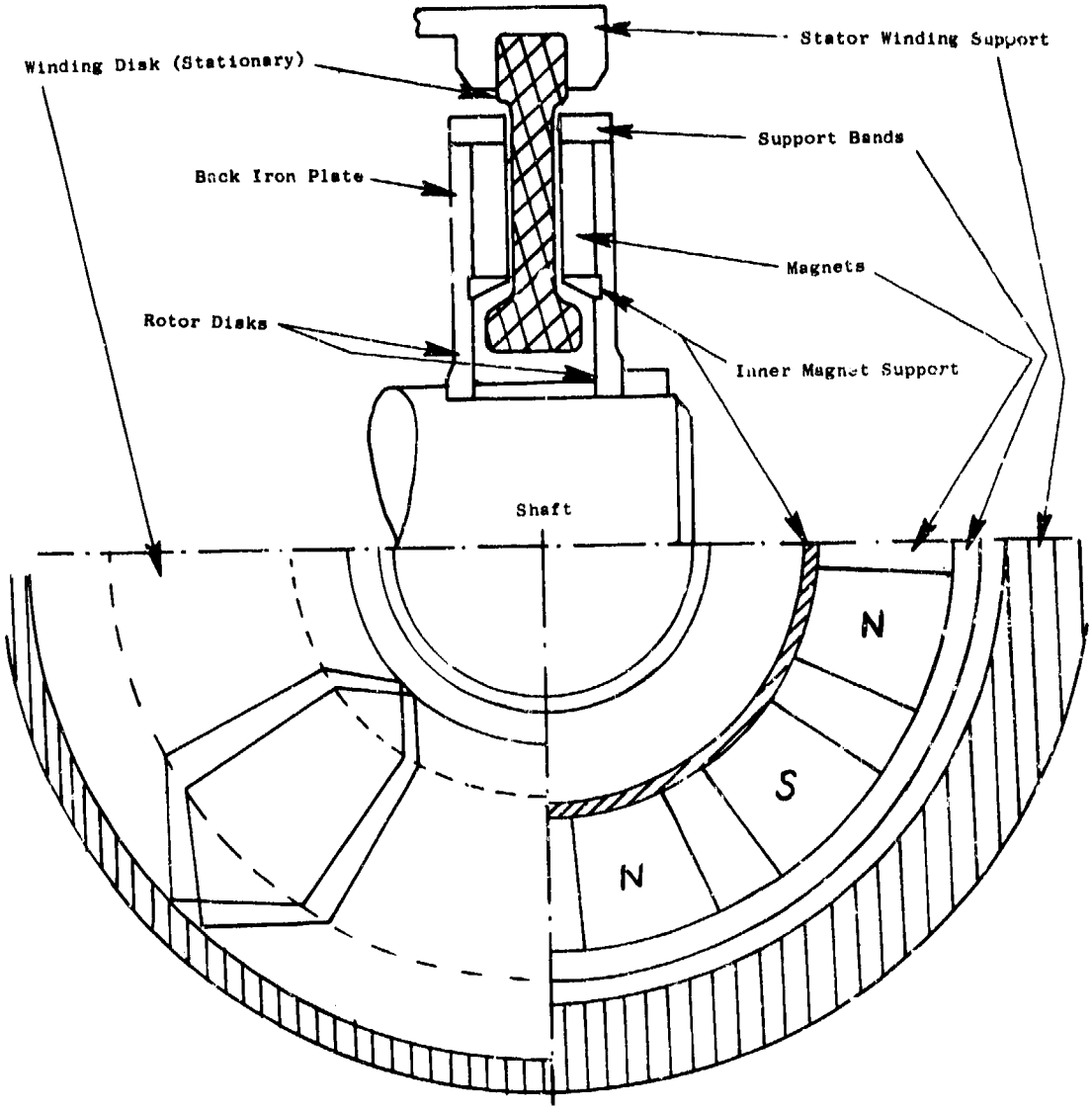

Figure 3-31. Disc-type Permanent Magnet Machine (Note: A double-disc unit in terms of the description in the report is shown.)

Preliminary investigations have shown that the disc-type machine exhibits a performance-diameter relationship different to that of a conventional cylindrical-type machine inasmuch as the power of the diameter in that relationship is bigger for the disc-type machine. The disc-type machine for optimum utilization has a large diameter. If more output power than can be handled by one disc is required, multiple discs can be stacked up

back-to-back. This eliminates the magnetic return path iron -- solid on the rotor and laminated on the stator -- between the units; only the first and last units require a magnetic return path.

For the sizing studies presented below, a number of machine variables, held constant as input parameters, are tabulated in Table 3-14. Initial studies involving magnet length, winding thickness (tw), current density (CD), winding space factor (SF), and number of pole pairs (P) have indicated that:

- Changing the magnet length up to two inches (per disc) produces a noticeable gain in machine efficiency. Beyond that, magnet weight and machine volume and weight are added without much improvement in efficiency.
- Increasing the product of the winding thickness, the space factor, and the current density, which is called current loading per unit length, J, up to a value of J = tw x CD x SF = 1500 A/in. results in significant decreases in magnet and machine volume and weight. Further increases in current loading produce only small weight and volume gains.

Table 3-14

CONSTANT INPUT VARIABLES FOR SIZING CALCULATIONS

Machine speed, rpm	168
Magnet strength (magnetization), Wb/m^2	0.85
Axial air gap (armature-magnet), in.	0.25
Power factor	1.0
Magnet outside radius, in.	55
Magnet inside radius, in.	40

These observations resulted in cross plots of the results versus current density, as shown in Figure 3-32. For this case, a magnet length of 2 in., a space factor of 0.5 (because no better value is available at present), and a current loading of 1500 A/in. have been selected. The number of disc units, as described before, necessary for a 40 000-hp output is the variable that determines the machine length (Lm).

The curves plotted in Figure 3-32 show the electrical losses in percent of the machine rating -- no iron losses are present since no iron is contained in the a-c flux path of this machine, the magnet weight (Mw), and the machine length (Lm). The latter is also representative for machine volume and weight, since the maximum rotor diameter is kept at 110 inches. The curves are plotted for P = 18, 24, and 36 pole pairs and illustrate the conflict between achieving low losses and low machine volume. However, the

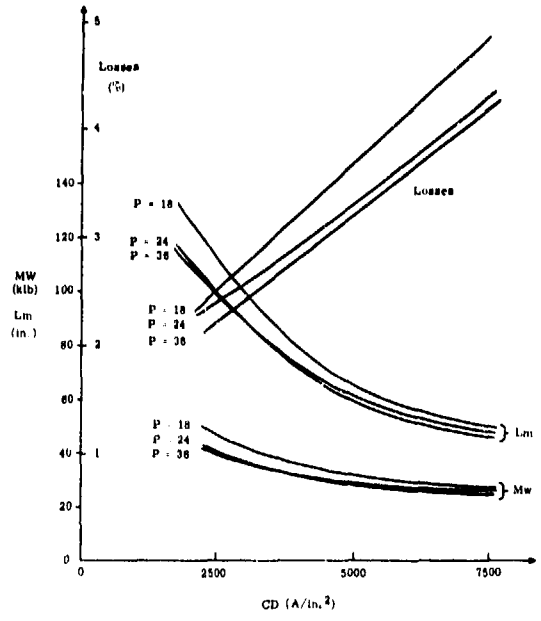

Figure 3-32.

Disc Machine Parameters Versus Winding Current Density for 40 000-hp, 168-rpm Machine (Ra = 55 in.)

results are significant because they indicate:

- The machine parameters show little sensitivity to the number of pole pairs.
- Over the range of current density considered, the variations appear to be reasonable.

Those results indicate a reasonable amount of design freedom in the choice of the machine parameters.

So far, an inside radius of the magnet and active winding discs of Ri = 40 in. has been used in the studies. To justify this selection, a plot of the machine parameters versus inside radius has been prepared (Figure 3-33), with the remaining parameters kept constant. This figure shows a broad minimum in losses and a similar gradual decrease in magnet weight over the range considered. However, the active machine length begins to increase rapidly at a rotor inside radius of about 40 in., hence the choice of this value.

The parameters of a machine selected from the midrange of the variables studied will be typical of a disc-type permanent magnet machine for the required rating. These machine parameters, which include all of the active parameters, are shown in Table 3-15. A detail mechanical design will have to establish the actual overall dimensions of the disc-type machine. However, if one compares the active volume of the disc-type machine, as defined by the active length and the magnetic outside diameter of the rotor, with the active volume of the cylindrical machine, as defined by the stack length and the stator punching outside diameter, the disc-type machine

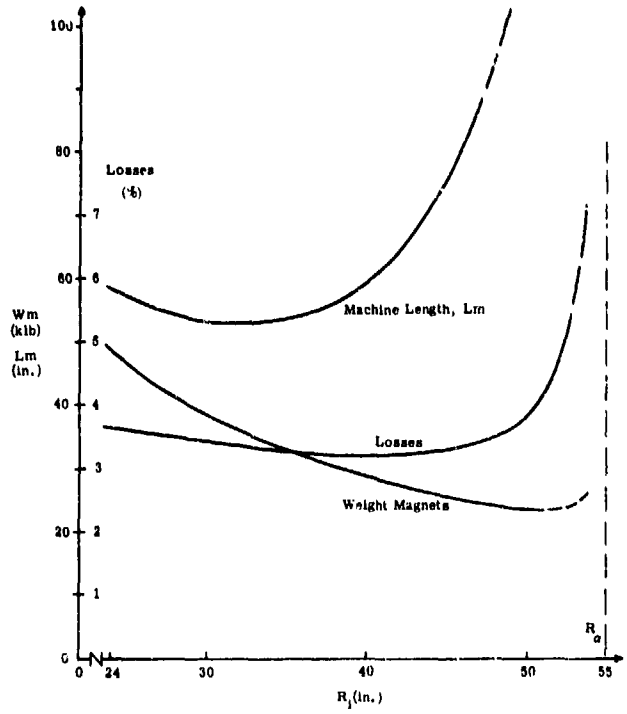

Figure 3-33.

40 000-hp, 168-rpm, Disc-type Machine Parameters Versus Inner Radius

Table 3-15

PARAMETERS OF TYPICAL DISC-TYPE MACHINE

Machine speed, rpm	168
Number of poles	48
Magnet outside radius, in.	55
Magnet inside radius, in.	40
Magnet strength (magnetization), Wb/m^2	0.85
Magnet axial half-depth, in.	1.0
Armature copper current density, $A/in.^3$	5000
Armature space factor	0.5
Armature current loading, A/in.	1500
Armature half-thickness, in.	0.6
Axial air gap, in.	0.25
Number of discs	16
Active length, in.	59.5
Magnet weight, klb	28.7
Copper weight, klb	13.4
Internal voltage, volts/turn	5.09
Terminal voltage, volts/turn	4.92
Power factor	1.0
Armature current, ampere turns/disc	125.6
Synchronous reactance per unit	0.25
Armature copper losses (d.c.), percent	3.2

compares favorably with

$$\text{Vact} = \pi \times 2 \times \text{Ra} \times \text{Lm} = 20\,600 \text{ in.}^3 \quad \text{(Disc)}$$

to the cylindrical machine with

$$\text{Vact} = \pi \times 2 \times \text{Ros} \times \text{Hi} = 27\,900 \text{ in.}^3 \quad \text{(Cylindrical)}$$

The significant differences between the two types of machines should be pointed out, since they determine, to a large extent, where one machine type would be preferred over the other.

- The disc-type machine achieves the best performance at large rotor diameters. This does not make the machine look advantageous where small diameters are required, as they are for the ship propulsion motors.
- The disc-type machines require at least twice as much magnet material as the cylindrical-type machines, which again makes them less attractive for low-speed, large-machine-size applications.
- The geometry of the disc-type machines, which calls for the flux path to be parallel to the axis of rotation, allows the mechanical rotor support structure to be outside of the magnetic path and not to interfere with it as it does for cylindrical machines. This would make the disc-type machine appear the preferred selection for high-speed applications, where mechanical strength considerations limit the rotor diameter.
- In general, more than one winding disc will be required. These discs will preferably be connected electrically in series in order to avoid circulating currents in the windings. Currents of this type are present when the discs are connected electrically in parallel, since one always has to allow for slight misalignments between discs. Each disc is a self-contained unit, which can be intentionally "misaligned" or, for that matter, can be mounted such that the alignment can be controlled by mechanically rotating the discs with respect to each other. This results in control of the output voltage, since the voltages of each disc add up geometrically

$$U \times e^{j\psi} = U_1 \times e^{j\psi_1} \hat{+} U_2 \times e^{j\psi_2}.$$

where: U and ψ are the amplitude and (arbitrary) angle of the two discs connected in series, and U_1 and ψ_1 or U_2 and ψ_2 are the voltage amplitudes and phase angles of the individual discs. Thus, changing the alignment of the discs will change the amplitude of the output voltage, making the disc-type machine amenable to external voltage control. This is not easily done for the cylindrical machine.

All of these points indicate that the disc-type machines are more advantageously utilized for the generator applications in a ship propulsion system than for the motor application.

CONCLUSIONS

In the preceding sections, permanent magnet motors and generators, as well as a wound-rotor synchronous generator, have been studied for application in a ship propulsion system.

The results for the cylindrical permanent magnet machines have been very promising. However, at the end of all of the studies, it was discovered that a mistake had occurred in the computer program. This error had the effect of requiring the magnets to be significantly stronger than those available today. Subsequent correction studies revealed that if the rotor can be constructed with more magnet volume than previously accounted for without interfering with the mechanical rotor structure to deliver the same flux densities in the air gap at full load, the same machine envelopes will be obtained as previously calculated. The differences will be found in the rotor weights, which will go up significantly. The stator and frame weights will not be affected by this as long as the air gap quantities can be maintained with the present magnet of nominally 21 MGOe energy level.

The corrected program studied the effect of magnet strength and magnet dimension in the circumferential direction. The results are shown in Figures 3-34 and 3-35. The magnets, originally specified, had the following data:

Energy level, MGOe	21
Flux density B_r, kG	9.38
Recoil Permeability	$\mu r = 1.05$

The flux density B_r was downrated to $B_r = 8.53$ due to reversible and irreversible temperature losses of B_r. This may be conservative for the two motors, but it is justified for the generators based upon previous experimental work. Figure 3-34 shows that the previous calculations would actually require magnets having an energy level of 55 MGOe. This energy level for rare earth permanent magnets is not expected to materialize in the foreseeable future. However, energy levels of 25 MGOe are presently being produced by several manufacturers, such as Brown, Boveri and Company, Ltd. in Switzerland and Hitachi, Ltd. in Japan. The same manufacturers and others in the United States, indicate that 30 MGOe and 35 MGOe magnets should be out of the laboratory within the next couple of years.

Figure 3-35 shows the relationship between machine weight and magnet length in circumferential direction. The point Lm = 1 p.u. means natural length, as defined previously. While the magnet weight shows a minimum, the machine weight tends to slowly decrease with increasing Lm. Thus, in

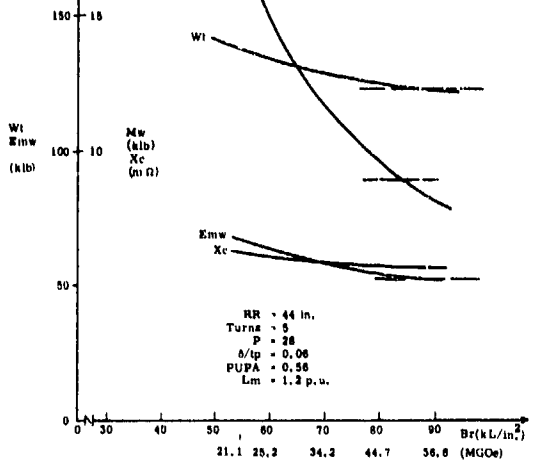

Figure 3-34.

Sensitivity of 40 000-hp, 168-rpm Machine Parameters to Magnet Strength

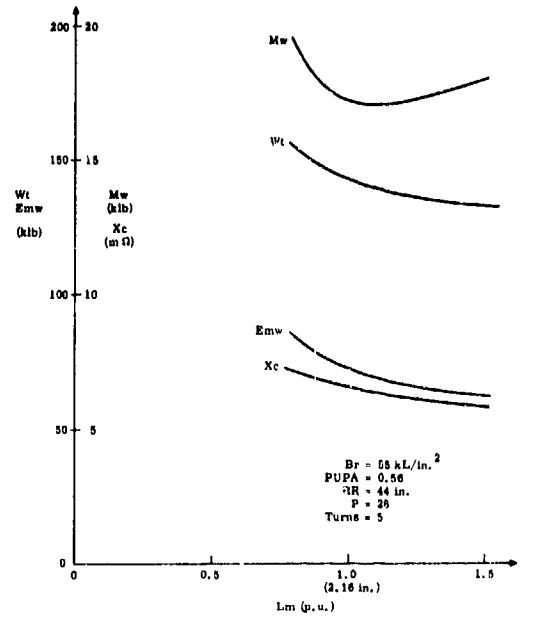

Figure 3-35.

Sensitivity of 40 000-hp, 168-rpm Machine Parameters to Magnet Length

contrast to previous calculations, an increase in Lm will reduce the rotor weight and correspondingly the total machine weight.

Figure 3-36 shows the corrected data printout for the 40 000-hp motor. The difference between this printout and the previous calculations, as shown in Figure 3-11, is found in the weights of the pole pieces and the magnets. The corrected machine weighs 8250 lb more for the magnets and 7150 lb more for the pole pieces, which amounts to 15 400 lb more for the complete machine. Thus, in a more detailed design, the corrected machine in the same envelope as before should weigh roughly 104 000 lb as opposed to 89 000 lb. If the 35-MGOe magnet material became available, the magnet

```
INDIVIDUAL PRINTOUT FOR PM-MACHINES(M)

ELECTRICAL DATA
TERM VOLT     320.0   TERM KW  30471.2   P F      1.00
GAP  VOLT     315.0   SHFT KW      0.     F        78.
PHASE CUR   31727.3                       RPM     168.

XSIG 0.7094E-03  FL      0.     BMG 0.6001E-03  PF      28.TURNS      5.
XAQ  0.6107E-02  DELTA   0.531  BMT 0.1200E-02  PUPA   0.36 PHASES    3.
XC   0.6212E-02  GAMA    0.603  BMP 0.1100E-02  GAP    0.296CIR     48.00
RW   0.1831E-03  COSD    0.862  BMY 0.1000E-02  CAEF   0.311  TPC      1.0
PLE  0.2576E 01  S1    720.00   CD     6000.00  KPKD   0.958  SF     0.660
KM       1.4233  KFI     0.9837  CAQ     0.6271  KF     0.92

DIMENSIONS
STATOR
RIS    44.296  RBS    46.308  ROS    47.451  ODFR   97.901
HI     90.733  OLEM   94.582  OLEC  152.836  OLMF  155.836
HY      1.113  TPP     4.937  CWDC    9.119
TS      0.387  WS      0.176  HSI     1.892  HST     0.150
ROTOR
RR     44.000  RIR    37.812  THR     0.340  THH     1.500
OLER   97.084  OLEB  152.836  OLMS  208.587
BEARINGS&SHAFT
DSHFT  27.876  ODB    55.751  DIS    22.301
MAGNETS
BR   0.000551  MYR     1.030  LM      2.586  HM      4.348

WEIGHTS
CU       7305.  SHR. R.    2532.  BEAR    36747.
CORE    17174.  POL. P.   12931.  SHFT     9602.
FRAME   19649.  MAGNETS   17139.  ROTOR   70404.
ENDB     4319.  HUB        9827.  EL M    66820.
STAT    66908.  ROT EM    42429.  TOT    137224.

LOSSES
PCU    552.9 PFET  59238.9  PFEY  30991.5  PFE     90.2  PTOT    643.2
```

Figure 3-36. Corrected Printout of 40 000-hp Motor

```
INDIVIDUAL PRINTOUT FOR PM-MACHINES(M)

ELECTRICAL DATA
TERM VOLT     320.0   TERM KW  15197.6   P F      1.00
GAP  VOLT     316.2   SHFT KW      0.     F       120.
PHASE CUR   15826.2                       RPM     450.

XSIG 0.1479E-02  FL      0.     BMG 0.6003E-03  PF      16.TURNS      4.
XAQ  0.1112E-01  DELTA   0.489  BMT 0.1201E-02  PUPA   0.60 PHASES    3.
XC   0.1224E-01  GAMA    0.563  BMP 0.1100E-02  GAP    0.236CIR     24.00
RW   0.2896E-03  COSD    0.883  BMY 0.1000E-02  CAEF   0.252  TPC      1.0
PLE  0.4019E 01  S1    288.00   CD     6000.00  KPKD   0.958  SF     0.660
KM       1.3803  KFI     0.9985  CAQ     0.6586  KF     0.92

DIMENSIONS
STATOR
RIS    20.236  RBS    22.038  ROS    22.965  ODFR   48.930
HI     90.661  OLEM   93.803  OLEC  128.885  OLMF  131.885
HY      0.927  TPP     3.927  CWDC    6.428
TS      0.441  WS      0.202  HSI     1.652  HST     0.150
ROTOR
RR     20.000  RIR    13.572  THR     0.340  THH     1.500
OLER   97.007  OLEB  128.885  OLMS  160.762
BEARINGS&SHAFT
DSHFT  15.939  ODB    31.877  DIS    12.751
MAGNETS
BR   0.000551  MYR     1.030  LM      1.544  HM      4.588

WEIGHTS
CU       2888.  SHR. R.    1145.  BEAR     6869.
CORE     7043.  POL. P.    7029.  SHFT     1478.
FRAME    8132.  MAGNETS    6164.  ROTOR   22897.
ENDB      919.  HUB        3647.  EL M    22437.
STAT    27916.  ROT EM    17985.  TOT     45334.

LOSSES
PCU    217.6 PFET  43673.6  PFEY  22127.0  PFE     65.8  PTOT    283.4
```

Figure 3-37. Corrected Printout of 20 000-hp Motor

weight would be reduced from 17 300 lb to 11 500 lb. If 55-MGOe material were ever to be economically produced, the rotor weight would be further reduced to 8900 lb. It is suspected one would pay excessive cost penalties for these 2600 lb (11 500 lb minus 8900 lb). It remains to be noted that the trade-off curves (shown before) change in absolute values, but not the general trends.

The 20 000-hp, 450-rpm motor was rechecked next. Figure 3-37 shows the new printout for a machine that has the same dimensions, turns, number of poles, and pole arc as the original design. The same results are apparent as for the larger machine. The envelope remains, but the rotor weight increases by 6860 lb, increasing the weight of the more detail design to roughly 44 500 lb without changing the electrical characteristics.

A brief check of the rotor structure indicates that because of increased weight and reduced structural area the rotor stresses for a similar construction will increase by a factor of four; the maximum stress in the dovetail design could go up to 16 000 psi. This is still within the capabilities of the materials used. However, more attention has to be paid to stress concentration factors, and a detail design would require more accurate analysis methods, such as finite element methods.

One thing should be pointed out: to achieve minimum weight, the original machine design was done by selecting the optimum pole arc. This pole arc is not the one for lowest weight for the corrected design, as illustrated in Figure 3-38. However, in order to maintain the same envelope, the pole arc was not changed. A detail design would take that into consideration; but, it would also push the reactance level to the limits allowed to reduce the air gap length somewhat for less magnet and rotor weight.

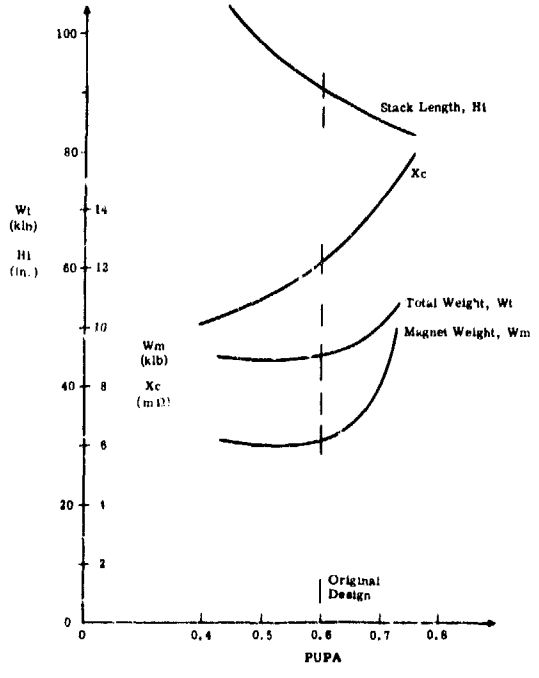

Figure 3-38.

20 000-hp, 450-rpm Motor Parameters Versus Pole Arc (Corrected design)

The redesign of the 20 000-hp, 3600-rpm generator confirmed what was expected before; the original envelope cannot be maintained since the rotor structure will not permit the required magnet height because of stress limitations. A closer analysis reveals that the combination of ampere loading (amperes per unit length of rotor circumference), stress limitations, and reactance requirements make the redesign "starved" of flux. The permissible magnet height is too small compared to the pole pitch of the 12-pole machine to allow sufficient flux squeezing in the air gap to make the desired gap flux density. Allowing that flux density to decrease, increases the stator length and thus the reactance.

On the other hand, increasing the number of pole pairs (and thus frequency) will achieve a better magnet-height-to-pole-pitch ratio and will result in an acceptable design from the machine standpoint. To prove the point, a redesign for 16 poles and 480 Hz was done with a sufficient rotor structure to permit 10 percent overspeed. In this case, the envelope stays almost the same, and the change in pole pairs will cover some of the increased weight due to the actual magnets available. The results are presented in Table 3-16 which shows the two computer designs and, for reference, the changed dimensions of the refined original design.

Based upon the experience with the 20 000-hp, 3600-rpm generator, one can predict that the redesign of the 5000-hp, 7200-rpm generator may become somewhat more difficult than the design for the 20 000-hp machine. However, since the interest in that machine is low, no redesign was performed.

In view of the results, the following trends are listed for the machinery part of the study:

- Two motors in the form of cylindrical permanent magnet machines appear feasible and practical.
- Two cylindrical permanent magnet generators appear somewhat marginal because of no regulation capability, rotor structure, and frequency, even though, as has been shown, the larger machine could be built.
- Disc-type permanent magnet machines appear to be desirable for the generator application because of their regulation capability and their rotor stress problem is less.
- Wound-rotor machine appears feasible as a 3600-rpm generator with an additional 64-kW excitation loss at cruise speed.
- Efficiencies of all of the machines look very good. However, it should be emphasized that due to the time harmonics created by the cycloconverter operation the actual efficiencies may be lower by a fraction of a point. The actual losses are extremely hard to

determine for a general case, because the system has not been defined to a detail level necessary for the exact loss prediction. This makes a trade-off between voltage regulation by the cycloconverter, with its increased harmonic losses, and voltage control by means of electrical excitation quite difficult at this stage.

Table 3-16

COMPARISON OF ORIGINAL AND CORRECTED 20 000-HP, 3600-RPM GENERATOR DESIGNS

Machine	Original Design	Refined Original Design	Corrected Design
Rotor Radius, in.	14.5	--	14.5
Frequency, Hz	360	--	480
Pole Pairs	6	--	8
Shrink Ring Thickness, in.	0.435	--	0.725
Magnet Height, in.	2.47	--	4.42
Magnet Length, in.	5.34	--	3.33
Xaq, mΩ	7.94	--	7.85
Xc, mΩ	--	--	8.69
Frame Diameter, in.	38.4	40.5	37.5
Frame Length, in.	66.7	54.4	66.9
Magnet Weight, lb	2108	2108	3146
Electromagnetic Weight, lb	8210	--	9355
Machine Weight, lb	14 177	13 000	14 946
Losses, kW	187.3	--	198.8
Stack Length, in.	44.4	44.4	44.6

Based upon the findings, it is concluded that, as a follow-on project, one should look into a detail design and analysis of a real well-defined propulsion system, consisting of cylindrical permanent magnet motors, cycloconverters, and either wound-rotor or disc-type permanent magnet generators. This effort would be followed by a hardware phase in which a scale model of the system should be built and tested to verify critical design components and procedures and system operation and performance.

Critical design areas that need more detail attention before a full-size system could be built are: 1) the permanent magnet pack and its containment structure, 2) the rotor dynamics, 3) a thermal analysis of the rotor and the stator, 4) the liquid-cooling approach outlined in the report, and 5) the question of the commutating reactance which in this study has been handled in a very conservative way. In addition, the techniques for assembling the rotor and the machine need detailed study, as well as the techniques for magnetizing the magnets after they are mounted in a rotor subassembly.

Section 4

POWER CONDITIONING

BASIC POWER CIRCUIT OF CONVERTER

The proposed basic building block of the propulsion system is shown in Figure 4-1, in which the machine windings are represented as EMF's in series with leakage inductance. The rectifiers are connected in three-phase groups and utilize symmetrical three-phase interconnections between the generator and the motor, which will result in a more symmetrical and uniform loading of both machines.

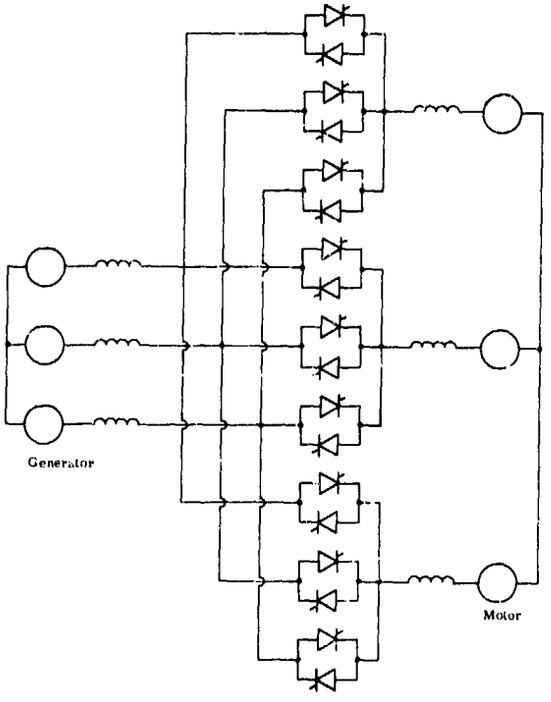

Figure 4-1.
Basic Converter Circuit

The complete ship propulsion system will consist of a number of similar "building blocks", fed from sets of three-phase generator windings. The windings will have a symmetrical mutual phase displacement and will feed sets of three-phase motor windings also having a symmetrical phase displacement. The machine design can also have parallel paired sets of windings which will be advantageous when some converters are disconnected to reduce losses when operating the ship at reduced power.

This particular converter circuit arrangement has been selected over a more usual six-pulse configuration in order to avoid the need for interphase transformers (in a six-pulse midpoint connection) or for separation of the motor phases (in a six-pulse bridge connection). With a direct connection

between the neutral points of the generator and the motor, the circuit shown in Figure 4-1 would produce a three-pulse ripple in the output. However, by eliminating the neutral connection between the motor and the generator, as proposed in Figure 4-1, the effective ripple is reduced and can approach the six-pulse value. Under these circumstances, it is expected that the leakage inductance of the motor can be made sufficiently high to effectively filter the current.

Converter circuits of this type sometimes employ "intergroup reactors" between the positive-current thyristors and the negative-current thyristors. When both groups of thyristors are allowed to conduct simultaneously, the reactors serve to limit the circulating current between the groups. However, since it is intended to eliminate the circulating currents entirely by preventing the simultaneous conduction of positive and negative group thyristors, intergroup reactors for this purpose are unnecessary.

In case of thyristor misfires, a surge current may sometimes flow in the same circulating current path during fault operation, and the reactors would limit such surges. However, since the faults are temporary and easily suppressed by proper remedial action, it is believed that the leakage inductance of the generator windings will be sufficient to limit the surge current and prevent damage.

Not shown in Figure 4-1 are the R-C snubbers that are necessary in most converter circuits in order to suppress transient voltage spikes during switching of the thyristors. The snubbers may be connected directly across each inverse-parallel pair of thyristor devices, or across the input or output lines. Also, it may be found desirable to insert small saturating reactors in series with each inverse-parallel pair of thyristors (Figure 4-1) to limit the reverse recovery current of the devices, thereby minimizing the snubber size and losses.

CONTROL

Converters must generally employ phase-angle lag firing to control both the magnitude and the waveform of the output voltage, e.g., industrial motor drives fed from a utility system must be operated in this manner. The present ship propulsion system would be similarly restricted if a permanent magnet generator is employed. When a field-controlled generator can be dedicated to the load, a decided advantage can be gained by using the field to regulate the magnitude of the output voltage. Considerable savings in the reactive load imposed on the generator and in the losses of the converter can be achieved.

The General Electric variable-speed, constant-frequency (VSCF) scheme for 400-Hz aircraft electrical power systems presently employs such a dedicated field-controlled generator. Since the specifications of that

system require high quality sinusoidal output, the converter must employ phase-angle lag firing to program the waveform. In general, the converter must be programmed to match the voltage waveform desired by the load, as modified by the need to also control the current waveform in a desirable manner.

If the ship propulsion motor in the present system is designed to generate a trapezoidal counter EMF, the converter should be controlled to match it and deliver a current consistent with efficient power transfer. In particular, the reactive power and the need for forcing voltages should be minimized.

RATING OF MACHINES WITH NONSINUSOIDAL WAVEFORMS

The power rating of electromagnetic apparatus designed for sine-wave operation is given as the product of the rms voltage, $E_m/\sqrt{2}$, and the rms current, $I_m/\sqrt{2}$, which equals the average power input (or output), $E_m I_m/2$. For nonsinusoidal waveforms, the actual rms current, I_{rms}, is still valid for determining the conductor size. However, the ferromagnetic size of the equipment is better related to the average voltage instead of the rms voltage, since the magnetic flux required is proportional to the area under the voltage curve. For nonsinusoidal voltage waveforms, an equivalent voltage rating, E_{eq}, is defined as the rms value of a sine wave having the same average value (or area) as the actual waveform. This will equal the average voltage, E_{av}, times the form factor for a sine wave:

$$E_{eq} = E_{av} \frac{\pi}{2\sqrt{2}} = 1.111\, E_{av} \qquad (4\text{-}1)$$

It is assumed that the physical size of a machine (volume and weight) is proportional to the product $I_{rms} E_{eq}$. The rating factor, F_r, is defined as this equivalent rating relative to the actual average power, P_{av},

$$F_r = \frac{I_{rms} E_{eq}}{P_{av}} \qquad (4\text{-}2)$$

For sinusoidal operation, $F_r = 1$, so any value in excess of unity is a measure of the size penalty paid for nonsinusoidal operation.

The combination of a trapezoidal voltage and a quasi-square current, having the same duration, β, as the flat-top of the voltage wave, is presented in Figure 4-2. The particular case $\beta = 2\pi/3$ is applicable to the proposed converter (Figure 4-1). The average value of voltage is

$$E_{av} = E_m \frac{\left(\beta + \frac{\pi - \beta}{2}\right)}{\pi} = E_m \frac{\pi + \beta}{2\pi} \qquad (4\text{-}3)$$

and the equivalent voltage rating is

$$E_{eq} = E_{av} \frac{\pi}{2\sqrt{2}} = E_m \frac{\pi + \beta}{4\sqrt{2}} \tag{4-4}$$

The rms value of the current is

$$I_{rms} = I_m \sqrt{\frac{\beta}{\pi}} \tag{4-5}$$

The average power with these waveforms is

$$P_{av} = E_m I_m \frac{\beta}{\pi} \tag{4-6}$$

Hence, the machine rating factor is

$$F_r = \frac{\pi + \beta}{4\sqrt{2}} \sqrt{\frac{\pi}{\beta}}$$

$$= 1.134 \text{ for } \beta = 2\pi/3 = 120 \text{ degrees} \tag{4-7}$$

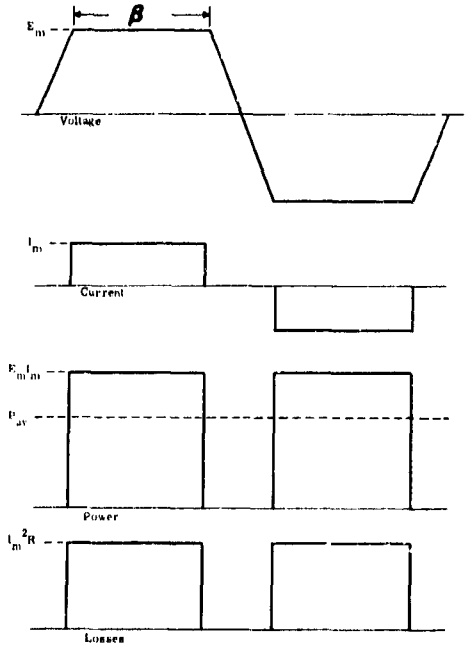

Figure 4-2.
Power and Losses with Trapezoidal Voltage and Quasi-square Current

CONVERTER SYSTEM RATING FACTORS

The rating of thyristors used in converter circuits is more difficult to calculate, especially for frequency converters of the type considered here. Because of the catastrophic breakdown characteristics of semiconductors subjected to overvoltages, their voltage rating must be determined by the peak instantaneous voltage, including allowances for long transients (such as generator overspeed) and short transients (such as recovery spikes).

The current rating of thyristors is mainly determined by the forward conduction losses, though both turn-on and turn-off switching losses become important at higher frequencies. In addition, the reverse recovery current of the devices results in inevitable losses that are dissipated elsewhere in the converter circuit, usually in the snubber damping resistors. To limit the recovery voltage spikes, the snubbers must dissipate more energy than the "inevitable" losses alone. Furthermore, the recovery of one device in a circuit usually generates voltage steps across other devices that are blocking at that time, causing losses in the associated snubbers. Then, the energy stored in the snubber capacitor is lost when the thyristor is turned on again. All of these switching and snubber losses can amount to more than the conduction losses, reducing the efficiency of the converter. While a preliminary estimate indicates that these effects are important in the proposed propulsion converter, only the conduction losses will be considered now.

The forward voltage drop across a thyristor is a nonlinear function of the instantaneous current. However, for the present study, it is reasonable to approximate the forward drop, v_f, by a constant component, v_a, and a linear resistive component, $R_a\, i_f$:

$$v_f = v_a + R_a\, i_f \tag{4-8}$$

The instantaneous power loss p_f is

$$p_f = v_f\, i_f = v_a\, i_f + R_a\, i_f^2$$

and the average loss P_f for one complete cycle is

$$P_f = v_a\, I_{av} + R_a\, I_{rms}^2 \tag{4-9}$$

where: I_{av} and I_{rms} are the average and rms values of the current in the device, which can be calculated from the circuit waveforms.

Unfortunately, the relative importance of I_{av} and I_{rms} depends upon the values of v_a and R_a for the particular type of device as well as the allowable value of the losses, P_f. The latter depends on the thermal parameters, such as the thermal resistance of the heat sinking system. Also, the thermal capacitance, which determines the junction temperature fluctuations about the average value, becomes especially important when the current waveform is highly pulsating, as in the present type of converter circuit.

Ignoring the thermal factors (or assuming they are the same for alternative circuits), two thyristor rating factors can be calculated for the converter circuits, based on the average and rms values of the current, respectively:

$$F_{av} = \frac{N E_{pk} I_{av}}{P_{av}} \qquad (4\text{-}10)$$

$$F_{rms} = \frac{N E_{pk} I_{rms}}{P_{av}} \qquad (4\text{-}11)$$

where: N = total number of thyristors in the converter

E_{pk} = peak voltage across a thyristor, neglecting transients

P_{av} = average power input/output of the converter

I_{av}, I_{rms} = average, rms current in each thyristor

RATING FACTORS FOR CONVERTER CIRCUIT OF FIGURE 4-1

This converter system operates ideally with trapezoidal motor and generator EMF's having $\beta = 2\pi/3$ (120 degrees), which should be practical to produce. As sketched in Figures 4-3 and 4-4, a mode of control is proposed in which the current waveforms for both machines are quasi-square with $\beta = 120$ degrees. To simplify the drawing, a particular frequency ratio ($f_m/f_g = 1/3$) and phase relationship has been assumed, such that all of the thyristors are loaded equally. Also, for clarity, phase-angle lag firing during commutation of the motor current has been ignored. However, rapid commutation of the motor current is feasible because the motor inductance can be small in this system, there being little ripple to filter.

In fact, for the ideal case depicted, there is no ripple voltage due to generator harmonics; when the EMF of one generator phase begins to fall, its duty is transferred to the next phase which has just attained the flat-top level, so that $E_g = E_m$. At any given instant, two phases of the generator are feeding two phases of the motor. The total power is equal to

$$2 E_m I_m = 2 E_g I_g \qquad (4\text{-}12)$$

and is constant, just as in a d-c or polyphase sinusoidal a-c system. Both machines are loaded uniformly at all times, and torque pulsations are eliminated (for the ideal case, which can be closely approached). The one phase of each machine that has zero current during a given interval also has a low EMF at that time; thus, it would be unable to contribute much additional power in any case. The rating factors of the two machines are equal, having the value of Equation 4-7, with $\beta = 120$ degrees:

$$F_{rg} = F_{rm} = \frac{5\pi}{8\sqrt{3}} = 1.134 \qquad (4\text{-}13)$$

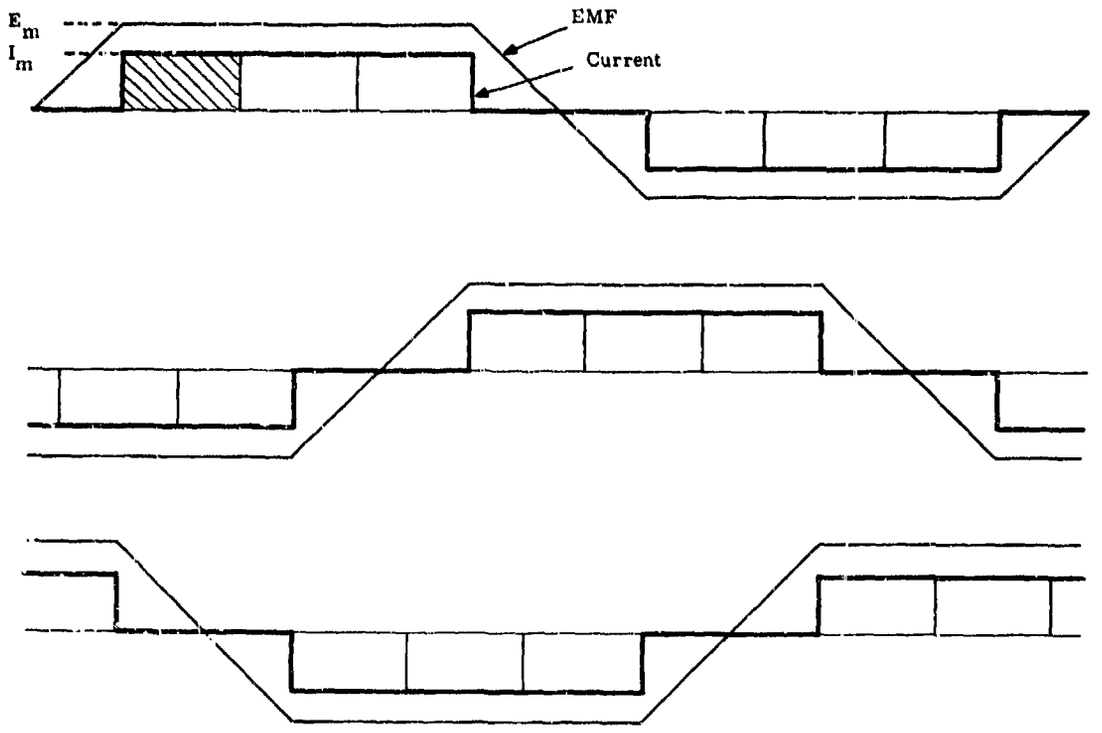

Figure 4-3. Motor EMF and Current Waveforms with Ideal Converter Operation

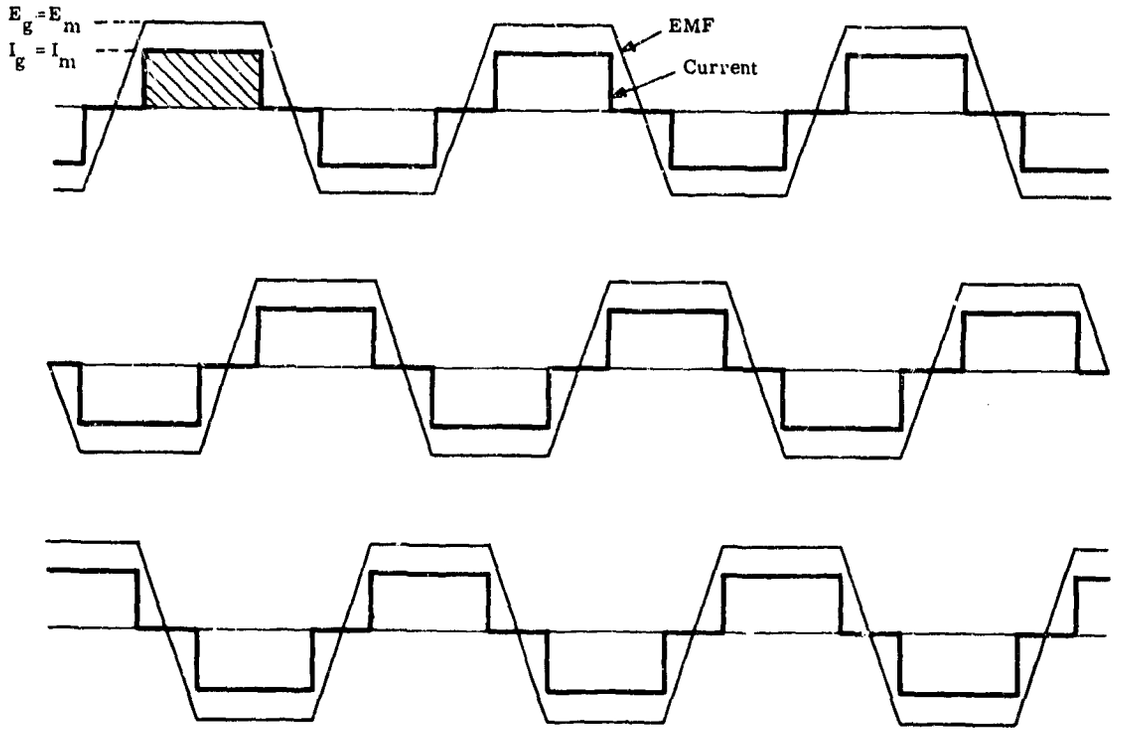

Figure 4-4. Generator EMF and Current Waveforms with Ideal Converter Operation

Since the phases in the converter (Figure 4-1) are interlinked, the entire circuit must be considered in computing the converter rating factors. The total number of thyristors is N = 18, and their peak voltage is

$$E_{pk} = 2\,E_g = 2\,E_m \tag{4-14}$$

The average power is the constant value

$$P_{av} = 2\,E_m\,I_m \tag{4-15}$$

At any one time, two of the eighteen (1/9) thyristors are conducting. The current in one device is shown by the hatched areas in Figures 4-3 and 4-4. The average and rms thyristor currents are seen to be

$$I_{av} = \frac{I_m}{9} = 0.111\,I_m \tag{4-16}$$

$$I_{rms} = \frac{I_m}{\sqrt{9}} = \frac{I_m}{3} = 0.333\,I_m \tag{4-17}$$

From Equations 4-10 and 4-11, the rating factors are found to be

$$F_{av} = 2 \tag{4-18}$$

$$F_{rms} = 6 \tag{4-19}$$

THYRISTOR SELECTION AND RATING

The largest thyristor presently available and having reasonable switching characteristics for operation above 60 Hz is the General Electric C712; this device has tentatively been selected for the proposed ship propulsion converter. It is available with a peak voltage rating of 2000 V (2100 V if the minimum junction temperature is limited to 0 C). The nominal current rating is 1000 A average, based on half-sine-wave conduction at 60 Hz and 65 C case temperature. The maximum allowable current under other standard conditions can be obtained from curves included in the published specifications. Unfortunately, none of these standard conditions pertain to the waveforms imposed by the present converter circuit.

However, examination of the maximum allowable current and corresponding energy loss data curves over the frequency range of interest (60 Hz to 400 Hz) reveals that the rated points correspond to a conduction loss of about 2000 W at 65 C case, reduced to 1200 W at 90 C case. Because of the poor form factor in this converter circuit, the switching losses are expected to be higher than usual. Also, operation near certain critical

frequency ratios, f_m/f_g, causes beat frequency effects that result in unbalanced sharing of the load between the thyristors in the circuit. To allow for such conditions, it will be assumed here that the allowable average conduction loss is 1200 W, but the case temperature must be limited to less than 90 C.

The forward conduction characteristic of the C712 thyristor (the maximum limit cell at 125 C junction) is presented in Figure 4-5. The normal peak current, I_m, in the converter circuit is expected to be less than 5000 A. The characteristic curve can be closely approximated in this range by Equation 4-8, with $v_a = 1.1$ V and $R_a = 0.34$ mΩ. The expressions of Equations 4-16 and 4-17 for average and rms currents, respectively, can be substituted into the average conduction loss formula (Equation 4-9), which is set equal to the allowable loss of 1200 W.

$$P_f = v_a \cdot 0.111\, I_m + R_a \cdot (0.333\, I_m)^2$$

$$1200 = 1.1 \cdot 0.111\, I_m + 0.34 \cdot 10^{-3} \cdot 0.111\, I_m^2 \qquad (4\text{-}20)$$

Solution of the quadratic Equation 4-20 for I_m yields

$$I_m = 4246 \text{ A} \qquad (4\text{-}21)$$

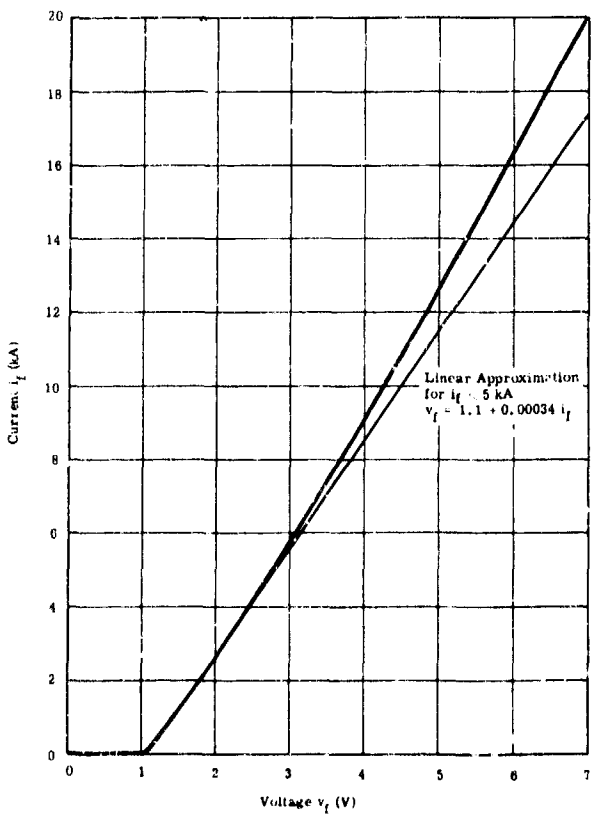

Figure 4-5.
Forward Conduction Characteristic of General Electric C712 Thyristor

CONVERTER FED BY A PERMANENT MAGNET GENERATOR

The rated crest operating voltage applied to the thyristors is 2 E_g in the converter. This value multiplied by the following factors may match the peak rated voltage of the devices, in this case 2100 V:

Generator voltage regulation factor	= 1.45	for a permanent magnet generator
Generator overspeed factor	= 1.07	for a permanent magnet generator
Machine transient factor	= 1.0	
Converter switching transient factor	= 1.35	
Converter switching commutating notch factor (This is the factor by which the generator voltage must be increased above the ideal value, E_g)	= 1.2	

The product of all of these factors is equal to 2.51.

In the case of the converter (Figure 4-1), the peak machine voltages are

$$E_g = E_m = \frac{2100}{2 \cdot 2.51} = 418 \text{ V} \tag{4-22}$$

The power delivered by each three-phase link is

$$\begin{aligned} P_{av} &= 2 E_m I_m \\ &= 2 \cdot 418 \text{ V} \cdot 4246 \text{ A} \cdot 10^{-6} \text{MW} \\ &= 3.55 \text{ MW} \end{aligned} \tag{4-23}$$

For a 40 000-hp motor having an assumed efficiency of 96 percent, the total power input required is

$$P_{total} = \frac{40\,000 \cdot 745.7 \cdot 10^{-6}}{0.96} = 31.1 \text{ MW} \tag{4-24}$$

Since the converter must be sized to provide 150 percent current for 150 percent torque during crash-back operation, the total number of 18-thyristor links required is

$$M = \frac{31.1 \cdot 1.5}{3.55} = 13 \tag{4-25}$$

and the total number of C712 thyristors is

$$NM = 18 \cdot 13 = 234 \tag{4-26}$$

POWER TRANSMISSION CABLES

Another consideration is the total number and current rating of the cables required between the converter and the motor. For the system shown in Figure 4-1, the rms current for the waveform in Figure 4-3 is

$$I_{rms(m)} = I_m\sqrt{\frac{2}{3}}$$

$$= 4246 \cdot 0.816 = 3465 \text{ A} \qquad (4\text{-}27)$$

The total number of cables is $3 \cdot 13 = 39$, having a total current capacity of $39 \cdot 3467 = 135,213$ A.

The number of power transmission cables can be reduced by increasing the voltage level of the system. If two thyristors are placed in series in each leg of the converter circuit shown in Figure 4-1, the voltage can be nearly doubled. A small derating due to imperfect voltage sharing across the series devices will occur. We can assume 7 instead of 13 transmission links, each delivering 3465 A per phase, as given by Equation 4-27, but operating at a voltage

$$E_g = E_m = 418 \cdot \frac{13}{7} = 776 \text{ V} \ .$$

CONVERTER FED BY A CONVENTIONAL FIELD-REGULATED GENERATOR

There is no difference in the basic circuit configuration in Figure 4-1 for a converter fed from a conventional generator. However, a significant reduction in size of the equipment and an improvement in efficiency will occur, because regulation of the motor voltage can now be accomplished by field-control of the generator instead of phase-control of the converter. The most important improvement is elimination of the generator voltage regulation factor (1.45) from consideration in the peak voltage rating of the thyristors. The no-load voltage of the generator can be maintained equal to the full-load voltage by reducing the field flux. Likewise, allowance for an overspeed factor (1.07) is unnecessary with field control.

The converter switching transient and the commutating notch factors remain as considerations in thyristor voltage rating. Using the same thyristors having a peak voltage rating of 2100 V, the rated machine voltages can be increased. Equation 4-22 becomes

$$E_g = E_m = \frac{2100}{2 \cdot 1.35 \cdot 1.2} = 648 \text{ V}$$

The power delivered by each three-phase link increases to

$$P_{av} = 2\, E_m\, I_m$$

$$= 2 \cdot 648\ V \cdot 4246\ A \cdot 10^{-6}\ MW$$

$$= 5.50\ MW$$

Therefore, the total number of 18-thyristor links can be reduced to

$$M = \frac{31.1 \cdot 1.5}{5.50} = 9$$

and the total number of C712 thyristors is

$$NW = 18 \cdot 9 = 162$$

In summary, for the conventional generator-permanent magnet motor system there can be a 4/13 (31 percent) reduction in the number of thyristors, machine windings, cables, and thyristor conduction losses over the permanent magnet generator-permanent magnet motor case.

The efficiency of the converter will also be improved by lower switching losses when the load is less than maximum, under which conditions the permanent magnet generator voltage would otherwise rise. Switching losses are proportional to the voltage across the thyristors when they are switched.

When field control of the generator is substituted for phase control of the converter, the phase delay can be minimal at all times and the power factor imposed by the converter on the generator will be high, even at reduced load. The losses in the generator will be smaller. The harmonic losses in the motor will be reduced because the output waveform of the converter is better with minimal phase delay.

If one were to design a converter for a conventional generator system using the new CXX 77-mm thyristor, a further reduction in converter size and weight could be achieved. Using the 2400-V peak rating of the CXX, the converter capability is changed as follows:

$$E_g = E_m = \frac{2400}{2 \cdot 1.35 \cdot 1.2} = 741\ volts$$

$$P_{av} = 2 \cdot 741 \cdot 4941\ A \cdot 10^{-6}\ MW$$

$$= 7.32\ MW$$

$$M = 6\ groups\ of\ 18\text{-}thyristor\ links$$

$$NM = 108\ thyristors$$

This will substantially reduce the number of thyristors and the number of power cables and resistors between the converter and the motor.

THYRISTOR PACKAGING AND POWER CONDITIONING MECHANICAL DESIGN

Two thyristors have been considered for this application, the General Electric C712, a 53-mm device which is commercially available, and the CXX, a 77-mm device presently in development. The C712 thyristor has a maximum junction temperature of 125 C, and suitable cooling systems must be provided so that this temperature is not exceeded when the system is operating under the most severe load conditions. Both air and liquid cooling have been considered, but an analysis made by W.H. Tobin of the General Electric Static Power Components Operation (SPCO) in Collingdale, Pa., indicates that only liquid cooling can be used if the crash-back condition persists for periods as long as two minutes. Air cooling could be used with the larger CXX device. However, the system study will use the C712 thyristor because of its present availability.

The chosen system using water cooling is described below, and estimates of its size and weight are presented. In addition, an estimate of the pump power needed to circulate the water is made. A comparison of the performance of the C712 and the CXX thyristors under different load conditions when they are cooled by either air or water is presented.

Each C712 thyristor will have a G18 water-cooled heat dissipator attached on both the cathode and anode sides, as shown in Figures 4-6 and 4-7. The G18 unit is a standard unit made by the General Electric Semiconductor Products Department in Auburn, New York. Higher performance heat dissipators are available as custom designs, but for this system study the standard unit is being used.

The weight of the thyristor, the two dissipators, and the mount is 9 pounds; its volume is 219 in^3. The power conditioning system will also need a saturable reactor for each pair of thyristors as well as associated snubbers; the weight of these has been estimated from a similar system to be about 33 lb for each pair of thyristors. Thus, the total weight of the 234-thyristor system with auxiliaries is estimated to be 6000 lb. The volume of the thyristors only would be 51 246 in^3. But, a more realistic packing density with reactors and snubbers estimated from the other system yields a volume of 540 000 in^3. This would fit in a cube 81 in. on an edge. This volume estimate is generous because the system on which it is based is a high voltage system, and more space was needed for voltage standoff. As such, this should be an upper limit for the volume of the system in this study.

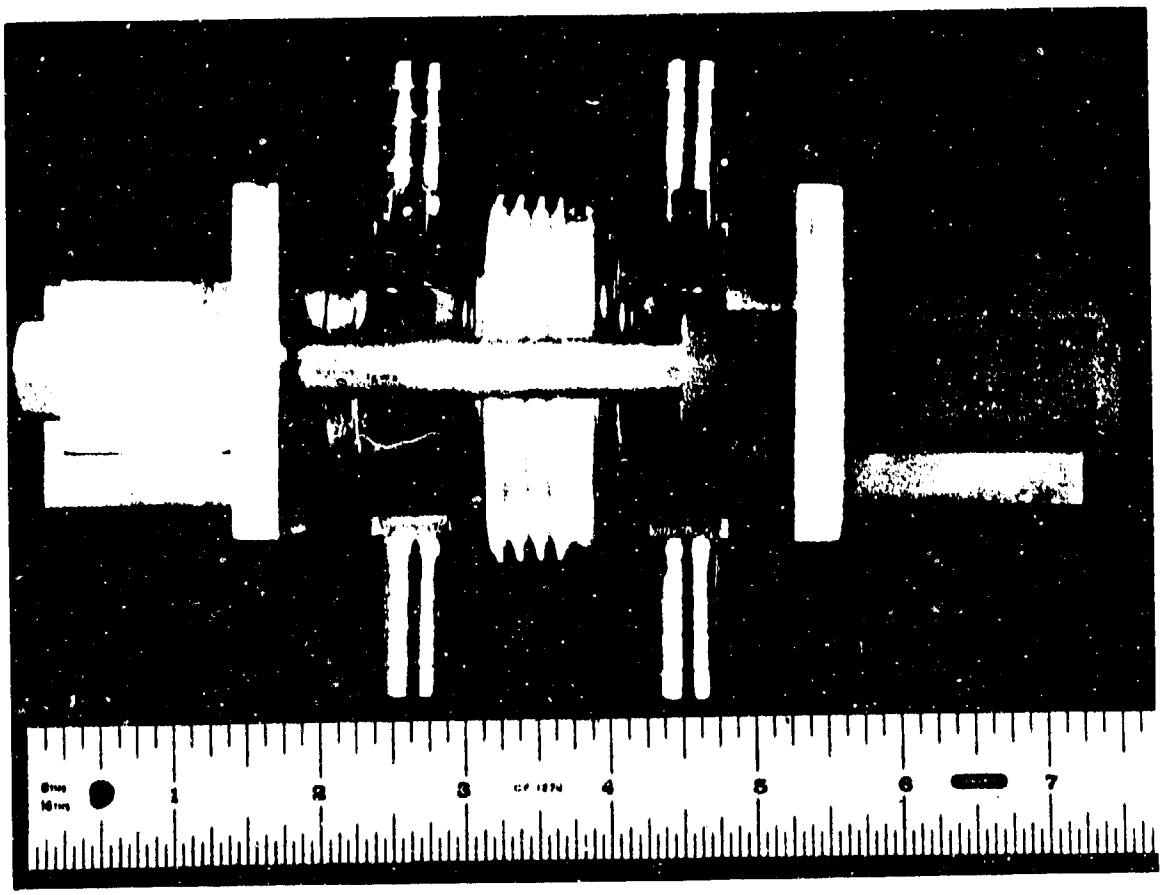

Figure 4-6. G-18 Water-cooled Heat Dissipator

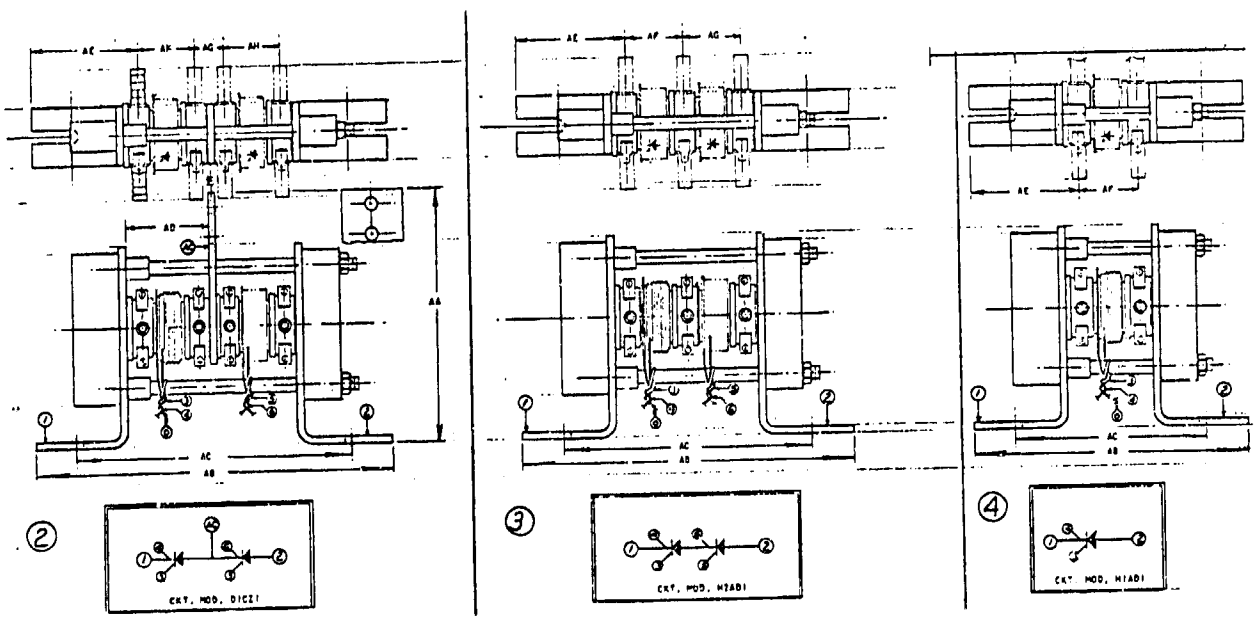

Figure 4-7. G-18 Water-cooled Heat Dissipator

The thermal resistance of a water-cooled system from thyristor junction to water varies with the flow rate of the water. A flow rate of between 2 and 3 gal./min has been found adequate for this system. The pressure drop across a G18 heat dissipator at a flow rate of 3 gal./min is less than 1.6 lb/in^2. Thus, for each thyristor the drop will be less than 3.2 psi. The pump power needed for each thyristor is 4.18 W. The power for the whole thyristor system will be 977 W. The pump power for the entire system will be still greater because of the pressure drop in the heat exchanger and the less than 100 percent efficiency of the pump. An estimate of 2 kW for the whole system is reasonable, because the 977 W for the thyristors is a worst-case estimate.

Both the weight and the volume of the system would be increased if air cooling had been used. This could be done with the C712 thyristor for the cruise and rated conditions, but not for crash-back. The weight of 234 air-cooled C712 devices with reactors and snubbers would be about 9750 lb, or about a 50 percent increase over the water-cooled weight. The volume of a single C712 air-cooled assembly would be about 315 in.^{3}, again about a 50 percent increase over the water-cooled volume. The change in the system volume would not be as great, however, because this is mostly determined by the snubbers, the reactors, and the mounting for voltage standoff.

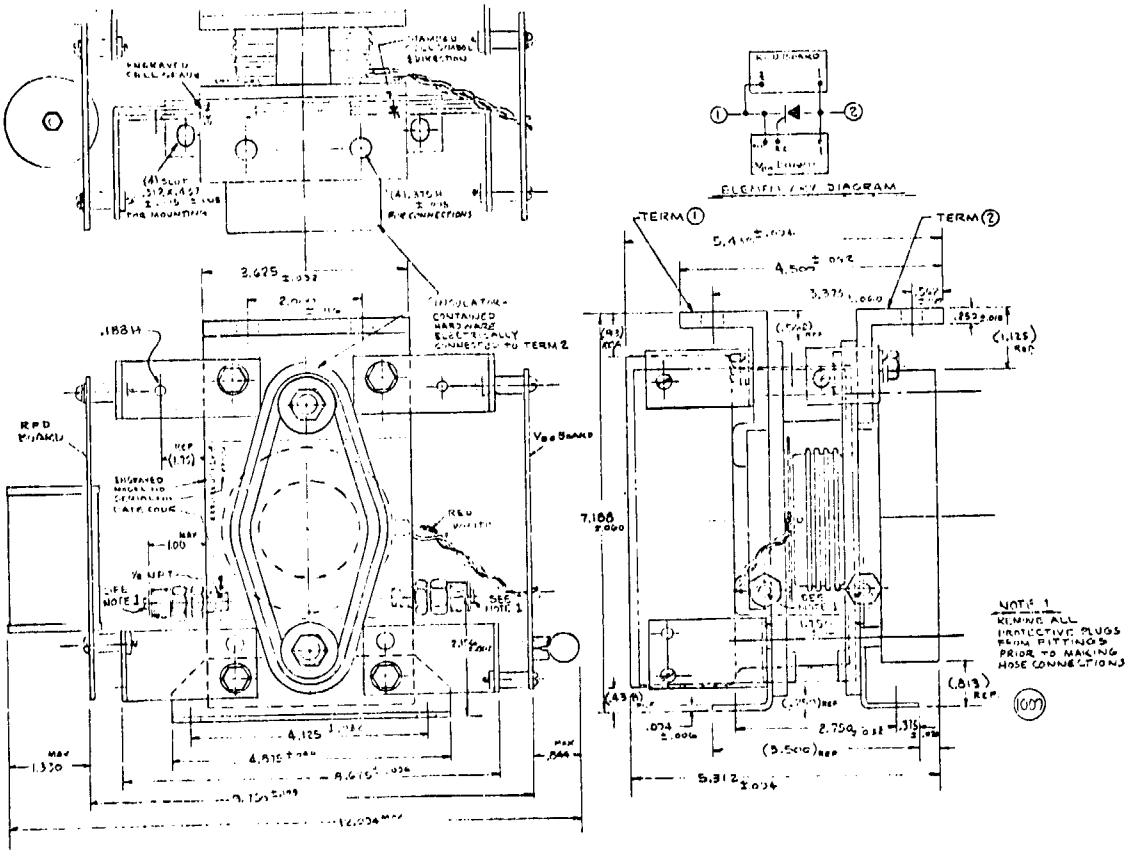

Figure 4-8. General Electric Freon 113-cooled Heat Dissipator

It is possible to use liquids other than water in liquid-cooled systems, but they must be chosen with care. For example, if an oil (Mobil Therm 600) is substituted for water at the same Reynolds number, the heat transfer will be decreased by a factor of 15. Such a change could be accomplished by redesign of the heat dissipator and an increase in the pump power, but it need not be done unless freezing of the water is a problem. Another solution to the freezing problem is the use of Freon 113 liquid. A high-efficiency aluminum heat sink which uses Freon 113 has been designed by the General Electric Static Power Components Operation (SPCO). At a flow rate of 1 gal./min, it has a thermal resistance almost as low as the G18 thyristor with water at 2 gals./min. This device is shown in Figure 4-8.

THERMAL ANALYSIS

W. H. Tobin's thermal analysis for the thyristors follows:

Specified Thyristors

712L/6RT107DB and CXX

2000 V 40 C to 0 C

2100 V 0 C to 125 C

Energy per Pulse	Average Power Dissipation
Assumptions	
Snubber dump	200 A
di/dt	100 A/μs
Pulse duration	925.9 μs
Reverse recovery current	700 A
Reverse voltage	100 V/μs to 2000 V max.

C712 Thyristor	Cruise	Rated	Crash-back
Peak current, A	849	2831	4246
Energy, W-s	1.73	6.15	10.5
Average device power losses, W	208	738	1260
ΔT_f, ^{o}C	5	9	13
Average system power losses, kW	48.7	172.7	294.8
CXX Thyristor			
Peak current, A	849	2831	4246
Energy, W-s	1.74	5.42	8.7

Average device power losses, W	209	650	1045
ΔT_f, ^oC	2.8	5	6
Average system power losses, kW	48.7	152.1	244.5

ΔT_f

The instantaneous rise of junction temperature above the average junction temperature

Thermal Requirement

Assumption -- crash-back condition for 2 min

Thermal Resistance for C712 Thyristor

With air cooling: $R_{\theta JA}$ = 0.07 C/W continuous
= 0.059 C/W 120 s

With water-cooled G18: $R_{\theta JW}$ = 0.053 C/W 120 s and continuous assembly

Thermal Resistance for CXX Thyristor

With air cooling: $R_{\theta JA}$ = 0.057 C/W continuous
= 0.046 C/W 120 s

With water cooling: $R_{\theta JW}$ = 0.040 C/W 120 s and continuous

Junction Temperature Calculation for C712 Thyristor

T_{jmax} = 125 C - 13 C = 112 C maximum allowable average junction temperature

Water cooling -- inlet 30 C, 2 to 3 gal./min

T_{jH_2O} = 30 C + 1260 (0.053) = 97 C (OK)

Air cooling -- 40 C air

T_{jair} = 40 C + 738 (0.07) + (1260 - 738)(0.059) = 122 C (too hot)

Junction Temperature Calculation for CXX Thyristor

T_{jmax} = 125 C - 6 C = 119 C maximum allowable average junction temperature

Water cooling 30 C inlet temperature

T_{jH_2O} = 30 C + 1045 (0.04) = 72 C (OK)

Air cooling -- 40 C air

T_{jair} = 40 C x 650 (0.057) + (1045 - 650)(0.046) = 95 C (OK)

SUMMARY

In summary, a water-cooled thyristor assembly using C712 devices can be used for all load conditions of this application. The assembly will weigh about 6000 lb and occupy a volume less than a cube 81 in. on an edge. The cooling pump power will be about 2 kW. A future device, the CXX, will permit the assembly to be used with either air or water cooling. The CXX thyristor has a higher current rating; thus, fewer of these need to be used in the system to control the power flow.

The CXX thyristor, which is presently in development, will probably become available in about one year. Its forward conduction characteristic has been measured; in the current range of less than 5000 A, it can be approximated by Equation 4-8, with V_a = 1.1 V and R_a = 0.22 mΩ. In addition, its voltage rating is 2400 V, instead of 2100 V, for the C712 thyristor. Using these new values, various systems currents, voltages, and powers have been reevaluated:

I_m	= 4941 A	Equation 4-21
E_m	= 478 V	Equation 4-22
P_{av}	= 4.72 MW	Equation 4-23
M	= 10	Equation 4-25
NM	= 180	Equation 4-26

Thus, with this new device for the permanent magnet generator-permanent magnet motor system, the total number of 18-thyristor links can be decreased from 13 to 10, and the total number of thyristors decreased from 234 to 180. The total number of cables would be decreased from 39 to 30.

To completely evaluate this new device, it needs to be operated in a system with required snubbers and reactors, then system losses, weights, and volumes can be determined for comparison with present thyristors. Because of potential savings in systems simplicity as well as weight and volume, it is recommended that evaluation of the CXX thyristor be completed and the device tested in systems applications. In addition, it is recommended that higher efficiency, liquid-cooled heat sinks and the C712 and the CXX thyristors be evaluated. It is also recommended that a breadboard circuit using the C712 thyristor be evaluated with the necessary snubbers to determine more precisely the losses that have been estimated in this study.

If the new CXX thyristor is used instead of the C712 with a conventional field-regulated generator, there can be a further reduction in equipment size and weight. The rated machine voltage can be increased.

$$E_g = E_m = 741 \text{ volts}$$

The power delivered by each three-phase link

$$P_{av} = 7.32 \text{ MW}$$

The total number of 18 thyristor links reduced to

$$M = 6$$

and the total number of thyristors will be

$$NM = 108$$

The number of cables required is 18.

Thus, there will be a reduction by more than a factor of two in the number of thyristors and cables in going from the permanent magnet generator with C712 thyristors to the conventional field-regulated generator with the new CXX device. It is estimated that the 40 000-hp converter volume will be about 230 ft^3 and the weight about 4500 lb.

Section 5

CONCLUSIONS

This study shows that permanent magnet motor electrical propulsion systems are practical for ship propulsion systems; such systems are relatively lightweight, have good efficiencies, and are unusually flexible.

One of the results of this study is that several technology areas need to be investigated further before large permanent magnet machines should be built for U.S. Navy applications. These areas are identified as:

- A manufacturing or process technology development program to demonstrate that high coersive force magnets can be packaged into subassemblies of a size and form necessary for use in large machinery.
- It has become apparent during this study program that for the performance characteristics, including losses and system trade-offs, to be meaningful a much better defined ship application is necessary before detailed analyses can be performed.
- The disc-type permanent magnet generator with its potential regulation capabilities needs to be investigated further. Such a study should include a detailed mechanical design and performance analysis of this machine as well as an investigation into the manufacturing and assembly problems associated with the disc-type machine.

Based on the results of this study, it is anticipated that a permanent magnet machine propulsion system is a prime candidate for electrical propulsion systems for new and existing ships.

General Electric's permanent magnet motor concept includes a very attractive feature in which low rpm machines can be operated and cooled by flooding with a cooling fluid such as water. This particular feature has advantages in large high power density machines, as pressurized and piped cooling systems tend to become complex and less reliable. This flooded motor concept is very appealing for use in ships such as the hydrofoil and, perhaps, the submarine. These two ship types are prime candidates for further studies involving permanent magnet machines.

The permanent magnet motor concept should also be applied to applications in the Navy for smaller horsepower machines, such as auxiliary and pump motors. Both fixed-speed and variable-speed machines should be studied with emphasis on reliability, ease of maintenance, and life-cycle costs.

The disc permanent magnet generator concept described briefly in Section 3, "Permanent Magnet Machine Trade-off Designs," of this report should

be given more consideration for ship service generator applications. This machine concept has received very little attention in the technical community and should be examined for the limits of its capabilities. The disc machine concept can also be applied to motors, with one unique advantage -- disc motors can be mounted on a single bearing common to the driven shaft.

General Electric is confident that the a-c propulsion system described in this report can be developed for these applications as a cost-effective propulsion system on a life-cycle cost basis.

APPENDICES

Appendix A

SYSTEM OPERATION

TWIN-SHAFT DESTROYER SHIP

The operator is provided with the following basic controls:

- Power selection switch
- Control power switch
- Throttle for each motor
- Start and stop switch for each turbine

STEP 1 -- DOCKSIDE

During this step, the propulsion plant is brought to a standby condition.

1. Control power is energized.
2. The generators to be used for the particular mission mode are brought up to idle speed and connected to the cycloconverter. The motors are deenergized as the thyristors are locked out and prevented from firing.

The power selection switch designates the number of generators that have to be used, and sets up the logic for automatically starting, connecting, disconnecting, and stopping the various generators according to the following selections:

1. No turbines
2. One port turbine for both motors
3. One starboard turbine for both motors
4. One turbine per motor
5. Two turbines per motor

The throttle for each motor has the following settings:

Open. In this position, the steady-state condition is that all of the generators called for by the power selection switch are connected to the line, with the turbine fuel flow at idle on all of the units.

Graduated rpm Scale. The desired steady-state propeller speed is obtained by moving the throttle to the proper position on the digital scale. The rpm range is a function of the number of turbines selected.

STEP 2 -- DOCKSIDE AND HARBOUR MANEUVERING
(Quarter-connected Power)

In this step, propeller speeds in either direction of rotation up to the level set by the connected power are available. One turbine for both motors will give propeller speeds up to 88 rpm. This is accomplished by setting each throttle level in the required direction to the desired speed value. The control is such that each cycloconverter receives firing pulses for the correct phase rotation and accelerates each motor to the selected speed. The turbine fuel is controlled automatically to achieve the turbine speed and horsepower that are consistent with the desired propeller speed.

If the motor direction is to be reversed, the throttle is moved to the desired setting in the opposite direction. The following sequence automatically occurs:

1. The turbine fuel is cut to idle.
2. The cycloconverter reverses the power flow, and the motor regenerative power is absorbed in the power turbine.
3. The cycloconverter reverses the phase rotation and accelerates the motor to the reverse speed selected. The turbine fuel flow is returned to automatic control for the speed and horsepower requirements.

STEP 3 -- INCREASED POWER (Half-connected Power)

In this step, one generator per motor is connected on-line for propeller speeds up to 125 rpm. This operation is accomplished as follows:

1. Leaving the throttle at any required value of speed, the operator moves the power selector switch to Position 3. This step automatically starts the necessary generator with the turbine fuel flow at idle.
2. The cycloconverters are phased off and the connected generator (supplying both motors) is disconnected, and the turbine fuel flow is set down to idle.
3. The generators are connected to their respective cycloconverters. The cycloconverters receive firing pulses for the correct phase rotation and accelerate each motor to the speeds selected on the throttles. The turbine fuel flow is automatically regulated for the speed/horsepower relationship determined by the power requirements.

STEP 4 -- HIGH SPEED (Full-connected Power)

In this step, two generators per motor are connected on-line for propeller speeds up to 168 rpm. The operation is accomplished as follows:

1. The operator moves the throttles to 168 rpm and the power selector switch to Position 4. This step automatically starts the two remaining generators with the turbine fuel flow at idle. The connected generators are operating the propulsion motors at 125 rpm.
2. The two remaining generators are now connected to their respective sections of the cycloconverter. These sections of the cycloconverters now receive firing pulses and are phased up and controlled to share the motor load for the 125-rpm operation. The turbine fuel flows on all of the turbines are automatically regulated for the speed/horsepower relationships determined by the power requirements.
3. All sections of the cycloconverters are now controlled to accelerate the motors to the 168 rpm value.

STEP 5 -- CRASH-BACK

In this step, power to the propellers is reversed, and the ship is brought stationary in the water as rapidly as possible. The operation is accomplished by moving both throttle levers to the maximum reverse position, which initiates the following sequence:

1. The turbine fuel on all of the units is cut to idle.
2. When the propeller speed drops to slip-speed braking, resistors are applied across the motor terminals. The resistor value is progressively reduced by shorting switches to maintain a motor phase current of 150 percent. The turbine fuel flow is automatically regulated to maintain the turbine speed as close as practicable to its minimum value.
3. With the remaining sections of the resistors applied to the motors, the motors are still turning ahead at slow speed, and the stator current has dropped to a relatively low value. The cycloconverters are controlled to supply power to the motor resistor combinations. Some of the power is used to reverse the direction of the motors, and some of the power is dissipated in the resistors.
4. When the motors reverse their direction of rotation, the braking resistors are removed from the circuit. The cycloconverters are controlled to accelerate the motors to the maximum speed obtainable. The turbine fuel flow is automatically regulated for the speed/horsepower relationships determined by the power requirements during this maneuver.
5. When the ship stops, the operator moves both throttles back to the reverse or forward speeds desired, and the control automatically brings the motors to those values.

STEP 6 -- POWER REDUCTION

In this step, power to the propellers is reduced by dropping the gas turbines. This is accomplished by the operator moving the power selection switch to the power combination position required.

1. The generators not required are automatically reduced in load and disconnected. The applicable turbine fuel flows are reduced to idle.
2. The still-connected power is automatically controlled to operate the propulsion motors at the speed set on the throttles, or to the maximum speed obtainable on that power configuration if the throttle position calls for a higher speed, if the throttle position would have to be reduced into the correct power zone for speed control of the motors.

HYDROFOIL SHIP

System operation will be identical to that described for the destroyer, except the one generator per motor represents full-connected power operation rather than the destroyer half-connected power. The equivalent propeller speed ranges would be: 1) half-connected power of one generator for two motors for propeller speeds of 0 to 890 rpm, and 2) full-connected power of one generator per motor for propeller speeds of 0 to 1200 rpm.

Appendix B

THE INFLUENCE OF MACHINE CHARACTERISTICS UPON THE WEIGHT AND VOLUME OF A SYNCHRONOUS GENERATOR

A machine characteristic important for the contemplated application of this machine is the commutating reactance, which is practically identical to the negative sequence reactance.

$$X_c \sim X_2 = \frac{1}{2}(X_d'' + X_q'') \qquad \text{(B-1)}$$

where: X_d'', X_q'' } subtransient reactances in direct, d, and quadrature, q, axes

If no amortisseur reactances are present, the subtransient reactances are equivalent to the transient reactance. Furthermore, if the field leakage reactance is large compared to the synchronous reactance in the direct axis, X_{ad}, one can simplify as a first approximation

$$X_c \sim \left(\frac{X_{ad} + X_{aq}}{2}\right) \qquad \text{(B-2)}$$

In other words, the synchronous reactances contribute significantly to the commutating reactance for a machine when the above approximations are valid. This indicates that when attempting to find a relationship between commutating reactance and machine volume and weight, one has to find a relationship between synchronous reactance level and volume. Qualitatively, that can be done as follows: the voltage produced in a synchronous machine can be written as

$$E_i = \omega \times W \times \xi \times \phi \qquad \text{(B-3)}$$

where: ω = rotational frequency
W = number of turns per phase
ξ = winding coefficient
ϕ = magnetic flux per pole

or with

$$\phi = \tau_p \times H_i \times B_g \qquad \text{(B-4)}$$

$$E_i = \omega \times W \times \xi \times \tau_p \times H_i \times B_g \qquad \text{(B-5)}$$

where: τ_p = pole pitch = $\frac{\pi D}{2p}$
p = pole pairs
B_g = average air gap flux density

Assuming the machine operates at constant speed and maximum allowable flux density, B_g (thus constant), the same voltage can be produced either through a large number of turns and a small pole area ($\tau_p \times H_i$) or through a small number of turns and a large area. The machine synchronous reactance is proportional to the number of turns squared and to the pole area.

$$X_{ad} \sim (W\xi)^2 \times \frac{\tau_p \times H_i}{\delta} \qquad \text{(B-6)}$$

where: δ = air gap length

Thus, when the stack length (and the pole area) is reduced and the number of turns is increased, to maintain constant voltage, the reactance of the new machine will be larger by $W \times \xi$,

$$X_{adl}/X_{ado} = W_1\xi_1/W_0\xi_0 \qquad \text{(B-7)}$$

e.g., a reduction in machine volume, though decreasing the stack length, results in an increase in reactance level.

A quantitative approach becomes more involved, as is shown below. The volume of an electrical machine consists of two parts: one is associated strictly with the end turns, the other is associated with the active part of the machine and can be written as follows:

$$V_2 = \frac{\pi}{4} \times H_i \times (D + 2 \times h_c + 2 \times h_s)^2 \qquad \text{(B-8)}$$

where: H_i = stack length
D = bore diameter
h_c = core height (behind slot)
h_s = slot depth

This neglects the frame contribution, which could be included as a $2 \times th_F$ term in the parentheses. For trend investigations, it is neglected for simplicity sake. For a machine with a number of poles larger than eight, the volume and weight contribution of the end-turn section has also been omitted to allow simpler relations to be developed. Its contribution can be estimated afterwards and added if necessary.

To tie the synchronous reactance level to the volume, we will use the relationship between current sheet and magnetic flux and torque produced in the machine

$$T = p \times D \times \frac{\pi}{4} \times A_{max} \times \phi \qquad \text{(B-9)}$$

Since the power output and the speed are assumed to be constant, we get

$$p \times D \times A_{max} \times \phi = \text{Constant} \qquad \text{(B-10)}$$

A_{max} can be replaced with

$$A_{max} = m \times W \times \xi \frac{2I\sqrt{2}}{\pi \times D} \qquad \text{(B-11)}$$

where: m = number of phases
I = rms current per phase

while ϕ can be replaced with

$$\phi = \tau_p \times H_i \times \frac{2}{\pi} \times B_{mg} \qquad \text{(B-12)}$$

where: B_{mg} = maximum flux density in the air gap

This results in

$$p \times D \times m \times W \times \xi \frac{2I\sqrt{2}}{\pi \times D} \times \tau_p \times H_i \times \frac{2}{\pi} B_{mg} = \text{Constant} \qquad \text{(B-13)}$$

or

$$p \times m \times W \times \xi \times \tau_p \times H_i \times B_{mg} \times I = \text{Constant} = C_1 \qquad \text{(B-14)}$$

The number of turns per phase, W, can be expressed as

$$W = \frac{S_1 \times T_{pc}}{a \times m} \qquad \text{(B-15)}$$

where: a = number of parallel circuits per phase
S_1 = number of stator slots
T_{pc} = turns per coil

for a two layer winding (two coil sides per slot).

Substituting Equation B-15 into Equation B-14, we obtain

$$p \times \frac{S_1}{a} \times T_{pc} \times \xi \times \tau_p \times H_i \times B_{mg} \times I = C_1 \qquad \text{(B-16)}$$

I/a equals the current per circuit, and thus per coil, and can be expressed as

$$\frac{I}{a} = \sigma \times W_{cu} \times h_{cu} \qquad \text{(B-17)}$$

where: σ = current density
W_{cu} = width of the conductor
h_{cu} = height of the conductor

Furthermore, for a two layer winding, one can approximate

$$T_{pc} \times \frac{I}{a} = \sigma \times \frac{W_s \times h_s}{2} \qquad \text{(B-18)}$$

where: W_s = width of slot

Equation B-16 can then be rewritten as

$$p \times S_1 \times \xi \times \tau_p \times B_{mg} \times \sigma \times H_i \times W_s \times h_s = C_1 \times 2 = C_2 \qquad \text{(B-19)}$$

This equation gives a relationship between the stack length, H_i, and the slot depth, h_s, when all of the other parameters are kept constant. B_{mg} and σ are supposedly at the maximum permissible values.

Equation B-19 can be utilized to replace H_i in Equation B-8.

$$V_2 = \frac{\pi}{4} \times (D + 2h_c + 2h_s)^2 \times \frac{C_2}{p \times S_1 \times \xi \times \tau_p \times B_{mg} \times \sigma \times W_s \times h_s} \qquad \text{(B-20)}$$

or

$$V_2 = C_3 \times \frac{1}{S_1 \times \xi \times B_{mg} \times \sigma \times W_s} \cdot \frac{(D + 2h_c + 2h_x)^2}{D \times h_s} \qquad \text{(B-21)}$$

This equation needs to be commented on. Equation B-18 equates the number of turns with the slot depth, while Equation B-19 gives us a relation between h_s and H_i. Thus, an increase in h_s means an increase in the number of turns and a decrease in H_i as is necessary to produce constant voltage in machines that only differ in the stack length and in the number of turns.

The next step is to find a suitable expression for the synchronous reactance.

$$X_{ad} = \omega \times \mu_0 \frac{2}{\pi} \times \frac{\tau_p \times H_i}{\sigma} \times \frac{C_{ad}}{\pi} \times m \times (W \times \xi)^2 \times \frac{1}{p} \qquad \text{(B-22)}$$

where: μ_0 = permeability of air

C_{ad} = pole form coefficient

τ_p and H_i can be substituted as before to obtain

$$X_{ad} = C \times \frac{S_1 \times \xi \times W_s}{(p \times a \times h_{cu} \times W_{cu})^2 \times \sigma \times m \times B_{mg} \times \sigma} h_s \qquad \text{(B-23)}$$

This expression relates X_{ad} to h_s.

Equations B-23 and B-21 are then combined to relate X_{ad} to the volume for machines of the same power and voltage output at identical speeds. These machines differ only in stack length and number of turns per coil and thus per phase (a is constant). The resulting function, X_{ad} versus volume and thus weight, is shown in Figure B-1. Since these investigations have been done for the purpose of finding out how the reactance of a given machine changes when the volume is reduced, both X_{ad} and V are referred to the original values X_{ado} and V_o. This curve is intended to show the trend, and other operating restrictions will have to be considered to determine the degree of applicability of the found function.

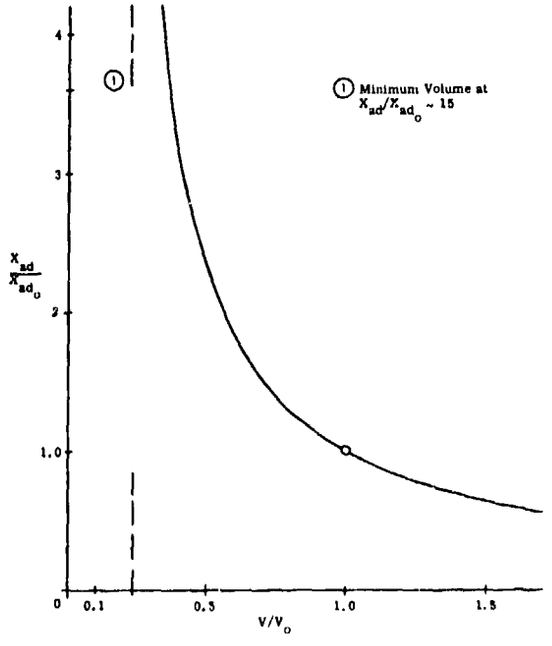

Figure B-1.

Relative Volume Versus Synchronous Reactance

Appendix C

REFERENCES

1. Bailey, L.J., Lafuze, D.L., Messenger, L.W., and Triebel, C.F., 150 kVA Samarium Cobalt VSCF Starter Generator Electrical System: Phase I, Final Report, No. AFAPL-TR-76-8, prepared for the Air Force Aero Propulsion Laboratory, Contract No. F33615-74-C-2037, General Electric Company, Schenectady, New York, March 1976.

2. Bailey, L.J. and Richter, E., Development Report on a High-speed Permanent Magnet Generator Utilizing Rare Earth Cobalt Magnets, paper presented at Second International Workshop on Rare Earth Cobalt Magnets and their Applications, Dayton, Ohio, 1976.

3. Stoehr, M., "Die Typenleistung kollektorloser Stromrichter Motoren bei verbesserten Motorschaltungen" ("The Rating of Brushless Converter Motors with Improved Motor Connections"), Archiv fuer Elektrotechnik, 1938, pp. 767-784.

DISTRIBUTION LIST

LCDR W. R. Seng
Scientific Officer
Office of Naval Research (Code 473)
800 N. Quincy Street
Arlington, VA 22217

Commander, Defense Contract Administration
Services District - Hartford
96 Murphy Road
Hartford, CT 06114

Director, Naval Research Laboratory (6)
Attn: Code 2627
Washington, DC 20375

Office of Naval Research (6)
Department of the Navy
Arlington, VA 22217
Attn: Code 102IP

Defense Documentation Center (12)
Building 5, Cameron Station
Alexandria, VA 22314

Office of Naval Research
Branch Office, Boston
495 Summer Street
Boston, MA 02210

LCDR Kirk Petrovic
Office of Naval Research (Code 211)
800 N. Quincy Street
Arlington, VA 22217

Naval Undersea Systems Center
Attn: T. Black, Code SB-331
Building 127
Newport, RI 02840

Naval Undersea Systems Center
Attn: Dr. John Brady, Code SB-3
Building 679
Newport, RI 02840

R. C. Hamilton
Institute for Defense Analysis
400 Army Navy Drive
Arlington, VA 22202

NAVORDSYSCOM
Attn: ORD 031C, M. F. Murphy
Washington, DC 20360

Mitchell Namy
A.C.O., DCASD
1000 Liberty Ave.
Pittsburgh, PA 15222

Dr. Michael Petrick
Associate Director for Advanced Programs
Engineering Division
Argonne National Laboratory
9700 South Cass Ave.
Argonne, IL 60439

Mr. Raymond J. Polcha
Code ECA
Naval Weapons Laboratory
Dahlgren, VA 22448

Dr. Robert Powell
Cryogenic Division
National Bureau of Standards
Boulder, CO 80302

H. O. Stevens
Code 2722
Naval Ship R&D Laboratory
Annapolis, MD 21401

Mr. Lou Jokl
U.S. Army Mobility Equipment R&D Center
(MERDC)
Main Building No. 312
Fort Belvoir, VA 22060

Dr. Robert Allen
David W. Taylor
Naval Ship R&D Center
Code 012
Bethesda, MD 20084

Mr. Nic Toffolo
Naval Ship Engineering Center
Code 6157C
Center Building
3700 East-West Highway
Prince Georges Plaza
Hyattsville, MD 20782

Mr. O. J. Remson
Headquarters
Naval Material Command (MAT) 033
Washington, DC 20360

Mr. John Harrison
David W. Taylor
Naval Ship R&D Center
Code 2722
Annapolis, MD 21402

Mr. Art Chaikin
Naval Sea Systems Command
Code 033
National Center No. 2
James Polk
2521 Jefferson Davis Highway
Arlington, VA 20360

Dr. Earl Quandt
David W. Taylor
Naval Ship R&D Center
Code 272
Annapolis, MD 21402

Dr. S. Koslov
Office of Asst. Secretary of the Navy
Research & Development
Pentagon 4E741
Washington, DC 20350

Dr. A. L. Bement
Defense Advanced Research Programs Admin.
Architect Building
1400 Wilson Blvd.
Arlington, VA 22209